THE CHARACTERISATION OF THE LEAD FLOTATION CIRCUIT AT BLACK MOUNTAIN MINING (PTY) LTD. USING THE FLOATABILITY COMPONENT MODEL APPROACH

By

Malikaah Galant

Thesis presented for the degree of

Masters of Science in Engineering

In the Department of Chemical Engineering

University of Cape Town

2015

SYNOPSIS

Black Mountain Mining (Pty) Ltd. (BMM) is a base metal operation that has been producing chalcopyrite-, galena- and sphalerite-bearing concentrates for over 30 years. Silver is recovered in the concentrates as a result of elemental substitution within the crystal lattice of chalcopyrite and galena minerals.

The primary objective of this study was to adapt the Floatability Component Model (FCM) as a simplified proof-of-concept model for the Lead flotation circuit of the BMM Concentrator based on plant- and laboratory-scale data. The model obtained, using the FCM approach in conjunction with the Woodburn and Wallin (1984) methodology, should give insight to the metallurgical team regarding the performance of the circuit based on the data pertaining to the feed characteristics of the Lead flotation circuit. Additionally, as a result of the known association of silver with galena minerals, an objective of the study was to be able to predict the response of silver based on the response of galena minerals. The model for the Lead flotation circuit of BMM Concentrator was developed in a single MS Excel spreadsheet and it was important that the raw data used to develop the model could be obtained easily, inexpensively and in a manner that was not disruptive to the operation.

The equation used to calculate the overall mineral recovery for each species, termed j in this study, was $R_{j,Total} = \frac{k_j\tau_A(1-R_{W,A})+ENT_jR_{W,A}}{(1+k_j\tau_A)(1-R_{W,A})+ENT_jR_{W,A}}$, which incorporates the flotation rate constant of the species j (k_j), the residence time of the flotation cell A (τ_A), the recovery of water in flotation cell A ($R_{W,A}$) as well as the degree of entrainment of species j (ENT_j). Based on the findings of Gorain and co-workers (1998), the flotation rate constant of each species was expanded in terms of the mineral's floatability constant (P), the bubble surface area flux of the flotation cell (S_b) and the froth recovery of the flotation cell (R_f), i.e. $k = PS_bR_f$.

Since this methodology had not been used internally at BMM before, Phase One of the study was aimed primarily at validating the flotation test procedure and the conservation of floatability in the Lead flotation circuit. Key findings from Phase One included validation that the batch flotation test procedure used in this study produced repeatable results that were within a 95% confidence level, that floatability of minerals was conserved when samples were stored for less than three hours and that silver recovery strongly correlated with galena recovery, although not linearly.

Phase Two of the study focussed on gathering circuit data by means of a circuit survey and hot batch flotation tests in order to characterise the Lead flotation circuit. The initial key findings from Phase Two were that the circuit was adequately stable when the circuit survey was conducted, the bubble surface area flux measured in the flotation cells was consistent with values measured at the Elura Lead Concentrator (Grano, 2006) and the overall

correlation of balanced and model predicted data was strong since majority (75,6%) of the data had a weighted sum of squared error less than 5. The experimental data from the 1st through 3rd Rougher tailings streams were more difficult to reconcile and it was likely that this was due to poor sample representivity.

In terms of the ore characteristics, galena, silver and sphalerite were characterised as having three floatability sub-classes, i.e. fast, slow and non-floating, and chalcopyrite was characterised as being slow floating and non-floating. The characterisation of three floatability sub-classes of galena was consistent with that obtained for the Red Dog (Runge et al., 1997) and Cannington (Welsby et al., 2010) operations. The amount of galena determined to be non-floating in the BMM circuit, i.e. 5.8%, was consistent with a mineralogy study conducted by Anglo Research Mineralogical Research Department in 2008 (Bramdeo et al., 2008) where it was found that 5,2% of the galena fed to the BMM Lead flotation circuit was locked and associated with gangue.

The Scavenger flotation cell was historically not always operational and would typically only be brought online when the feed grade to the circuit was high and/or there was difficulty achieving the target galena circuit recovery. At the time of the circuit survey, the Scavenger flotation cell was found to be performing inefficiently with respect to mineral recovery and this was reinforced by the low model fitted froth recovery of all species in this flotation cell. Since the gas dispersion of the cell appeared to be within a normal operating range, as indicated by the S_b data that compared well to the Elura Lead Concentrator (Grano, 2006), it suggested that the operational froth depth was not optimal. The sub-optimal performance of the circuit in terms of slow floating galena not being recovered in the Scavenger flotation cell was supported by the findings from a mineralogy study conducted by Anglo Research Mineralogical Research Department (Bramdeo et al., 2008) which found that the Lead flotation circuit tailings contained liberated galena within the optimal size range for galena flotation.

It was concluded that the model obtained could be used to predict the galena response in the Lead flotation circuit since the model predicted galena recovery was within a 99% confidence level of the average historical BMM galena recovery obtained with similar Lead feed grade. However, the model could not be used to accurately predict the response of silver. Lastly, it was concluded that the modelling methodology used in this study was sufficiently rigorous that it could indeed be used to identify possible areas of improvement and could simulate adequately the effect of a parameter being tested by means of a desktop study. This has the potential to dramatically reduce the time taken to study the effect on the circuit as a result of making process changes and has the potential for significant cost savings in optimizing the operation of the Lead flotation circuit.

ACKNOWLEDGEMENTS

I would like to thank my supervisors, Professor Cyril O'Connor and Jenni Sweet. The journey of this MSc started as far back as 2010 with our on-site meeting at Black Mountain, and it had many hiccups along the way. The start of this MSc relationship showed me their passion and commitment towards the project. Their individual strengths, guidance and direction throughout the various stages of the project and compilation of the dissertation ensured that I got the most out of this MSc, especially from a perspective of personal growth. Their assistance was invaluable.

I would also like to thank my husband and family. Their support, especially over the last stretch of my MSc, encouraged and motivated me to finish it to the best of my ability. I definitely would not have been able to complete it without their invaluable support. Although my father is not alive to celebrate in this accomplishment, I am certain he would have been extremely proud.

Last, but certainly not least, I would like to thank Black Mountain Mining (Pty) Ltd. for making the resources and time available to me to do all the necessary testwork and data collection for this project. A special mention to the previous and current concentrator management team, metallurgists, Analytical Laboratory personnel and the UCT students who played a role in making this project a reality.

GLOSSARY

a	is the model parameter related to the volumetric flow rate of concentrate used to calculate water recovery to concentrate, dimensionless
Avg	is average
b	is the model parameter related to the volumetric flow rate of concentrate used to calculate water recovery to concentrate, dimensionless
BMM	is Black Mountain Mining (Pty) Ltd.
Calc'd	is calculated
$C_{j,A}$	is the mass flow of species j exiting flotation cell A in the concentrate stream, $\frac{kg}{hour}$ or $\frac{t}{hour}$
$C_{ij,A}$	is the mass flow for sub-class i of species j exiting flotation cell A in the concentrate stream, $\frac{kg}{hour}$ or $\frac{t}{hour}$
Chalcopyrite	is the mineral with empirical formula $CuFeS_2$
Cu	is copper metal
d_{32}	is the Sauter mean bubble diameter, mm
ENT_j	is the degree of entrainment for species j in the overall recovery calculation, dimensionless
ENT_M	is the degree of entrainment of valuable mineral species in the Warren (1985) method, dimensionless
ENT_G	is the degree of entrainment of gangue species in the Warren (1985) method, dimensionless
f_A	is the fraction of the feed entering the flotation cell A, dimensionless
F_D	is froth depth, mm or cm
$(FD)_{k=0}$	is the froth depth when the flotation rate constant is zero, mm or cm

F_j	is the species j in the feed to the circuit, $\frac{kg}{hour}$ or $\frac{t}{hour}$
F_M	is the indication of true flotation found by extrapolating the trendline of the valuable mineral recovery to the y-axis in the Warren (1985) method, %
F_S	is the flow rate of solids in the concentrate stream, $\frac{m^3}{hour}$
g/t	is grams per ton
g_{GA}	is the enhancement factor of gangue for the flotation cell A (dimensionless)
g_{jA}	is the enhancement factor of species j for the flotation cell A (dimensionless)
g_{ijA}	is the enhancement factor for sub-class i of species j for the flotation cell A (dimensionless)
HIRA	is Hazard Identification and Risk Assessment
J_g	is the superficial gas velocity, $\frac{cm}{second}$
k	is the first order flotation rate constant, min^{-1}
k_c	is the collection zone rate constant, min^{-1}
kg/h	is kilograms per hour
k_j	is the first order rate constant of species j, min^{-1}
k_{ij}	is the first order rate constant for sub-class i of species j, min^{-1}
L/min	is litres per minute
ml	is millilitres
ml/min	is millilitres per minute
m^3	is cubic metres
Mtpa	is million tons per annum
ppm	is parts per million, and the equivalent of g/t

P	is the inherent mineral floatability, dimensionless
Pb	is lead metal
P_{ij}	is the inherent mineral floatability for sub-class i of species j, dimensionless
R	is metal or mineral fractional recovery
$R_{j,Total}$	is the fractional overall mineral recovery for species j by true flotation and entrainment
$R_{f,A}$	is the fractional recovery of particles into the froth
$R_{f,i,A}$	is the fractional recovery of particles of a specific species i into the froth
$R_{ij,Batch}$	is the fractional recovery for sub-class i of species j in the batch flotation test
R_G	is the fractional recovery of gangue material by entrainment into the concentrate
R_M	is the fractional recovery by true flotation of the valuable mineral at a specific flotation in the Warren (1985) method
R_W	is the fractional recovery of water into the concentrate
$R_{W,A}$	is the fractional recovery of water into the concentrate for flotation cell A
rpm	is revolutions per minute
$S_{b,A}$	is the superficial bubble surface area flux for flotation cell A, $\frac{1}{min}$
$S_{b,Batch}$	is the superficial bubble surface area flux of a batch cell, $\frac{1}{min}$
tph or t/h	is tons per hour
t_{at}	is the bubble-particle attachment time (e.g. microseconds)
t_i	is the induction time, i.e. time for liquid film to thin to a critical film thickness (e.g. microseconds)

t_r	is the time required for the film to rupture and form the three-phase contact nucleic hole (e.g. microseconds)
t_{tpc}	is the time required for the three-phase contact line expansion (e.g. microseconds)
$T_{j,A}$	is the mass flow of species j exiting flotation cell A in the tailings stream, $\frac{kg}{hour}$ or $\frac{t}{hour}$
$T_{ij,A}$	is the mass flow for sub-class i of species j exiting flotation cell A in the tailings stream, $\frac{kg}{hour}$ or $\frac{t}{hour}$
Q_w	is the volumetric flowrate of water in the concentrate stream, $\frac{m^3}{hour}$
V_A	is the volume of flotation cell A, m^3
W_W	is the mass recovery of water to the concentrate at a specific flotation time (%) in the Warren (1985) method
τ_A	is the residence time of flotation cell A, minutes
τ_{Batch}	is the residence time of the batch flotation cell, minutes
$X_{j,A}^{-1}$	is the inverse of the connection matrix for species j, dimensionless
Zn	is zinc metal

TABLE OF CONTENTS

LIST OF FIGURES

LIST OF TABLES

LIST OF EQUATIONS

1 INTRODUCTION

1.1 Subject of the study

This study was concerned with the characterisation of the Lead flotation circuit at Black Mountain Mining (Pty) Ltd.

1.2 Background

Black Mountain Mining (Pty) Ltd., commonly referred to as BMM, is located in the Northern Cape province of South Africa. The mining area is located approximately seven (7) kilometres from the small town of Aggeneys, a mining town developed in the late 1970's to accommodate the personnel working for the mining company. The ore deposits belonging to BMM are exploited for the contained copper, lead, zinc and silver metal along with other minerals.

Due to the remote location of the mine, infrastructure required to run the mine is also located quite a distance from the mine. Water is supplied from the Pella Water Board, located approximately 60 kilometres from Aggeneys, and the railway siding used to transport the concentrates from the mine to the Saldanha Port is located approximately 170 kilometres from Aggeneys. Figure 1.1 illustrates a section of the South African map showing the location of Aggeneys, highlighted with a red circle, relative to other small towns in the Northern Cape region. Figure 1.2 shows a section of the mining area of BMM, with the Concentrator located on the far right and the old Broken Hill shaft located towards the centre of the figure.

Figure 1.1: The location of Aggeneys relative to other towns (Photo courtesy of BMM)

Figure 1.2: A section of the mining area of BMM (Photo courtesy of BMM)

Although exploration for economical reserves started in 1929, the potential of the deposits in the vicinity of Aggeneys was only realised in 1971 when Phelps Dodge conducted an extensive diamond-drilling program. Prior to 1980, the production of lead concentrate in South Africa was very low and erratic, and it was only after BMM started production that South Africa became a net exporter of lead concentrates (Snodgrass, 1986).

The BMM mine has been in operation for over 30 years and the ore deposit treated at the Concentrator has varied over the lifetime of the mine. Similarly, the feed composition to the mine as well as the feed throughput of the Concentrator has changed dramatically. The Concentrator was initially designed to treat approximately 1.2 Mtpa but is currently targeting an annual throughput 50% higher, i.e. 1.8 Mtpa.

Although the feed composition has changed, the amount of lead- and zinc-bearing minerals per ton of ore treated have always greatly outweighed that of the copper-bearing minerals and have, therefore, contributed significantly more towards the profitability of the mine due to the magnitude of concentrate volumes produced and sold. Furthermore, in recent years the lead concentrate sales have been the biggest contributor to the profitability of the BMM business (Company snapshot 2015-2016).

In order to adapt to the changing processing requirements, it is imperative that there is a good understanding around problem areas causing reduction in metal recovery and concentrate quality, and in effect profitability, as well as knowledge to help with the identification of possible improvement areas. Typically, this is done by the operators means of trial and error during the day-to-day operation, or by means of laboratory-scale testwork generally conducted to test possible alternatives like reagents. The online approach of trial

and error could have negative impacts on the operation causing loss in metal recovery or poor concentrate quality, and it could be time-consuming. The laboratory approach is very time-consuming, since it requires assay analysis to be done by the Analytical Laboratory, and the results achieved from the testwork are not always achieved in the plant-scale operation.

In the mining industry, each day could pose different challenges that hinder achieving the performance targets. When problems arise during the day-to-day operation, it is not common for the cause to be easily identified since the flotation process itself is made up of various sub-processes. The inefficiency of any of these sub-processes could affect the efficacy of the overall flotation process. Furthermore, when dealing with a complex ore, it is even more complicated to identify the cause of the problem.

An added disadvantage to this problem is that the reporting of the flotation performance is not always done throughout the day but is rather done using data collected over a 24 hour period, which is the case for BMM. Due to the delay in reporting, metal losses or poor concentrate quality cannot always be dealt with proactively.

In light of the complexity of the flotation process, testwork is normally conducted on a laboratory-scale in order to minimize the interaction of variables and maintain single parameter testing. However, the results of process improvement testwork conducted as laboratory-scale tests can very rarely be extrapolated accurately to predict the results that will be observed in the plant-scale operation. Plant-scale testing, or trials, is therefore the ideal method to be used when testing process alternatives but the results obtained from the trials cannot always be proven to be a direct result of the parameter being tested, and may also cause undesired losses in recovery, and revenue, or downstream instability.

Owing to the complexity of the ore being treated at the BMM Concentrator, it was important to develop a simple and robust methodology that could be used by the in-house metallurgists to easily troubleshoot problems or to identify areas of improvement. Any improvements in the Lead flotation circuit could have a marked effect on the revenue generated by BMM and so this was chosen for the proof-of-concept study.

1.3 Scope and limitations of the study

The scope of the study was limited to the Lead flotation circuit of BMM. This was due to the known stability of the circuit, based on operational information, as well as the profitability of the circuit, which implies that any possible improvement would result in additional profit for the company. Furthermore, it only focussed on the Roughing and Scavenging stages, which focuses on maximising lead metal recovery. The Cleaner stage was omitted from the scope due to poor access for sampling at the time the circuit survey was conducted. Lastly, the

species considered in the data analysis of this study were chalcopyrite, galena, sphalerite, silver and the non-sulphide gangue, which was termed the remainder in this study.

1.4 Plan of development of the dissertation

The dissertation will begin with a literature review focussing on a brief overview of the Black Mountain Mining (Pty) Ltd. company, flotation and the sub-processes of flotation as well as modelling of flotation processes. Thereafter, the results obtained from the study will be highlighted and discussed. Based on these results, conclusions and recommendations will be made.

2 LITERATURE REVIEW

2.1 Black Mountain Mining (Pty) Ltd.

South Africa's mining industry includes the mining and processing of a variety of base metals, PGM's, diamonds and coal. Lead is one of the metals found in base metal ores and is extracted at Black Mountain Mining (Pty) Ltd and is one of the world's most widely used metals in the industrial world whereby almost half of the world's annual production is consumed to produce car batteries (Chamber of Mines of South Africa, 2014). This study focused on the recovery of lead metal, as well as other minerals and metals, in the Lead flotation circuit at BMM.

When underground mining started at BMM, ore was processed from the Broken Hill and Swartberg orebodies. Due to the sulphide-nature of the ore, i.e. the Broken Hill and Swartberg orebodies containing chalcopyrite, galena and sphalerite at varying compositions, flotation was used to produce copper, lead and zinc concentrates at the Black Mountain Concentrator (Concentrator). The Life of Mine (LOM) of the Broken Hill orebody was nearing the end when, in 1999, it was discovered through surface drilling that the orebody extended further underground (Chamber of Mines of South Africa, 2014). The orebody extension is known as the Deeps orebody. A project to sink an additional shaft as well as a ventilation shaft was approved in the year 2000 and mining of the Deeps orebody commenced in 2003.

2.2 Processing of Deeps ore

The Deeps orebody is made up of several ore types, which are then further classified into four general ore types and are shown together with the typical metal content per type in Table 1.1 (Jenniker, 2005).

Table 1.1: Description of the ore types of the Deeps orebody (Jenniker, 2005)

Ore type		Description	Grades (%)		
			Cu	Pb	Zn
1	Type A	Made up of a variation of three Quartz-Magnetite ores (QM 1 - QM3) where the magnetite content is above 10%	0.31	2.8	2.92
2	Type B	Made up of Quartz-Magnetite ore QM4 which has magnetite content above 10%	0.64	0.43	5.17
3	Type C	Made up of Garnet-Amphibole-Magnetite iron formation, Garnet-Magnetite iron formation and Amphibolite-Magnetite iron formation ores	0.19	6.76	2.17
4	Type D	Massive-Sulphide, where sulphide content is above 25%, and Sulphidic-Quartzite, where sulphide content is below 25%	0.89	10.05	3.58

In terms of BMM standards, the feed grade of Type A is fairly typical, Type B would be referred to as a low galena-bearing and high chalcopyrite- and sphalerite-bearing ore type, Type C would be a high galena-bearing ore type and Type D would be a high chalcopyrite- and galena-bearing ore type.

The Deeps ore is mined underground at various depths using the Cut and Fill as well as Blasthole Stoping methods. Typically, the mined ore, consisting of different ore types, undergoes a degree of blending underground to prevent too many spikes and dips in terms of feed grade to the Concentrator. However, this is not always possible due to mining conditions underground. The mined ore undergoes Primary Crushing underground, by means of a Jaw Crusher, before being further crushed on surface by means of a Secondary and Tertiary Cone Crusher. The crushed product enters the Milling Circuit where it undergoes two-stage grinding using a Rod and a Ball mill, and is classified in terms of particle size using double-stage hydrocyclones. The overflow from the second stage of hydrocyclones is the flotation feed.

Anglo Research Mineralogical Research Department (ARMRD) conducted mineralogical studies of the feed to the flotation circuit (Brand & Horsh, 2006) and of streams within the flotation circuits (Bramdeo et al., 2008). The results of the study conducted in 2006 showed that the predominant minerals of the BMM ore was made up of magnetite and gangue, while the sulphide component of the feed stream was made up of pyrrhotite and sphalerite as the most abundant sulphide minerals followed by galena, chalcopyrite and pyrite (Brand & Horsh, 2006). The gangue minerals (Bramdeo et al., 2008) were composed primarily of quartz (23,8%), Fe-oxides (23,0%) and FeMn-silicates (16,9%). Chalcopyrite is the copper-bearing mineral, galena is the lead-bearing mineral and sphalerite is the zinc-bearing mineral of the BMM Deeps ore (Brand & Horsh, 2006: 2). The silver found in the ore generally occurs as a substitution element in the crystal lattice of galena (argentiferous galena) and chalcopyrite, and would occur as Pb-Sb-Ag-Cu-Fe-S or Ag-Cu-Fe-S respectively (Rozendaal & Stalder, 2007).

In the Copper flotation circuit chalcopyrite is concentrated from around 1% to 78%. The flotation tailings of the Copper flotation circuit is thickened to increase the density of the stream fed to the Lead flotation circuit. In the Lead flotation circuit, galena is concentrated from approximately 4% to over 80% galena. The Lead flotation circuit's tailings is fed directly to the Zinc flotation circuit where sphalerite is concentrated from approximately 5% to 73%. This is based on the 2013 financial year metallurgical performance of BMM.

Due to the complex nature of flotation, as well as the polymetallic composition of the Deeps orebody, each concentrate consists of varying amounts of contaminants. Some of these contaminants pose problems for further processing at smelters that treat BMM's concentrates. It is, therefore, of utmost importance to manage the relationship of concentrate grades and metal recovery.

2.3 Introduction to flotation

Flotation was initially patented in 1906 and is currently used widely across the world to extract valuable minerals from complex ores using the difference in surface properties between the desired and undesired material (Wills, 1988). The difference in hydrophobicity is an example of one of the properties, and is the principle flotation is based on.

When designing a Concentrator, the required flotation volume per stage and the circuit configuration is determined based on the feed to the Concentrator, in terms of parameters such as grade and throughput, as well as the target product specifications. The required flotation volume is related to the residence time required for successful mineral extraction or recovery. This is typically calculated as a ratio of the volume of the flotation cell to the volumetric flow rate of the tailings stream exiting the flotation cell (Nelson et al., 2009). The

required flotation volume could either be made up of a long bank of small cells or a short bank of larger cells. It has been found that, from a financial perspective, it is better to use a short bank of larger cells (Sutherland, 1981), since this would reduce capital requirement when starting up and would also require less maintenance time and operating cost. However, this may not always be the case for complex ores.

Following on from the number of cells in each bank, the way these banks are interconnected is also important. Historically, the point where recycle streams are reintroduced into the circuit would be such that, with mixing within the cell, there is not a significant impact on the grade of the material (Taggart, 1945 as cited by Sutherland, 1981). However, this only considered the grade of the material and not the natural inclination for the mineral to float, which should be considered when designing plant layouts.

The stages of the flotation process and the purpose of these stages, as described by Rao in 2003, are namely:

- Conditioning stage: During this stage, various reagents are added to the pulp in order to make the differences of the surface properties of the desired and undesired material more apparent. Each conditioner cell is equipped with an agitator to ensure homogenous mixing of the pulp and reagent fluid. At BMM, the Copper flotation circuit tailings stream is pumped to the Copper Tails Thickener where the slurry is thickened before passing through three (3) 20m^3 conditioning tanks. In the Conditioning stage, lime solution is added in the first conditioner, depressant in the second conditioner, and the collector and frother are added in the third conditioner. More detail about the reagents used at BMM will be given in subsequent sections.

- Roughing stage: The Roughing stage is the first stage of active flotation and provides sufficient retention time to achieve the target recovery. During this stage of flotation, a large portion of the unwanted tailings is eliminated. This, thereby, reduces the volume of slurry reporting to the next stage. At BMM, the conditioned slurry is pumped to the Rougher bank where it is floated in a series of three (3) OK40 tank cells.

- Scavenging stage: This stage is used to recover as much as possible of the desired, valuable material remaining in the pulp. The tailings stream exiting the Scavenging stage, i.e. the Scavenger tailings, is the final tailings of the flotation circuit. The Scavenger concentrate usually contains a high proportion of locked middlings, and typically undergoes regrinding depending on the mineral of interest. With reference to BMM, depending on

the ore type and Concentrator feed conditions such as feed grade, the Rougher tailings may be scavenged by a single OK30 tank cell. The Scavenger concentrate is recirculated to the 1st conditioning tank and the Scavenger tailings is pumped to the Zinc flotation circuit.

- Cleaning stage: The purpose of the Cleaning stage is to produce target concentrate grade. This is often accompanied by eliminating entrained material that was recovered in the Roughing stage, and by exploiting the differences in flotation rates of high grade particles and locked middlings. Dilution in the Cleaning stage promotes the rejection of entrained material. With reference to BMM, the combined Rougher concentrate (i.e. concentrates recovered from the 1st through 3rd Rougher flotation cells) is cleaned in one (1) OK30 tank cell and the Cleaner concentrate is pumped to the Lead Concentrate Thickener, before being filtered in a vertical filter press. The Cleaner tailings stream is recirculated to the Copper Tails Thickener.

Figure 2.1 shows the circuit configuration of the Lead flotation circuit, as described above.

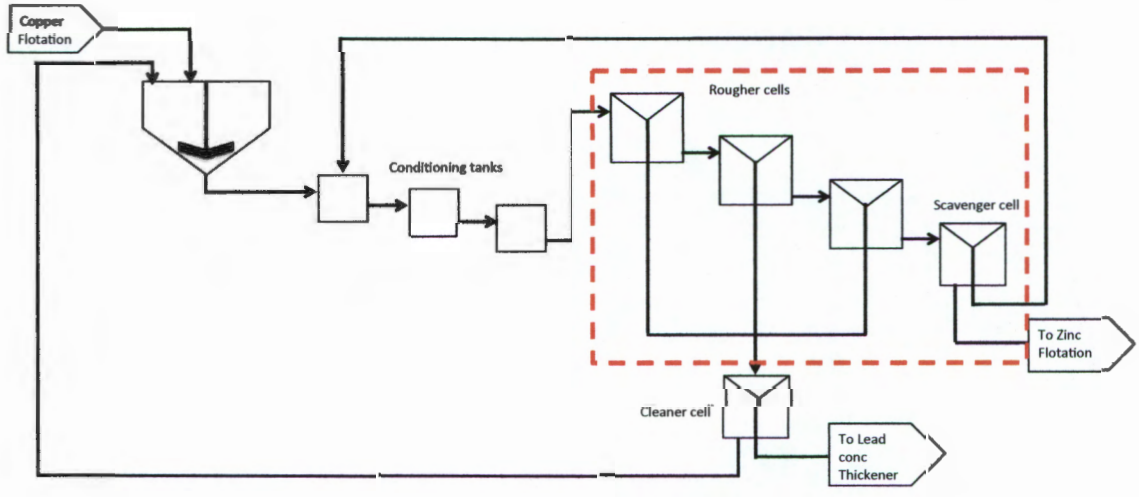

Figure 2.1: Circuit configuration of the Lead flotation circuit at BMM

The scope of the study was limited to the Roughing and Scavenging stages as indicated by the red box in Figure 2.1.

It is the belief of some researchers, such as Sutherland (1981), that although the arrangement of the flotation circuit has an effect on metallurgical performance, there is greater sensitivity to flotation conditions and selectivity in the flotation bank. These parameters are a direct result of the chemical conditions within the flotation cell. However, it is the author's view that the synergy between all aspects of flotation, including the equipment, the mineral

characteristics and the chemical conditions of the flotation circuit, results in the overall metallurgical performance.

2.4 Sub-processes of flotation

As described by Vera and co-workers (1998), in the view of a hydrophobic mineral, the overall flotation process is made up of four (4) sequential sub-processes. Therefore, the effectiveness of the overall process is a direct result of the effectiveness of each of these sub-processes. Looking at the sub-processes on a macro-level, they are described as follows:

1. Collision of particle and bubble
2. Attachment of particle to bubble
3. Transport of the loaded bubbles
4. Recovery of concentrate

To better understand how these sub-processes could be affected, the following sections describe the above-mentioned sub-processes in more detail.

2.4.1 Exposing the mineral surfaces

Mined ore is made up of a mixture of heterogeneous solidified phases, which are mainly crystalline. Crystalline phases represent various minerals and non-crystalline phases are made up of material such as coal, glass and resin. In the case of crystalline phases, the mined ore is crushed and ground with the objective to free the minerals from gangue and reduce the size of solids within the size range required for the separation technique that will be used. This action of freeing the minerals is referred to as the liberation of minerals (Leja, 1982). A liberated mineral surface is required, for example, for reagents to adsorb onto.

The BMM Concentrator uses a rod mill and ball mill operated in open and closed circuit configuration respectively, in order to reach a target grind of 65% passing 75μm in the flotation circuit feed, which is fed to the Copper flotation circuit.

With the use of a rod mill as the primary mill, the particle size distribution (PSD) is kept fairly narrow such that over-grinding does not occur in the secondary mill, i.e. the ball mill (Crowson, 2006). Due to galena being a fairly soft mineral, over-grinding and slimes generation can easily occur (Bowen, 1962; Shanthaveerappa et al., 1995). In the past, the target grind for BMM was a lot finer, at approximately 74% passing 75μm. However, due to the polymetallic nature of the ore, it posed significant problems regarding metal loss of galena entrained into the copper concentrate. This resulted in poor quality copper concentrate and

due to the high content of lead metal in the copper concentrate, it could not be sold (Nel, personal communication 2008).

The mineralogical study conducted by Brand and Horsh in 2006 showed that a grind of 65% passing 75μm was sufficient to liberate 95% of the sulphide particles. The galena minerals exhibited the highest degree of liberation and the galena grains were typically smaller in size compared to the other mineral grains. This is, therefore, the target grind for the Comminution circuit.

2.4.2 Preparing the exposed surfaces for flotation

As mentioned in Section 2.3, the difference in hydrophobicity, or wettability, is the principle on which flotation is based. As mentioned by Kawatra (2011), particles can be described as those that are easily wettable by water, i.e. hydrophillic, and those that are water-repellent, i.e. hydrophobic. In the case of a slurry mixture of hydrophobic and hydrophillic particles coming into contact with bubbles distributed into the slurry, the hydrophobic particles will tend to attach to the air bubbles and travel to the surface. Since not all minerals are naturally hydrophobic, this section describes what it entails to render a particle hydrophobic.

Kawatra (2011) continues to say that there are various degrees of wettability and in order to achieve selectivity in the flotation process, it is imperative to ensure the surfaces of the valuable mineral particles are more hydrophobic than the undesired gangue minerals.

When it is required to increase the hydrophobicity of a mineral, chemicals known as collectors are used. Collectors adsorb onto the mineral surface and, in so doing, reduce the stability of the layer separating the mineral surface from the air bubble. The reduction in stability is to such an extent that the particle is able to attach to the bubble on contact (Wills, 1988).

Alternatively, when it is required to reduce the hydrophobicity of the mineral, to render it hydrophillic and thereby prevent the minerals from floating, chemicals referred to as depressants are used (Wills, 1988). Some more detail pertaining to depressants and collectors, with reference to the BMM operation, is given in Sections 2.4.2.1 and 2.4.2.2.

2.4.2.1 *Reducing gangue hydrophobicity*

The sulphide minerals present in the Deeps orebody are naturally floating. Therefore, due to the sequential flotation process used at the BMM Concentrator, it is imperative that the undesired sulphide mineral(s) of that particular flotation circuit are depressed to prevent recovery to the incorrect concentrate, i.e. galena and sphalerite are depressed in the Copper flotation circuit and sphalerite is depressed in the Lead flotation circuit. Depression is,

therefore, the first step in the Conditioning stage in the Copper and Lead flotation circuits at BMM.

Since the Zinc flotation circuit follows on from the Lead flotation circuit, ideally all the sphalerite has to be depressed in the Lead flotation circuit to minimise the recovery of payable zinc metal to the lead concentrate. To do this, cyanides are widely used to depress sphalerite in copper-lead-zinc ores. The depression of sphalerite is achieved by the simultaneous addition of sodium cyanide (NaCN) and zinc sulphate ($ZnSO_4$) solutions. Zinc cyanide is formed when adding the combination of the two reagents and once formed precipitates on the sphalerite mineral preventing collector adsorption and rendering it hydrophillic (Wills, 1988).

If NaCN is added to an acidic solution hydrogen cyanide (HCN) gas would be formed and is toxic. Due to the use of NaCN at BMM, the pH of the Lead circuit feed is monitored by means of an online pH meter, and the pH is controlled to be approximately 7.8 at all times by the addition of lime solution in the first conditioning stage. In the event that the pH drops below a desired level, the feed of NaCN and $ZnSO_4$ is stopped automatically due to interlock control.

2.4.2.2 *Enhancing valuable mineral hydrophobicity*

Once the undesired minerals are depressed, i.e. sphalerite minerals in the case of the Lead flotation circuit at BMM, a single collector or multiple collectors are added in the Conditioning stage. As described by Wills (1988), collectors can be classified as being either ionizing or non-ionizing. Ionizing collectors are widely used in flotation and are asymmetrical in structure and heteropolar, which means they are made up of a non-polar hydrocarbon group and a polar group. The polar group reacts with water while the non-polar hydrocarbon radical has water-repellent properties.

Sodium ethyl xanthate (S.E.X.) is an example of an ionising collector. It is a sulphydryl anionic collector typically used in sulphide flotation (Wills, 1988) and is used in the Lead flotation circuit at BMM to enhance the hydrophobicity of galena minerals. The structure of this compound is shown in Figure 2.2.

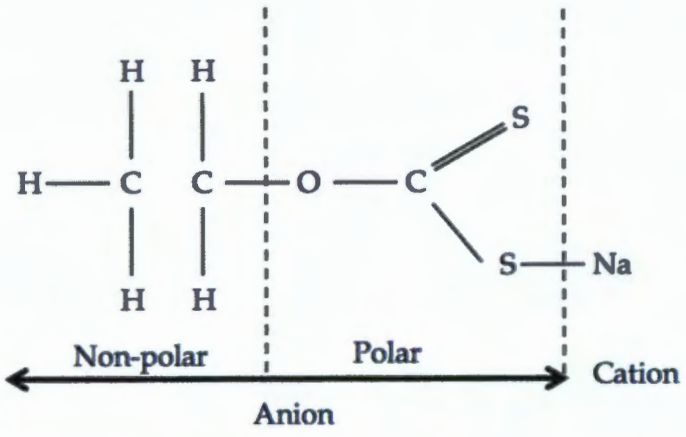

Figure 2.2: The molecular structure of S.E.X. (after Wills, 1988)

As can be seen in Figure 2.2, the S.E.X. collector consists of an anion as well as a sodium cation. In the Lead flotation circuit, the S.E.X. solution is added in the third conditioner and is also added on an adhoc basis at the feed box of the Scavenging flotation cell when required. At BMM the amount of collector added to the circuit is controlled by the operator by increasing or decreasing the volumetric rate within an allowed range, i.e. the high and low limits assigned to control loop. Although the operators adjust the volumetric rate of addition, this is based on the known concentration of the collector and the calculated desired grams per ton (g/t) to be added.

2.4.2.3 *The resulting floatability of minerals*

Once the mineral surface has been liberated and the hydrophobicity altered, i.e. the undesired minerals are rendered hydrophillic and the desired minerals are rendered hydrophobic or the degree of hydrophobicity is enhanced, the minerals would have varying degrees of ore floatability.

Ore floatability is the propensity of the particles in a stream to float (Runge et al., 2003b) and is also described as the reason for bubble-particle attachment (Collins et al., 2009). This means that minerals will either float or won't float, and for floating minerals this would be at various rates. In essence, the ore floatability affects where the mineral would be recovered along the flotation bank.

Runge and co-workers (2003a) cited work done by previous authors, such as Imaizumi and Inoue in 1963 and Runge and co-workers in 1997, which mentions that the floatability of a mineral in the ore cannot be described by a single number, but rather by a distribution and is dependent on properties such as the particle size, reagent coverage, degree of liberation, surface composition, particle shape and density. Provided these properties remain unchanged down a flotation bank and there is no oxidation, agglomeration or additional reagent

addition, it is assumed that the floatability of a particle in a discrete property class is a constant, inherent value.

2.4.3 Creating the correct hydrodynamic conditions for flotation

Although ore floatability is an important aspect of the flotation process, other factors also have an influence on the overall flotation performance. Examples of these are the circuit design (e.g. the number of cells, arrangement of cells, etc.), operating conditions of the cell (e.g. froth depth and air flow rate) and the chemical conditions of the pulp (e.g. pH, percent solids, etc.).

2.4.3.1 *Generating an optimal bubble size distribution*

There are three types of flotation cells commonly used in industry, namely the conventional, tank and column cell. Conventional and tanks cells are equipped with an agitator, made up of a rotor and stator, and one of the roles of the agitator is to generate and disperse bubbles within the cell. Figure 2.3 shows a schematic of a conventional cell to better describe how bubble formation takes place.

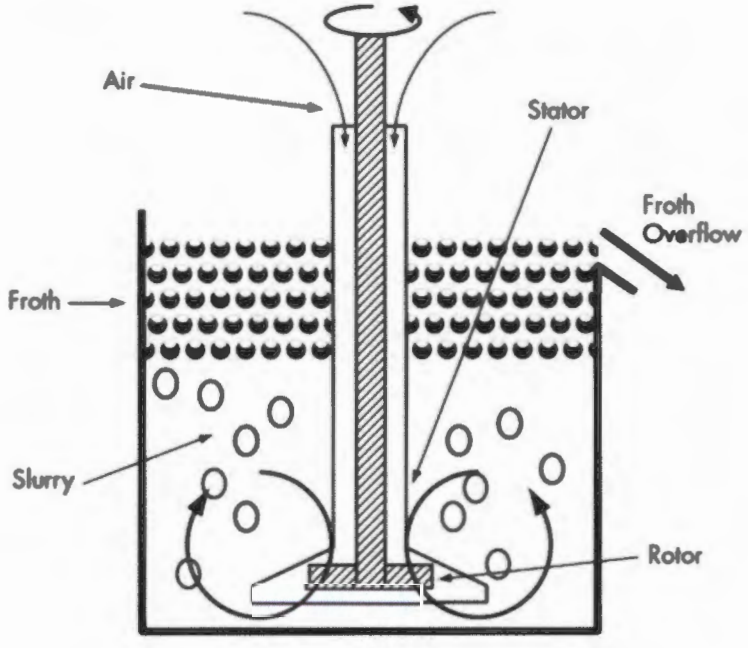

Figure 2.3: Schematic of a conventional cell (Kawatra, 2011)

While the agitator is rotating, air is either pulled into the cell through the action of the impeller (self-induced) or is introduced into the flotation cell down the shaft of the impeller by means of an air blower (forced air). Bubbles are generated by the shearing action of the rotating impeller (Ata, 2012) and are distributed into the pulp zone by means of the stator, which has holes in it. In a forced air cell the airflow or velocity entering the cell can be

controlled whereas in a self-aerated cell it cannot be controlled independently of the other cell operating conditions.

Kawatra also mentioned that in order to ensure a high probability of bubble-particle contact and attachment, it is imperative that the size of the bubbles is not too large relative to the size of the particles. In the event that the bubble size is too large, it could result in the particles being swept past the bubble without making contact. However, if the bubble is too small it may not have sufficient buoyancy to lift the particle to the surface.

2.4.3.2 *Preventing coalescence*

The bubble size observed in a flotation cell is a result of two (2) processes. The first process is the bubble generation by means of the flotation cell equipment, as mentioned above, while the second process is by means of coalescence (Nesset et al., 2006). Harris (1976), as cited by Nesset and co-workers (2006), mentioned that in most cases frother is added to retard coalescence, which is considered more important in controlling the bubble size as compared to the primary generation process, i.e. bubble generation. Frothers are also used to stabilise the bubbles such that they remain well dispersed in the slurry and will form a stable froth that will be recovered as the concentrate.

The efficiency of the frother has a direct result on the stability of the attachment of the mineral to the bubble surface. Due to interactions between the frother, mineral particle and reagents, a suitable frother for a particular ore can only be selected after reagent screening. At BMM, Senfroth 6005 is used in all flotation circuits. Senfroth is a poly propylene glycol produced by Senmin. It is dosed as a concentrated solution, i.e. as received by the manufacturer, and the dosage is controlled by the operators by means of volumetric flow rate in the same manner as the collector.

2.4.3.3 *Modelling gas dispersion*

Gas dispersion is defined as the collective term for bubble size distribution, gas holdup and superficial gas velocity (Gomez & Finch, 2007). As mentioned by Gorain and co-workers (1995a), although the importance of bubble size and the influence it has on flotation was recognised and researched as early as 1920 by researchers such as Nevett (1920) as well as Bennett and co-workers (1958), it was highlighted by Diaz-Penafiel and Dobby (1994) that these studies were conducted in ideal conditions due to restrictions in obtaining actual bubble size data from industrial flotation cells.

Between 1995 and 1997, Gorain and co-workers conducted a series of investigations to determine which of the gas dispersion parameters was best suited to describe gas dispersion in a flotation cell. All tests were conducted on an industrial flotation cell and looked at how

each of the above-mentioned parameters were affected by a change in impeller type, impeller speed and gas flow rate.

With respect to bubble size distribution (Gorain et al., 1995a), gas holdup (Gorain et al., 1995b) and superficial gas velocity (Gorain et al., 1996), the authors found that each of these could not individually completely describe gas dispersion. This was due to the fact that the results achieved and the trends observed when varying the operating parameters, were dependent on both the impeller type and speed (bubble size and gas holdup) or on the impeller type alone (superficial gas velocity).

The last study in this series of investigations was conducted by Gorain and co-workers in 1997 and looked at the effect bubble surface area flux had on the flotation rate constant. It was shown in the study that of the three parameters they had previously tested, the superficial gas velocity had the best correlation with the flotation rate constant and was directly proportional at lower airflow rates. However, the relationship at high airflow rates was not clear. This outcome supported what was seen by Laplante and co-workers in 1983, i.e. since the superficial gas velocity is a measure of the rate at which air passes through the flotation cell it does not distinguish whether the air is made up of small or large bubbles (cited by Gorain and co-workers, 1997)).

This gave rise to investigating the correlation between the bubble surface area flux (S_b) and the flotation rate constant of a flotation cell. Gorain and co-workers found that S_b was a good descriptor of the gas phase dispersion properties in a flotation cell since it had a linear relationship with the flotation rate constant regardless of the impeller type, impeller speed or gas flow rate.

S_b is calculated from the superficial gas velocity and the Sauter mean bubble diameter using Equation 2.1.

Equation 2.1: Bubble surface area flux

$$S_b = \frac{6J_g}{d_{32}}$$

where: S_b is the bubble surface area flux $(\frac{1}{sec})$

J_g is the superficial gas velocity $(\frac{m}{second})$

d_{32} is the Sauter mean bubble diameter (m)

In practice, when measuring the bubble diameter and superficial gas velocity, the units of measure are millimetres (mm) and centimetres per second ($\frac{cm}{second}$) respectively.

2.4.4 Attaching particle to bubble

As described by Nguyen and Schultze (2004), in order for a particle to become attached to a bubble, they have to be in close proximity to each other. When a particle and bubble collide, during the process of the bubble rising and the particle being mixed in the pulp zone of the flotation cell, the liquid film between the particle and bubble thins and ruptures. Upon rupture, a nucleic hole is formed resulting in a three-phase contact between particle, bubble and liquid (water). The attachment of the particle to bubble would be weak, or ineffective, and effective attachment is only achieved with additional drainage of the liquid film and, in effect, the expansion of the three-phase contact line. The attachment process is, therefore, defined as the sequence of three (3) steps, namely the drainage of the film, rupture of the film and the expansion of the three-phase contact line. This is shown mathematically in Equation 2.2 (Albijanic et al., 2010).

Equation 2.2: Bubble-particle attachment time

$$t_{at} = t_i + t_r + t_{tpc}$$

where: t_{at} is the bubble-particle attachment time (e.g. microseconds)

t_i is the induction time, i.e. time for liquid film to thin to a critical film thickness (e.g. microseconds)

t_r is the time required for the film to rupture and form the three-phase contact nucleic hole (e.g. microseconds)

t_{tpc} is the time required for the three-phase contact line expansion (e.g. microseconds)

The attachment time can be used to give insight into the hydrophobicity of minerals, with and without the use of reagents, since a shorter attachment time indicates to a highly hydrophobic mineral particle and long attachment time indicates a weakly hydrophobic mineral particle. Additionally, the components used to calculate the attachment time of mineral particles are strongly affected by the physical properties of the mineral particles and bubbles, as well as the solution chemistry of the flotation system (Albijanic et al., 2010).

It is the belief of some researchers, including Stechemesser and Nguyen (1999), Albijanic and co-workers (2010) as well as Subasinghe and Albijanic (2014), that the attachment sub-process is the critical stage that defines the efficiency of the overall flotation process.

Although methods are available to establish and model bubble-particle attachment, it would require specialised equipment, such as induction sensors, and was therefore not within the scope of this study.

2.4.5 Transporting loaded bubbles and recovery of concentrate

After bubble-particle attachment occurs, for a mineral particle to be recovered into the concentrate, the loaded bubble has to travel from the pulp zone into the froth zone and thereafter into the concentrate launder. This could be viewed as selective transportation of particles from the pulp to the froth zone. As previously mentioned, frothers are added in the flotation system to stabilise the froth, and thereby play a role in the recovery of particles from the pulp to the froth zone. As previously mentioned in Section 2.4.3.1, reagent screening is required to ensure a suitable frother is used for a particular ore. Good frothers produce a froth that is just stable enough to allow for the transfer of the desired mineral to the collecting launder of the cell (Wills, 1988).

Although smaller bubbles have a greater surface area for mineral attachment, they also have a greater surface area to carry more water into the froth as a film between bubbles. Typically undesired, hydrophillic minerals are transported to the froth zone within this film layer by entrainment. The transportation of entrained minerals and gangue could be viewed as an unselective transport mechanism. Similarly, very fine desired mineral particles are entrained into the froth phase by this same mechanism. Water recovery is, therefore, an important variable in flotation since this could have a detrimental impact on your concentrate quality (Kawatra, 2011).

2.4.5.1 *Froth recovery*

As described by Kawatra (2011), although mineral particles could attach to the bubbles within the pulp zone, the hydrophobic particles could detach prematurely during the process of transportation from the pulp to the froth zone. A study conducted by Johansson and Pugh in 1992 showed that the degree of hydrophobicity of particles influence the froth stability whereby highly hydrophobic particles destabilise the froth and moderately hydrophobic particles have a stabilising effect on the froth (cited by Ata and co-workers (2003)), . When the froth is not stable enough it results in the hydrophobic, desired minerals to detach and drop back into the pulp. As mentioned by Vera and co-workers (1999), although researchers recognised the significant role the froth zone had in determining the flotation process and

performance, such as the work conducted by Feteris and co-workers in 1987, for a long time the flotation process was modelled as a pulp-based system.

As a result of this, in 1999 Vera and co-workers set out to investigate the froth zone by means of a single parameter, the froth recovery. Froth recovery is defined as the efficiency of the transfer process of attached particles recovered by true flotation from the collection zone of the cell to the froth zone (Vera et al., 1999). It is the understanding of the author that froth recovery is a parameter that is related to the sub-process of recovery of concentrate, but more so related to the recovery of solids into the concentrate by true flotation, and as mentioned by Vera and co-workers (1999) it is independent of mixing regimes and lumps together all possible mechanisms taking place in the froth zone. The two assumptions made for the study conducted by Vera and co-workers (1999) were that transport of particles from the pulp to the pulp-froth interface was only a result of the pulp zone, and transport of particles from the froth to the launder was only a result of the froth zone.

Vera and co-workers also show in the outcomes of the study that factors that influence the sub-processes of bubble formation, bubble-particle attachment as well as recovery of concentrate, as described in earlier sections, also have an effect on the froth recovery. These factors are the airflow rate, frother concentration and dosage, froth depth, impeller speed as well as impeller design.

While the impeller design remains largely unchanged during operation of the flotation cell, the froth recovery could be optimised by means of improving the other variables listed above. Some examples of improvements that may be incorporated are froth crowders, radial launders, or changing the frother used, i.e. type and/or concentration.

2.4.5.2 *Modelling froth recovery*

Vera and co-workers (1999) showed in the study that the froth recovery could be determined mathematical based on experimental data. The experimental procedure entailed laboratory-scale flotation tests conducted in a high S_b flotation cell, developed by the Julius Kruttschnitt Mineral Research Centre (JKMRC), operated continuously. This specialised flotation cell produced S_b values, which were comparative with those, achieved in industrial or plant-scale flotation cells. The key parameter tested in this study was the effect of varying froth depth and it was determined that the froth recovery could be modelled by the following equation, assuming a perfectly mixed system and first order rate process.

Equation 2.3: Froth recovery as a function of rate constants

$$R_f = \frac{k}{k_c} = 1 - \frac{FD}{(FD)_{k=0}}$$

where: R_f is the fractional froth recovery (%)

k is the flotation rate constant ($\frac{1}{min}$)

k_c is the collection zone rate constant ($\frac{1}{min}$)

FD is the froth depth ($e.g.\ cm$)

$(FD)_{k=0}$ is the froth depth when the flotation rate constant is zero ($e.g.\ cm$)

As cited by Alexander and co-workers (2003), Burgess (1997) as well as Alexander and co-workers (2000) validated the assumption that a first order rate process is observed in a large flotation cell and, hence, Equation 2.3 can be applied to model the froth recovery.

Based on the outcome of the study conducted by Vera and co-workers in 1999, it is important to note that the froth recovery parameter is associated with each individual flotation cell and a global froth recovery value cannot be applied for an entire flotation bank or circuit. This is due to the change in mineralisation of the froth, particle size, the operating conditions of the cell in terms of aeration rate, froth depth and impeller speed, as well as the change in hydrophobicity of minerals present at the head compared to the end of the flotation bank (Savassi et al., 1998; Vera et al., 1999; Pugh, 2005).

Other researchers, such as Alexander and co-workers (2003), have also proposed the use of experimental techniques to determine the froth recovery of industrial, plant-scale flotation cells. The proposed technique was a combination of the work conducted by Savassi and co-workers (1997) and Vera and co-workers (1999). Although Alexander and co-workers mention that the primary objective of the proposed methodology was to be "simple, inexpensive and non-intrusive", it requires significant sampling and assay analysis which could result in it being costly and time-consuming when the froth recovery of more than one cell has to be determined at various operating conditions.

Therefore, the froth recovery of flotation cells can be modelled experimentally using the Vera and co-workers (1999) and Alexander (2003) methods. However, in order to do so it requires significant testwork and/or specialised equipment. For the modelling of froth recovery of both methods discussed above, it would entail significant operational changes, i.e. varying the froth depth, and for each operational change a circuit survey around the flotation cells

would have to be conducted. This would be time-consuming, expensive and disruptive to the operation.

A simple approach is to treat froth recovery as a model fit parameter that is calculated during the model calibration process, like the component mass fraction or floatability. The model fitted froth recovery would, therefore, not be correlated explicitly to the operating conditions of the flotation cell and cannot be used to optimise the flotation circuit in a quantitative manner. However, the froth recovery per cell and mineral could still be compared qualitatively in order to guide any optimisation efforts.

2.4.5.3 *Entrainment*

As described above, entrainment is the flotation mechanism where water and suspended solids, in the pulp zone, enter the froth between the rising loaded bubbles. In the study conducted by Singh (2013), the author cited work conducted by Engelbrecht and Woodburn (1975) that described entrained particles as being typically small in size with a low density and are, hence, recovered in the upward movement of the rising bubbles. This is as a result of the net upward flux of the water. Particles that are entrained are, therefore, not attached to the bubble and can be made up of desired and/or undesired minerals (Wang et al., 2015).

2.4.5.4 *Modelling entrainment*

As mentioned in a review by Wang and co-workers (2015), various methods to quantify entrainment have been developed including that of Trahar in 1981, Warren in 1985 and Ross in 1989 who used batch flotation tests as the experimental method. The objective of the batch flotation tests conducted was to distinguish how much of the total metal recovered was recovered by true flotation and how much was due to entrainment.

Wang and co-workers (2015) explains that Trahar (1981) assumed that when conducting a batch flotation test using frother and collector, this represented the recovery of true flotation, and a test conducted using only frother represented the recovery by entrainment. This method was found to be insufficient in quantifying entrainment based on three (3) factors. The first being that true flotation could occur without the presence of collector, the second being that fine particles could be slightly hydrophobic and be recovered by true flotation and the third being that some frothers act as collectors. Therefore, using the method as set out by Trahar, the entrainment of solids could be over-estimated.

Warren (1985), as described by Wang and co-workers (2015), conducted the batch flotation tests by varying the water recovery under the same chemical conditions. The water recovery was varied by changing the froth height, or froth depth, and the froth removal rate. Figure 2.4 is a graphical representation of the batch flotation test results obtained using the Warren

(1985) method for cassiterite ore from which recovery by true flotation and entrainment were calculated.

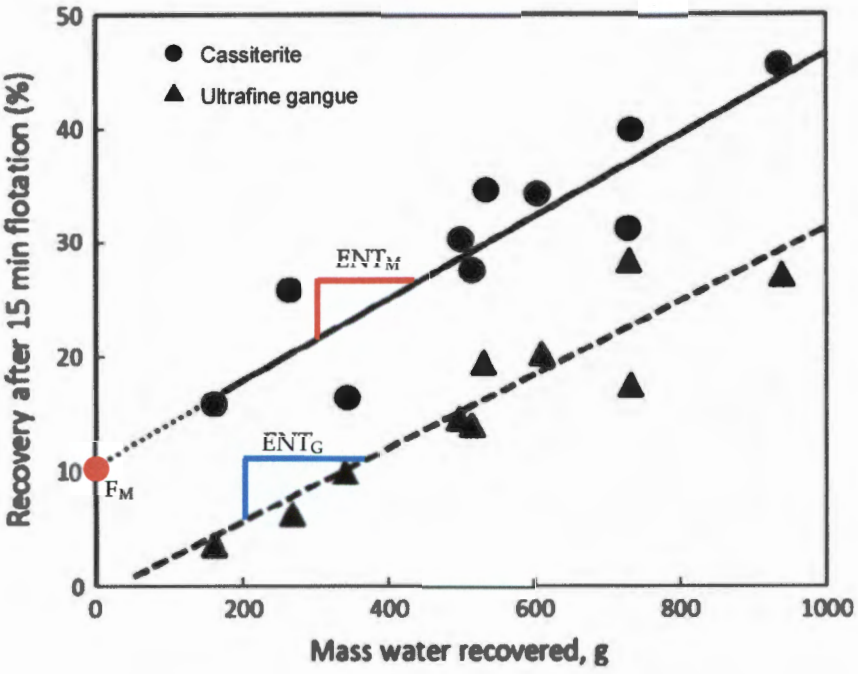

Figure 2.4: Determination of true flotation and entrainment of ultrafine cassiterite and ultrafine gangue as a function of water recovered (Warren, 1985)

From Figure 2.4 the trendline of the ultrafine cassiterite recovered was extrapolated to determine the intercept (F_M, indicated with the red circle) of this trendline with the mineral recovery axis, i.e. the y-axis, and F_M indicated the true flotation of cassiterite. The slope of the two trendlines, i.e. ENT_M and ENT_G, indicated the degree of entrainment of cassiterite and gangue respectively, and was determined by using two data points, e.g. mineral recovery and mass of water recovered after five (5) minutes flotation time and 15 minutes flotation time.

Warren (1985) then calculated the recovery by true flotation and that of entrainment based on the data inputs determined from the graphs, as described above, by using the Equation 2.4 and 2.5.

Equation 2.4: Recovery by true flotation (Warren, 1985)

$$R_M = F_M + ENT_M W_{Water}$$

where: R_M is the recovery of the valuable mineral at a specific flotation (%)

F_M is the indication of true flotation, found by extrapolating the trendline on the y-axis, i.e. mineral recovery axis

ENT_M is the degree of entrainment of the valuable mineral cassiterite

W_{Water} is the mass recovery of water to the concentrate at a specific flotation time (%)

Equation 2.5: Recovery by entrainment (Warren, 1985)

$$R_G = ENT_G W_{Water}$$

where: R_G is the recovery of the gangue at a specific flotation time (%)

ENT_G is the degree of entrainment of gangue

W_{Water} is the mass recovery of water to the concentrate at a specific flotation time (%)

As mentioned by Wang and co-workers (2015), besides the fact that the method outlined by Warren was time-consuming since numerous tests were conducted to establish both curves shown in Figure 2.4, it was also found that an accurate recovery by entrainment could not be achieved since the degree of entrainment varies with a change in froth height. Therefore, this method cannot be used to calculate the recovery by entrainment in the laboratory-scale system, i.e. batch flotation cell, and be applied to the plant-scale operation.

Similarly to Trahar (1981) and Warren (1985), Ross (1989) developed the approach that to quantify the recovery by entrainment, two transfer factors were defined. The first, X(t), was defined to describe the entrainment process while the second factor, Y(t), was defined to describe the total (true and entrained) recovery. Although this method is easy and simple, it cannot necessarily be used successfully on high grade samples, such as concentrates, since even at the end of the batch flotation test, composites of valuable minerals and gangue could be recovered which would not be representative of entrainment.

Wang and co-workers (2015) mentioned that beyond the experimental methods proposed by Trahar (1981), Warren (1985) and Ross (1989), many other modelling techniques have been developed and could be sub-divided into two categories, i.e. models that predict the entrainment flow directly and those that incorporate other parameters to thereby determine the entrainment flow.

Furthermore, as mentioned by Wang and co-workers (2015), the methods that were historically developed were based on specific types of flotation cells and cannot easily be applied to a different cell design since this has an effect on entrainment. Since many factors influence entrainment, for example particle size, the methods found in literature typically only focussed on a selected parameter. Therefore, when modelling entrainment in flotation cells, a general model should be used and it should be based on the most important variable.

As mentioned above, the method by Warren (1985) could not predict an accurate recovery by entrainment since the degree of entrainment varies with froth height as well as particle size. Savassi and co-workers (1998) mentioned that although there are six (6) parameters identified in literature that affect entrainment, the most useful is the partition curve between the degree of entrainment and particle size which encompasses the effect particle size has on the degree of entrainment. This is an extension of the Warren (1985) method and gives a much better estimation on recovery by entrainment.

However, when information regarding particle size is not available and the Savassi and co-workers (1998) method cannot be used, the simplest form of the equation can be used as shown in Equation 2.5, i.e. Warren (1985) method.

2.4.5.5 *Modelling water recovery*

For all mathematical descriptions of the degree of entrainment, the actual recovery by entrainment is strongly dependent on the water recovery for which many detailed models have been developed. These include parameters such as froth residence time, drainage and first order kinetics for water recovery, as highlighted by Zheng and co-workers (2006). However, to obtain these additional parameters could be time-consuming and costly, and was therefore not the preferred approach for this study.

As cited by Zheng and co-workers (2006), a simple method developed by Alford (1990) is currently used in the JKSimFloat software package and is shown in Equation 2.6.

Equation 2.6: Water recovery

$$Q_W = aF_S{}^b$$

where: Q_W is the concentrate water flow rate $\left(e.g.\ \frac{m^3}{hour}\right)$

F_S is the concentrate solids flow rate $\left(e.g.\ \frac{m^3}{hour}\right)$

a and b are dimensionless numbers, and are determined by fitting experimental data to Equation 2.6

As mentioned by Zheng and co-workers, the usefulness or applicability of this model depends on whether the a and b model parameters remain constant over the flotation circuit or bank and for different operating conditions. In the study conducted by Zheng and co-workers, they found that the a and b model fitted parameters were different at low and high aeration rates. In a plant-scale operation this could be validated for the system by conducting a circuit survey at low and high aeration rates and comparing the a and b model fitted parameters for each scenario.

2.5 Modelling the flotation process

2.5.1 Flotation as a first order rate process

As highlighted by Herbst and Flintoff (2012), since as far back as 1935 it has been shown that flotation follows a first order process and can be expressed by Equation 2.7.

Equation 2.7: First order rate process based on mineral concentration

$$\int -\frac{dC}{dt} = kC_j$$

When assuming a perfectly mixed environment, which represents the plant-scale flotation cell, the recovery of species j can be calculated using the flotation rate constant of species j, k_j, and the residence time of the flotation cell A, τ_A.

Equation 2.8: Recovery for plant-scale flotation cells

$$R = \frac{k_j \tau_A}{1 + k_j \tau_A}$$

Alternatively, as cited by Collins and co-workers (2009: 199), when considering a plug flow environment, which represents the batch-scale flotation cell, the recovery of species j can be calculated by the following equation which incorporates the batch-scale flotation rate constant of species j, $k_{j,batch}$, and the cumulative flotation time of the batch test, τ_{batch}.

Equation 2.9: Recovery for batch flotation cells

$$R_{j,Batch} = \left(1 - e^{-k_{j,Batch}\tau_{Batch}}\right)$$

2.5.2 Determining the total mineral recovery

As cited by Welsby (2010), by using the equation developed by Savassi and co-workers (1998) to incorporate the entrainment mechanism, the overall mineral recovery can be calculated as follows by Equation 2.10. Although Savassi and co-workers (1998) based this on sized

particles, the same is true for unsized particles since there is mass conservation in a flotation system. The expanded equation for species j is shown in Equation 2.10.

Equation 2.10: Total mineral recovery by true flotation and entrainment (Savassi, 1998)

$$R_{j,Total} = \frac{k_j \tau_A (1 - R_{W,A}) + ENT_j R_{W,A}}{(1 + k_j \tau_A)(1 - R_{W,A}) + ENT_j R_{W,A}}$$

where: $R_{j,Total}$ is the overall mineral recovery for species j by true flotation and entrainment (fraction)

k_j is the rate constant for species j ($\frac{1}{min}$)

τ_A is the residence time of flotation cell A (minutes)

$R_{W,A}$ is the water recovery to the concentrate of flotation cell A (fraction)

ENT_j is the degree of entrainment for species j (dimensionless)

For this study, it was assumed that the contribution of entrainment to the recovery of the sulphide minerals, i.e. chalcopyrite, galena and sphalerite, was negligible, i.e. $ENT_j = 0$ in Equation 2.10 for these sulphide minerals. Furthermore, it was assumed that the non-sulphide gangue (the remainder) was only recovered by entrainment, i.e. $k_j = 0$ for the remainder in Equation 2.10.

2.5.3 Defining the overall rate constant

Various mathematical models can be found in literature that makes use of the flotation rate constant to predict mineral recovery from experimental data. As cited by Brezani (2010), these models either make use of a single flotation rate constant, including the Klimpel model (Klimpel 1980), or two (2) flotation rate constants each describing floatability classes, such as the Kelsall model (Kelsall 1961) and modified Kelsall model (Jowett 1974). As mentioned by Ramlall and Loveday (2015), these mathematical models are based on the assumption that mineral recovery is by true flotation only, i.e. the mineral is transported to the froth by bubble-particle attachment.

As previously mentioned, batch-scale information cannot be extrapolated to confidently predict plant-scale performance. Therefore, when a prediction of plant-scale performance is required, mathematical models that incorporate the plant-scale flotation rate constant is imperative.

As mentioned in Section 2.4.5, froth recovery is related to mineral recovery by true flotation since it is defined as the efficiency of the transfer process of attached particles from the collection zone of the cell to the froth zone (Vera et al., 1999). Additionally, based on testwork conducted on a variety of plant-scale flotation cells, operated at various aeration rates, froth depths, impeller types and speeds, it was demonstrated that the flotation rate constant can be characterised by three parameters. These characteristics are the particle floatability, the bubble surface area flux and the froth recovery of the cell (Gorain et al., 1998). This relationship is shown in Equation 2.11.

Equation 2.11: Flotation rate constant as a function of P, S_b and R_f

$$k = PS_bR_f$$

where: k is the flotation rate constant ($\frac{1}{min}$)

P is the particle floatability (dimensionless)

S_b is the bubble surface area flux ($\frac{1}{min}$)

R_f is the fractional froth recovery of the cell

As can be seen in Equation 2.11, the rate of flotation is determined by characteristics of both the particle (P) and the sub-processes of flotation (S_b and R_f). Particle floatability has been shown to be described by a distribution based on size, mineralogy, liberation and reagent coverage and remains constant for a particular component or species provided that there is no oxidation, agglomeration or reagent addition down the bank (Runge et al., 2003b).

All species, valuable and gangue, can be sub-divided into sub-classes. There are a number of sub-classes and combinations of sub-classes that can be used to categorise minerals, for example, particle size, degree of liberation and mineral floatability. However, the sub-class categorisation is dependent on the information available and the parameter of importance for the study being done. An example of an approach applied where a combination of sub-classes was used is the study conducted by Welsby and co-workers (2010) where the galena minerals, which was the mineral of interest, was categorised into floatability per discrete size-by-liberation sub-classes. Another approach which has been used was that of Runge and co-workers (1997) where the unsized galena minerals were categorised by mineral floatability only.

In this study, the minerals and the remainder (gangue) were classified into two floating classes, i.e. fast and slow floating, as well as a non-floating class. Therefore, it was assumed that for each species three (3) sub-classes exist. This assumption is supported by work done

by Welsby and co-workers (2010) and Runge and co-workers (1997), where it was shown that three (3) sub-classes were sufficient to describe galena minerals.

With this in mind, and by combining Equation 2.8 and Equation 2.11, the recovery of the sub-classes of a mineral by true flotation in a flotation cell can be calculated as per Equation 2.12.

Equation 2.12: Recovery by true flotation for plant-scale flotation cells as a function of P, S_b and R_f

$$R_{i,j} = \frac{P_{i,j} S_{b,A} R_{f,A} \tau_A}{1 + P_{i,j} S_{b,A} R_{f,A} \tau_A}$$

where: $R_{i,j}$ is the recovery for sub-class i of species j by true flotation (%)

$P_{i,j}$ is the particle floatability for sub-class i of species j (dimensionless)

$S_{b,A}$ is the bubble surface area flux of flotation cell A ($\frac{i}{min}$)

$R_{f,A}$ is the fractional froth recovery of the flotation cell A (%)

2.6 Linking of flotation units into circuits

Flotation simulation software packages, such as Cycad, MetSim, ModSim, HSC, UsimPac and JKSimFloat, incorporate various models to predict the sub-processes of flotation, linked into flowsheets for full circuit simulation. These software packages have been developed to assist metallurgists with the prediction of plant-scale performance. However, licences and training are required in order to use the software. BMM does not have access to any of the above-mentioned packages.

Another approach to modelling a flotation circuit is to do so using MS Excel and this can be achieved by using the Woodburn and Wallin (1984) matrix algebra. Woodburn and Wallin (1984) proposed a decoupled kinetic model to simulate the tailings flow in a flotation circuit (cited by Sweet (1999) and Mathe and co-workers (2000)). In order to predict the circuit flow, the methodology makes use of simultaneous equations to balance the mass of all species across the flotation circuit. This is achieved by using a matrix of enhancement factors and the connection matrix of the circuit under consideration.

The enhancement factor for a species is defined as the ratio of flow of the species in a concentrate stream, to that of the flow of the same species in the tailings stream from the flotation cell A. This is illustrated in Equation 2.13.

Equation 2.13: Enhancement factor

$$g_{jA} = \frac{C_{jA}}{T_{jA}}$$

where: g_{jA} is the enhancement factor of species j for the flotation cell A (dimensionless)

$C_{j,A}$ is the mass flow of the species j exiting flotation cell A in the concentrate stream $(e.g. \frac{g}{min} \text{ or } \frac{t}{hour})$

$T_{j,A}$ is the mass flow of the species j exiting flotation cell A in the tailings stream $(e.g. \frac{g}{min} \text{ or } \frac{t}{hour})$

The connection matrix is a matrix representation of the layout or connection between the units in the flotation circuit being investigated, and it incorporates the streams entering and leaving each flotation cell.

In the connection matrix the columns represent the streams produced by a flotation cell, and the rows represent the flotation cell each stream is entering. To represent the production of two (2) separate products from the flotation cell (A), the term $-(1 + g_A)$ is used in the diagonal cells. To represent a tailings stream from one flotation cell entering another flotation cell, the number 1 is used. To represent a concentrate stream from one flotation cell (A) entering another flotation cell, the term g_A is used. For all terms mentioned above, the subscript A refers to the flotation cell A from which the stream originates. Figure 2.5 shows a simplified flowsheet of the Lead flotation circuit that was considered in this study.

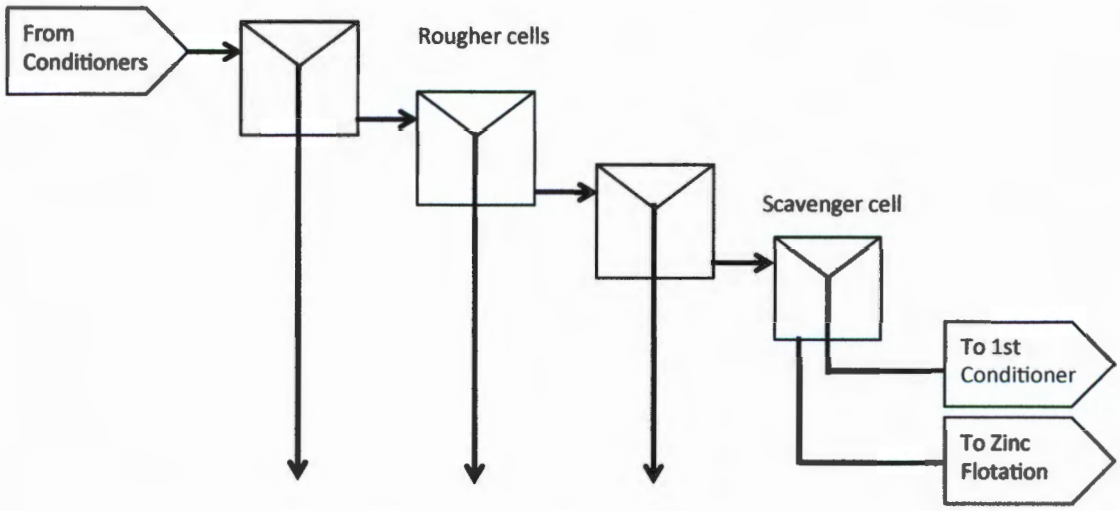

Figure 2.5: Simplified Lead flotation circuit flowsheet considered in this study

With reference to Figure 2.5, Table 2.1 is the connection matrix for the scope of this study. Since there are four (4) flotation cells in the Lead flotation circuit under investigation, it is a 4 x 4 matrix and deals with all streams entering and leaving each flotation cell. For ease of explanation, row and column numbers have been assigned to Table 2.1. As an example, the 1st Rougher flotation cell will be used and the information is represented in Column 1 of Table 2.1. This cell is only fed from the conditioning tanks and, therefore, no stream produced by any other flotation cell enters the 1st Rougher flotation cell directly. The diagonal is marked with $-(1 + g_{R1})$. The tailings stream from the 1st Rougher flotation cell then feeds the 2nd Rougher flotation cell, and this is represented by the 1 in Column 1, Row 2. The concentrate from the first Rougher goes to the Cleaner cell which is not within the boundary conditions of this study, and so the remainder of the cells in Column 1 are zeros.

The same procedure is applied to the 2nd and 3rd Rougher flotation cells as well as the Scavenger flotation cell. It must be noted that the Scavenger concentrate is considered to be an exit stream within the boundaries of this study. Therefore, no concentrates are recycled directly and no stand-alone g_A terms appear in the connection matrix.

Table 2.1: The connection matrix of the Lead flotation circuit

		Column Number			
		1	2	3	4
Row Number	Received by cell	Produced by cell			
		1st Ro	2nd Ro	3rd Ro	Scavenger
1	1st Ro	$-(1+g_{R1})$	0	0	0
2	2nd Ro	1	$-(1+g_{R2})$	0	0
3	3rd Ro	0	1	$-(1+g_{R3})$	0
4	Scavenger	0	0	1	$-(1+g_S)$

Assuming that first order kinetics holds true for the flotation circuit, and by manipulation of the recovery calculation, the enhancement factor, g_{ijA}, is calculated as per Equation 2.14.

Equation 2.14: Enhancement factor for true flotation as a function of k and τ

$$g_{ijA} = k_{ijA}\tau_A$$

where: g_{ijA} is the enhancement factor of sub-class i of species j in flotation cell A (dimensionless)

k_{ijA} is the rate constant of sub-class i of species j in flotation cell A ($\frac{1}{min}$)

τ_A is the residence time of flotation cell A (minutes)

When applying Equation 2.11, the enhancement factor can be calculated as follows in Equation 2.15.

Equation 2.15: Enhancement factor for true flotation as a function of P, S_b, R_f and τ

$$g_{ijA} = P_{ij} S_{b,A} R_{f,A} \tau_A$$

where: g_{ijA} is the enhancement factor of sub-class i of species j in flotation cell A (dimensionless)

P_{ij} is the floatability of sub-class i of species j (dimensionless)

$S_{b,A}$ is the bubble surface area flux of flotation cell A ($\frac{1}{min}$)

$R_{f,A}$ is the froth recovery of flotation cell A (fraction)

τ_A is the residence time of flotation cell A (minutes)

As mentioned in Section 2.5.2, it was assumed for the purposes of this study that only the remainder was recovered by entrainment. By manipulating Equation 2.5 and using Equation 2.13, which states that the enrichment of a species is the ratio of the mass flow of the species in the concentrate stream to the mass flow of the species in the tailings stream, the enrichment of the gangue can be calculated using Equation 2.16.

Equation 2.16: Enhancement factor for entrainment

$$g_{G,A} = \frac{ENT_G R_{w,A}}{1 - R_{w,A}}$$

where: $g_{G,A}$ is the enhancement factor of the remainder for the flotation cell A (dimensionless)

ENT_G is the degree of entrainment of the remainder (dimensionless)

R_w is the fractional water recovery

2.7 Using the Floatability Component Model approach

An interpretation of the work done by Runge and co-workers in 1997 is that when considering inherent mineral floatability, using plant-scale flotation data is insufficient due to the fact that the flotation cells within the bank would operate at different operating conditions.

In the investigation Runge and co-workers, therefore, incorporated batch flotation tests done on samples collected directly from the plant to determine the inherent floatability of various streams. The methodology used by Runge and co-workers assumed that at a relatively high gas rate, very shallow froth depth and strictly controlled operating conditions, any dropback of particles from the froth phase was prevented and thereby assumed 100% froth recovery in the batch flotation cell. This implied that the froth recovery achieved in the plant-scale flotation cell was relative to that achieved in the batch flotation test. The rate constant calculated for these batch flotation tests would, therefore, only be a function of the measured batch cell S_b and the mineral floatability, which was assumed to be the same as the floatability in the stream from which the sample was collected. They termed these "hot floats" as the batch flotation tests were done immediately after sample collection, while the sample still maintained all the characteristics as that of the circuit stream and was still literally warm from the energy provided by the mill and the flotation cells.

Therefore, the basis of the Floatability Component Model (FCM) is to use both circuit survey and laboratory-scale testwork data in order to derive the most accurate representation of the circuit by using both unit specific and stream specific parameters (Runge et al., 2003b). When developing a model using the FCM approach, it is assumed that the mineral floatability for the various sub-classes of the species is conserved in the flotation circuit provided that no floatability altering events take place within the circuit, e.g. oxidation, reagent addition, etc. By conducting the hot batch flotation tests on multiple streams, the additional information obtained from the tests assists in developing the constraints of the model in order to ensure a robust fit.

When considering the equation used to calculate recovery by true flotation in a batch process, the equation can be expanded with the substitution of the flotation rate constant in terms of the mineral floatability, bubble surface area flux and the fractional froth recovery. This could be further expanded based on the sub-classes of the species. For hot batch flotation tests, Equation 2.17 is simplified since the froth recovery from a hot batch flotation test is assumed to be 100%, as a result of the shallow froth used to conduct the tests.

Equation 2.17: Recovery by true flotation for batch flotation cells as a function of P, S_b and R_f

$$R_{j,Batch} = \left(1 - e^{-P_{i,j}S_{b,Batch}R_{f,Batch}\tau_{Batch}}\right) = \left(1 - e^{-P_{i,j}S_{b,Batch}\tau_{Batch}}\right)$$

where: $R_{i,j,Batch}$ is the batch recovery for sub-class i of species j by true flotation (%)

$P_{i,j}$ is the particle floatability of sub-class i of species j (dimensionless)

$S_{b,Batch}$ is the bubble surface area flux of the batch flotation cell ($\frac{1}{min}$)

τ_{Batch} is the discrete flotation time for the batch flotation test conducted (minutes)

When the FCM approach is combined with the Woodburn and Wallin (1984) matrix methodology, this allows a flotation circuit to be modelled using a single MS Excel spreadsheet, which could be easily adapted in future.

3 OBJECTIVES OF THE RESEARCH AND HYPOTHESES

This chapter discusses the objectives of the study as well as the hypotheses that were made.

3.1 Objectives of research and key questions

The primary objective of this study was to adapt the FCM as a simplified proof-of-concept model for the Lead flotation circuit of the BMM Concentrator based on plant- and laboratory-scale data. The model obtained, using the FCM approach in conjunction with the Woodburn and Wallin (1984) methodology, should give insight to the metallurgical team as to whether or not the Lead flotation circuit is performing optimally based on the data pertaining to the feed characteristics of the flotation circuit.

This methodology would also have to be easy to adapt to other flotation sections and have a relatively short turnaround time for results. The data used to develop the methodology would have to be obtained easily, inexpensively and by using non-disruptive techniques.

The main question addressed in this study is thus:

1. Can a simple, robust and user-friendly model of the Lead flotation circuit be developed for use on-site at BMM?

Aside from this question, the study explores the association of silver metal with galena minerals and seeks to determine whether the modelling approach could predict the response of silver metal as a result of the response observed for galena minerals.

Hence a secondary question addressed in this study, which is of major economic importance to the Concentrator, is the following:

2. Can the response of silver metal be predicted using the simple modelling approach?

3.2 Hypotheses

In addressing these questions, the following hypotheses were proposed:

1. It is hypothesised that the FCM approach can be used as the basis for the development of a simple model of the Lead flotation circuit at BMM that will still be able to give useful insights to the metallurgical team in terms of circuit optimisation. This hypothesis is based on the fact that an approach similar, but slightly more complex to that used in this study, has been used by Welsby and co-workers (2010) which incorporated a fully calculated

experimentally and analytically expensive approach, while a very simplistic approach has been used by Runge and co-workers (1997) to model the behaviour of a flotation circuit. Both of these investigations were conducted in a Lead flotation circuit.

2. It has been generally observed on Concentrators treating similar orebodies as that being treated at BMM that silver metal is generally associated with galena-rich ores and, therefore, it is reasonable to expect that the predicted response of silver metal using the model should be similar to the response of the galena minerals.

Based on these hypotheses and the key questions, the experimental procedure was developed.

4 EXPERIMENTAL PROCEDURE

The study comprised two phases, referred to as Phase One and Phase Two. The focus of Phase One was primarily the validation of the batch flotation procedure that would be used in the study during the circuit survey as well as the validation of conservation of floatability. Phase Two was focussed on gathering circuit data by means of a circuit survey such that the Lead flotation circuit could be mass balanced and modelled in order to identify possible circuit performance improvement areas. This section outlines the general safety and preparation aspects of tasks conducted at the BMM Concentrator as well as the methodology used in Phase One and Phase Two in order to obtain their respective results.

4.1 General safety

In the mining industry, safety is crucial to ensure sustainable production. At the BMM Concentrator the employees believe in and live by a safety motto, which is "If you cannot do it safely, do not do it". This implies that a task, however simple or complex, should not be done if there are significant hazards and risks that cannot be guarded against.

Due to the fact that the surroundings and conditions could change on a continuous basis, it is important to ensure that day-to-day tasks include a review of the risk assessment. This is achieved by a summarised version of a risk assessment, referred to as the hazard identification and risk assessment (HIRA) that typically takes approximately two (2) minutes to complete. Before any task can commence, employees complete a HIRA in the area where the task will take place.

Furthermore, the mine is governed by a set of rules that is referred to as Golden Rules. The Golden Rules outline the basic rules which every employee, contractor and visitor has to adhere to while on BMM's premises. Since the Golden Rules are applicable for the entire mine, the specific hazards and risks of the Concentrator are briefed to employees, contractors and visitors in the form of a site induction. The site induction highlights all additional hazards, risks and rules that are applicable at the Concentrator. These include the risk of lead-bearing dust inhalation and ingestion, the risks associated with the use of hazardous chemicals, the risks and procedures for working in a confined space as well as the dangers and precautions of working in areas where there is an accumulation of water.

With respect to this study, the importance of safety precautions were highlighted regarding the calibration of pH meters and the manner in which sampling was conducted. As highlighted in Section 2.4.2.1, the pH meters used in the laboratory and Concentrator were calibrated at regular intervals to ensure the pH reading given by the equipment was as accurate as possible. It was also important in this study to assess the sampling locations since

all samples had to be attained in a safe manner. This implied that the location of the sampling point had to be easily accessible and the probability of injury for the person collecting the sample had to be minimal. Examples of injures that could have resulted from sampling were muscular strain and falling from heights.

4.2 General preparation for tasks

Adequate planning for a circuit survey should take place in advance to understand the resources and equipment needed, including safety equipment. In order to ensure that no contamination of samples occurred during the circuit survey, all sampling equipment had to be thoroughly washed and dried before use. This ensured that all measurements, whether in terms of mass, volume or for assay purposes, were accurate and representative of the situation. In some instances, mass measurements were required by means of a scale. To ensure that the mass measurements were accurate, the scale, which was used, had to be compliant with calibration standards, i.e. calibrated annually by an independent and accredited company, and zeroed before measurements were taken.

4.3 Equipment used in this study

Various types of equipment were used for various purposes in this study. This section gives a brief description of the equipment and the purposes of the equipment with respect to this study.

4.3.1 Sample cutters

Sample cutters are used to ensure that a sub-sample is taken from a stream and the sub-sample is representative of the entire stream. Three types of sample cutters were used in this study, i.e. pelican sample cutter, dip sample cutter and ice cream containers. The sample cutter selection in this study was based on the conditions under which the sample had to be collected. The types of sample cutter used for specific streams are described later in this section. Figure 4.1 shows an example of the pelican sample cutters used in the study.

Figure 4.1: An example of the pelican sample cutters used in the circuit survey

As per sample cutter selection guidelines, the aperture of the sample cutter used should not be less than three (3) times than nominal top size of the stream being sampled, and should be at least 1cm for slurry sampling (Bartlett, 2002). The pelican sample cutters used in the circuit survey had an aperture/width of approximately 1cm that allowed the sample, with a top size of approximately 150 microns, to freely enter the sample cutter.

4.3.2 Sample buckets

Sample buckets used at BMM are plastic buckets that have lids and handles. The lids are to ensure that the samples are protected from being spilt and/or contaminated during transportation, and the handles are required such that it can be carried in a convenient manner. For this study, the volume of the sample buckets varied from five (5) to 20 litre buckets. The size of the bucket used was dependant on the size or volume of the sample that was collected.

4.3.3 Water bottles

Water bottles were used in various applications during the study and the standard volume of water bottles used was 500ml. Generally, the metallurgical team used them to rinse out settled solids from buckets or containers. During this study, the water bottles were used during sampling, filtration of bulk samples as well as during the batch flotation tests.

4.3.4 Volumetric cylinders

During certain tasks in this study, the addition of water to dry solids samples was required. Volumetric cylinders were used to measure the amount of water added. In order to standardise any possible error in measurement, the same volumetric cylinder was used for all instances where water addition had to be measured.

4.3.5 Sample splitting equipment

When large samples had to be reduced to smaller sub-samples, sample splitting equipment was used. This ensured that the sample was reduced but still maintained all the characteristics of the large bulk sample. In the Metallurgical Laboratory, this was achieved by means of a 10-way rotary splitter. The rotary splitter was equipped with a conical feed chute, a vibrating feeder, a turntable as well as 10 sample beakers. Ideally, the sample beakers should have contained identical sub-samples of the bulk sample, both in terms of the amount of sample and the characteristics. These characteristics include the particle size distribution, sample composition in terms of assay and the mineralogy. During scoping studies, the validity of this was verified.

4.3.6 Stopwatch

Stopwatches were essential equipment during this study since it was used as a measure of time during the batch flotation tests as well as during mass flow measurements.

4.3.7 pH meter

As mentioned previously in Section 2.4.2.1, sodium cyanide is used in conjunction with zinc sulphate in the Lead flotation circuit at BMM to depress sphalerite minerals. Sodium cyanide is a potentially dangerous chemical when added to solutions with an acidic nature. In this study pH control was of utmost importance, both from a safety and process point of view, and the pH was measured by means of pH meters in the Concentrator and the Metallurgical Laboratory.

In order to ensure that the instrumentation gave accurate readings, it was calibrated on a regular basis. This was done by means of buffer solutions supplied by the manufacturer of the pH meter. The buffer solutions cover a broad range of pH values, from very acidic to very alkaline.

4.3.8 Batch flotation cell and concentrate containers

Bench-scale batch flotation tests are a means of minimising the interaction of process parameters in flotation such that a single variable is altered and the results thereof can be

analysed, i.e. single parameter testing. The procedure for a batch flotation test is dependent on various parameters, one of which is the parameter to be tested for. Batch flotation cells are used to conduct these tests and the setup of the machine is a scaled down version of plant-scale equipment.

For the purposes of this study, a modified Leeds flotation cell was used. The modified cell allowed for varying and controlling the impeller speed, the airflow as well as the pulp level. While adjusting the airflow and agitation using the control speed dials, the level was controlled by the addition of water to the cell.

Figure 4.2: 3 L modified Leeds cell used for batch flotation tests

Depending on the analyses or results that were desired from a flotation test, the concentrates were either collected in a single container or in various individual containers. Collection into a single container would allow the overall recovery to be calculated, if this was of importance, while collection into various individual containers allowed for each individual concentrate per flotation time to be analysed. In other words, if the kinetic recovery profile needed to be calculated which represented a flotation bank, concentrate collection would have to be in individual containers. For the purposes of this study, individual concentrate containers were used since it was important to characterise the recovery profile for each stream that batch flotation tests were conducted on.

4.3.9 Filtration equipment

In order to obtain a dry solids sample, slurry samples are filtered using various types of filtration equipment. For the purposes of this study, large volume slurry samples were filtered using a laboratory-scale pressure filter while smaller batch flotation concentrate samples were filtered using filter paper placed in sieves. In the past at BMM, it was found that if a small slurry sample was filtered using the laboratory-scale pressure filter, either the filter would be damaged after prolonged use or the filter paper would tear and this would jeopardise the integrity of the sample since some of the sample mass was lost. The methodology of allowing the water to naturally drain from the concentrate sample, i.e. by inserting the filter paper in the sieves, has been standard practice for small slurry samples in the BMM Metallurgical Laboratory for at least the past 10 years.

4.3.10 Bench-top scales

One of the most crucial, yet simple, types of measurements that are taken by the metallurgical team in this study was mass measurement. In the Metallurgical Laboratory, mass measurements were done by means of bench-top scales, which were calibrated by external certified personnel on an annual basis. As with the volumetric cylinder, the same bench-top scale was used during this study such that any inherent bias was maintained for all measurements.

4.3.11 Ovens

After filtration, samples are typically not completely dry and in order to remove all moisture retained within the sample, it is placed in the oven for drying. The standard temperature used for the ovens in the Metallurgical Laboratory was 105°C since it was found that at this temperature the sulphur contained in the samples did not burn off (Mentoor, personal communication 2011). However, a recommendation was made that for all samples that required further testing, such as batch flotation tests, these samples were dried in ovens pre-set at 60°C. This was done to ensure that the surface of the solids did not potentially oxidise and negatively affect the results obtained from the batch flotation tests (O'Connor, personal communication 2011). All ovens used at BMM Concentrator were equipped with temperature control, and this allowed for the temperature to be adjusted when required.

4.3.12 Bubble sizer

The Anglo Platinum Bubble Sizer, manufactured by Stone Three in South Africa, is a portable device used to measure the bubble size distribution and the superficial gas velocity directly in the flotation cell. This was used to obtain certain information pertaining to the cell parameters

of the various flotation cells in this study. More detail of the bubble sizer is given in Section 4.4.2.3. Figure 4.3 shows an example of the Anglo Platinum Bubble Sizer.

Figure 4.3: An example of the Anglo Platinum Bubble Sizer (Naik and van Drunick, 2007)

4.4 Circuit survey procedure

The data collected from the circuit survey was reconciled such that a steady state mass balance could be achieved. This required assay samples to be collected and flow rates to be measured on key process streams. Furthermore, hot batch flotation samples were taken to assist with the model development. Lastly, equipment measurements were required to define the operating parameters for the model. The following sections describe how these various measurements were obtained.

4.4.1 Determination of sampling points

In order to model the Lead flotation circuit using the FCM approach, data from all major streams in the circuit were obtained and hot batch flotation tests were conducted on the feed stream to each flotation cell as well as the tailings of the circuit. Figure 4.3 shows the section of the Lead flotation circuit as per the scope of this study as well as all the sampling points used.

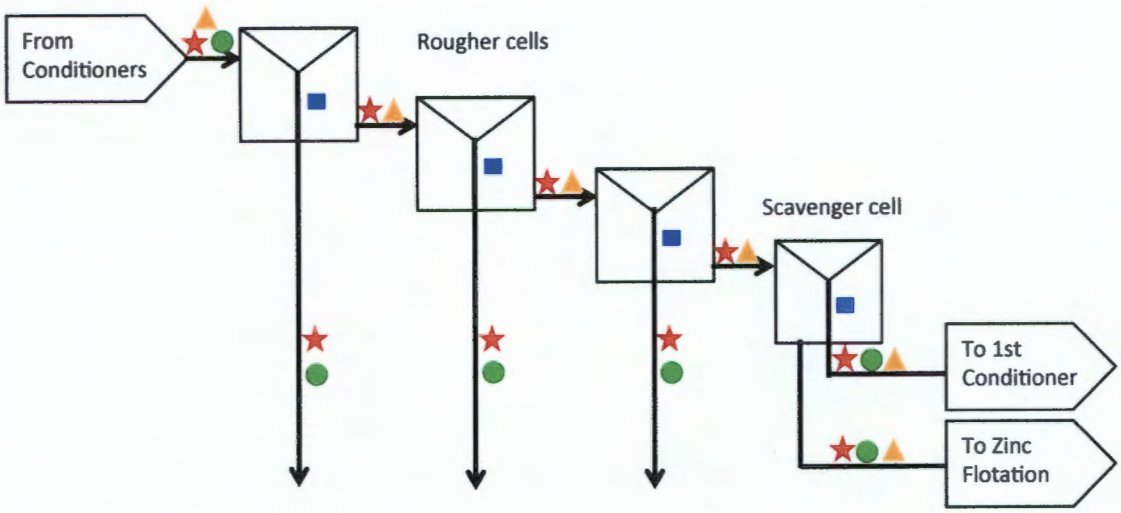

■ is a flotation cell sampling point for S_b

★ is an assay and percent solids sampling point

● is a slurry mass flow rate sampling point

▲ is a hot batch flotation test sampling point

Figure 4.4: Lead flotation circuit considered in this study showing sampling points

As previously mentioned, the scope of this study was from the Rougher feed to the Scavenger tailings. With this in mind, the three (3) Rougher concentrate streams, the Scavenger concentrate stream as well as the Scavenger tailings stream were seen as product streams. The circuit was, therefore, referred to as an "open circuit".

The samples collected for assay and percent solids determination was done in triplicate in the event a sample was compromised during transportation to the Metallurgical Laboratory (spilled or contaminated), during preparation for the analytical analysis, etc. Six (6) samples were collected to calculate the mass flow of certain streams and the frequency of sampling is described in Section 4.4.2.1.

4.4.2 Sampling techniques

A flotation circuit is never at complete steady state and small fluctuations in feed tonnage, feed grade and slurry density occur continuously. In order to smooth out the effects of fluctuations, multiple sample increments are taken during a circuit survey that are then composited to form the final sample. The more increments are taken, the better the representation of the operation of the circuit during the period of the circuit survey. However, the longer the circuit survey the higher the risk that a major disturbance affects the circuit operation. Therefore, there is a practical compromise between survey duration and sample

increments. Although there are statistical methods to calculate the minimum sample requirement based on the expected variance of the stream data (Hathaway et al., 2008), it has been found during recent surveys conducted by MPTech (Sweet, personal communication 2015) that 10 increments are required to obtain a reasonable mass balance and seven (7) is the minimum number of increments provided this is accompanied by multiple flow rate measurements of concentrate streams.

4.4.2.1 *Number of sample increments*

In scoping the circuit survey, it was found that a sample interval of 15 minutes was sufficient to allow all stream assay samples to be collected. In order to collect at least 10 samples or measurements, the circuit survey would have had to be 2,25 hours long. It was decided to extend this to a full three (3) hours provided the circuit remained at a reasonable steady state for this duration. This frequency allowed the composite samples collected to reflect the possible fluctuations or changes observed in the flotation circuit during the period of the circuit survey.

The mass flow samples were taken every 30 minutes, with the first measurement taken 30 minutes after the start of the circuit survey. The longer sampling interval for mass measurement sampling was due to the constraints associated with manpower during the circuit survey as well as the location and distance between the sample points.

Over the three (3) hour period a total of 13 sample increments were collected for stream data, i.e. to determine the composite assay and percent solids of the circuit streams, and six (6) mass flow samples of the selected streams.

4.4.2.2 *Stream samples*

In the Lead flotation circuit at BMM, slurry is transported from one place to another using three (3) main routes, namely pumping out of a sump, overflow of a launder or lip, and flow under gravity. The best-suited samplers for these streams are described below.

Pumped streams:

Some of the streams in the Lead flotation circuit are discharged into sumps before being pumped to the following location. These streams are the Rougher feed, overall Rougher concentrate, Scavenger concentrate and Scavenger tailings streams. The mass flow rates of these streams vary greatly from one another.

Due to the fact that these streams are discharged into a sump, representative sampling was best achieved by using a pelican sample. The use of a pelican sample cutter ensured that best

practice was used in taking samples and due care was taken to move the entire sampler at a steady speed across the width of the stream. The handle design of the pelican sampler allowed for maximum control when collecting the sample in a safe manner.

With each cut, the sampler's volume was partially filled and once the sampler was completely full, as per standard practice at BMM, the contents were deposited into the respective sample bucket. The process of collecting the sample by cutting across the stream and depositing it into the bucket was repeated until the required sample volume was obtained. Due to the solids content of the slurry, settling of solids could occur fairly quickly. To ensure that the complete sample, and more specifically all the solids, was deposited into the sample bucket, the standard practice at BMM was employed, i.e. the sampler's contents was agitated by swift back and forth motion. When the agitation was done correctly, negligible amounts of solid particles were left behind in the sampler.

The slurry mass flow sample for all required streams, besides the Rougher feed stream, was collected by placing the sample bucket under the discharge point for a certain period of time. The Rougher feed could not be sampled in the same manner since access to the discharge point, i.e. at the feedbox of the 1st Rougher flotation cell, was very difficult. Due to this constraint, it was decided to obtain the average mass flow of the slurry for the Copper Tails Thickener underflow stream and reconcile the Rougher feed mass flow. This was possible since the slurry mass flow of the Scavenger concentrate was obtained during the circuit survey.

Lip samples:

The individual Rougher concentrate flows over the lip of each of the Rougher flotation cells, into a collection launder. The pipes of the individual concentrate streams merge and the combined Rougher concentrate is discharged into the overall Rougher concentrate sump. Due to the piping configuration, a cross cut sample per individual concentrate stream was not possible and instead a flexible container was used to collect the assay and percent solids sample at the lip of the flotation cells. For ease of implementation and accessibility, a 2L ice cream container was used. When collecting the lip samples the ice cream container was held against the lip of flotation cell and was swept across the perimeter of the flotation cell that was accessible until the volume of the container was filled. This was repeated on average three (3) times such that there was sufficient sample available for assay analysis.

For the mass flow rate samples, the time duration over which each sample was collected was recorded so that the mass flow could be determined. In order to store the sample until returning to the Metallurgical Laboratory to measure the mass, the individual samples were collected using large plastic bags that were sealed using cable ties. The bags were stretched

and kept open in an almost rectangular shape, to allow the froth to flow into the bag for the sampling time. The mass flow measurements obtained were then scaled up using a ratio of the width of the bag, in the open position, to the perimeter of the flotation cell. Therefore, it was assumed that the flow of concentrate over the lip of each of the flotation cells was uniform across the entire perimeter of the flotation cell.

For both sampling methods, the surface area for sample collection was found to be sufficient and allowed for free flow of the froth into the sampler. Although the bubbles collected were of high volume, the solids load on the bubbles was small and the sample container had to be filled at least twice per sampling interval to ensure sufficient solids for assay analysis. Furthermore, it was found that due to the reagent addition, the froth sample was sticky and would not easily be deposited into the sample containers but had to be rinsed out with water. Since water recovery was a crucial parameter in the study, the water used to wash out the sampling containers was recorded. This enabled the original percent solids of the froth sample to be calculated.

Gravity flow:

The intermediate tailings streams, i.e. 1st through 3rd Rougher tailings, are internal streams that flow via gravity from the preceding flotation cell to the next. These streams generally have a high mass flow rate. Due to the fact that the stream was not visible, a certain degree of error was inherent for sampling this stream. For the purposes of this study, the samples were collected as dip samples using a sampler that was available on site, similar to that shown in Figure 4.5. The sampler was positioned towards the tail box of each flotation cell so as to collect the pulp as it was exiting the flotation cell. Due to the fact that the sampler was submerged into the flotation cell, the safety risks associated with the sampling had to be taken into account, i.e. moving parts within the flotation cell. This was managed by ensuring that the sampler was submerged in a vertical position, and at a safe distance away from the moving parts of the flotation cell, i.e. the agitator and dart valves.

Figure 4.5: Sampler used to obtain dip samples (Naik and van Drunick, 2007)

Once the sampler was lowered to the desired depth, the handle was pulled upwards and kept in the open position for approximately one (1) minute before being closed. The sampler was then carefully pulled to the top of the cell and the exterior of the sampler was rinsed while ensuring the sampler remained in the closed position. The sampler was then placed over the respective sample bucket and the contents were deposited into the container. Due to the fact that only one sampler was available, the cleaning of the sampler between sampling of the different intermediate tailings streams was crucial. This was done using process water available close to the flotation cells.

4.4.2.3 *Equipment measurements*

The Anglo Platinum Bubble Sizer was used to measure the bubble size distributions and the superficial gas velocity directly in each of the flotation cells. The bubble sizer is made up of a sampling tube that is attached to a viewing chamber. The sampling tube was lowered into the flotation cell and bubbles within the flotation cell travelled into the sampling tube. The bubbles were photographed with a digital still camera. The images were processed using proprietary image analysis software, and the bubble size distribution was determined. This enabled the bubble surface area flux (S_b) to be calculated for the cell, using Equation 2.7. A metallurgical assistant collected the superficial gas velocity (J_g) and Sauter mean bubble diameter (d_{32}) measurements for each of the flotation cells and used the methodology as per the Anglo Platinum Bubble Sizer to calculate what the S_b values were. However, the raw data pertaining to the J_g and d_{32} measurements were not recorded and only the calculated S_b values

were recorded at the time of the circuit survey. The S_b values obtained from the circuit survey were, therefore, the only information regarding gas dispersion within the circuit under investigation.

4.5 Batch flotation test procedure

As mentioned in Section 4.3.8, batch flotation tests are a means of minimising the interaction of process parameters in flotation, such that a single variable is altered and the results thereof can be analysed. For the purposes of this study, two types of batch flotation tests were performed, namely repeatability flotation tests and hot batch flotation tests. Some tasks before, during and after the tests were common between the repeatability and hot batch test procedures.

In the case of testing for the repeatability of the batch flotation procedure, a dry sample was prepared for flotation and various parameters, including reagent and air addition, were kept standard. This ensured that the environment was maintained in all repeat tests and it was assumed that the only variance in results was as a result of human error.

In the case of the hot batch flotation tests, a slurry sample was collected from the flotation circuit and was floated without the addition of reagents, such that the slurry characteristics were not altered.

The repeatability of flotation tests were conducted to confirm that results obtained from all batch flotation tests were representative and reliable while the hot batch flotation tests were conducted to quantify the floatability of minerals in the Lead flotation circuit. The 3L modified Leeds cell used during this study is shown in Figure 4.1 (cf. Section 4.3.8).

4.5.1 General preparation and tasks for all batch flotation tests

4.5.1.1 *Preparation required before tests*

1 The pelican sample cutter, sample buckets and laboratory filters were cleaned in the Metallurgical Laboratory.
2 The sample buckets were dried and the lids labelled using masking tape and a permanent marker, e.g. Cu Tails underflow #1. The empty sample buckets were weighed and the mass of each was recorded.
3 Where required, a permit to work was completed. The Production Foreman was informed that sampling would take place in the flotation circuit. A HIRA was completed to ensure that all hazards and associated risks for the task were identified.

4 All the concentrate containers used in the flotation test were cleaned and labelled. Each empty concentrate container was then placed on the bench-top scale in order to record the empty weight of the concentrate container.

5 During the flotation test, concentrate or froth was generally washed off the scraper in order to ensure the entire froth sample was collected in the concentrate container. Since water recovery was a parameter that had to be monitored in this study, the mass of wash water was recorded such that it could be deducted from the overall water recovered in each concentrate. Two water bottles were numbered and filled, and the mass of each was recorded. The use of bottle "1" and "2" was alternated such that the end mass could be recorded after use between concentrates.

4.5.1.2 *Transferring the sample to the flotation cell*

1 Due to the solids content of the sample that was tested, this had to be agitated to avoid settling of solids in the cell. In both bench- and plant-scale flotation cells, when the agitator is started with a load in the cell, it could cause damage or complete failure to the agitator and installed motor. A small amount of slurry was, therefore, added and the agitator was started at a low speed. The agitation speed was regulated by means of the agitation control dial. Once the entire slurry sample was added to the cell, the agitation speed was set at 1 140 rpm, which was found to be the optimal speed during prior scoping tests. The optimal speed of 1 140 rpm resulted in sufficient mixing where the solids were suspended without causing a boiling effect on the surface of the pulp.

2 Before all batch flotation tests, a syringe was used to collect a feed sample from the Leeds cell. This was done by placing the syringe next to the agitator, at a safe distance, and ensuring the opening of the syringe was below the pulp level. Approximately 10ml of slurry was taken since this ensured sufficient mass of solids for assay purposes.

4.5.1.3 *General batch flotation procedure*

1 When the batch test commenced, the air valve was opened such that the airflow was maintained at 2.5 L/min. Once the air was opened, the flotation test was officially started and this was referred to as zero minutes.

2 In order to minimise dropback once a particle entered the froth phase, the pulp-froth interface was set to one (1) cm from the lip of the flotation cell and the froth was scraped at regular intervals of 15 seconds. The interface was maintained by adding water to the cell. The required water addition was calculated from the average water recovery in the scoping flotation tests conducted prior to the repeatability tests, and the water flow rate of the make-up water was adjusted accordingly. The water pipe was then placed at the back of the cell, at a designated point, and the pipe's outlet was placed below the

pulp-froth interface to ensure that the water did not immediately get recovered in the froth. The water level was adjusted by adding approximately 7.0 ml/min of water.

3 As mentioned in Section 4.3.8, for the purposes of this study it was important to define the kinetic recovery profile for the flotation tests conducted. Hence, multiple concentrates were collected into individual concentrate containers. Table 4.1 shows concentrates that were collected as well as the wash water bottle used for each of the individual concentrates.

Table 4.1: Concentrate name and wash water bottle used for batch flotation tests

Concentrate name	Wash water bottle
30 seconds	1
1 minute	2
2 minutes	1
3 minutes	2
7 minutes	1
11 minutes	2
15 minutes	1
20 minutes	2

The concentrate name refers to the cumulative flotation time that elapsed. Therefore, the 30 seconds concentrate comprises of two scrapes, i.e. collected 15 seconds and 30 seconds cumulative flotation time, since 30 seconds would have elapsed from the time where the air valve was opened. The one (1) minute concentrate was collected in a separate concentrate container and this would also have been made up of two scrapes, i.e. 45 seconds and one (1) minute, since a total of one (1) minute of flotation time would have elapsed from the time where the air valve was opened.

4 After concentrate collection, each of the concentrate containers was weighed and the mass recorded. The total weight included the weight of the concentrate container, the solids recovered in the froth, the water recovered in the froth as well as the wash water used to clean the scraper into the bucket.

5 The wash water bottle was weighed such that the end weight could be recorded. This end weight was the start weight for the next use, e.g. the end weight of wash water

bottle 1 after the 30 seconds concentrate would be the start weight for the 2 minutes concentrate.

6 The contents of the concentrate container were then transferred to the filter paper placed on the sieves, as described in Section 4.3.9. Another water bottle was used to wash out any residual solids from the concentrate container. Once most of the water had drained, the filter paper with concentrate samples were placed in sample dishes before being placed in the oven to dry.

7 Once the total flotation time had elapsed, i.e. 20 minutes, the air valve was closed and the agitator speed was set to zero. The machine was then switched off and unplugged. The tailings of the test were washed into a bucket.

4.5.1.4 *Preparation of samples for assay*

1 The tailings sample was transferred into the pressure filter, ensuring all residual solids was washed out using wash water. The filter cake was then placed into a sample dish before being placed in the oven to dry.

2 Once the samples were dry and cooled, the mass of all the flotation test samples, i.e. feed, concentrates and tailings, were recorded. The feed and concentrate samples were transferred to sample bags to be submitted for assay analysis. The tailings sample, due to its size, was split using the 10-way rotary splitter. A representative portion of the tailings sample was bagged and submitted for assay analysis.

The various samples were analysed for lead and silver content. The decision to restrict the analysis to only lead and silver at this stage was due to the fact that they are the desired minerals to be recovered in the Lead flotation circuit and their reproducibility was, therefore, important.

4.5.2 Experiments to test repeatability of batch flotation procedure

The batch flotation tests would be seen as repeatable if the results obtained from the three (3) tests met one (1) or both of the set criteria. The first criterion was that the results fit within a 95% confidence level and the second criterion was that the relative standard deviation was below 5% and the error of the reconciled feed grade was below 10%.

It was decided that the most ideal sample to conduct the repeatability testwork on was the Copper Tails Thickener underflow sample, which was collected at the sample point used for metallurgical monitoring. This sample had no Lead flotation circuit reagents added and so it allowed for the controlled addition of reagents in the bench-scale unit.

In order to conduct repeatability of flotation tests, a large sample was collected, prepared and thereafter floated. The tests were deemed repeatable when complying with one or both of the

prescribed measures mentioned above, i.e. the 95% confidence level and the guideline of the standard deviation of the cumulative recovery and the error of the reconciled feed grade.

4.5.2.1 *Feed sample requirements*

It was advised that the percent solids of the repeatability flotation tests was set at 35% (O'Connor, personal communication 2011). Therefore, with the solids density, the desired percent solids and the volume of the batch flotation cell known, the required mass of the solids and dilution water were calculated. The mass of solids required per test was calculated to be approximately 1.4kg. Therefore, it was decided that the total bulk sample had to contain approximately 7.0kg solids such that the testwork could be conducted in triplicate, as mentioned above, and sufficient sample would be available if any of the tests had to be re-done. Due to the high relative density of the underflow stream, three sample buckets were used to collect the bulk sample to ensure that the load per bucket did not exceed the 25.0kg manual handling limitation of the mine, and was manageable to carry to the Metallurgical Laboratory.

4.5.2.2 *Sample collection and preparation*

All steps outlined in Section 4.5.1.1 were followed prior to sample collection and preparation. The steps listed below depict the order of tasks that was followed for the sample collection and preparation for the repeatability tests.

1 The sample valve was opened completely and allowed to run until the stream showed that the sampling point's tap had a full flow. The pelican sample cutter was swept across the stream until the volume was filled. The contents of the sampler were deposited into the sample bucket as per Section 4.4.2.2. The second cut was placed into bucket 2 and the third into bucket 3 so that all three buckets contained as closely as possible identical samples. This was repeated until the three (3) sample buckets were completely filled.
2 The lids were placed on the buckets to ensure that the sample was not spilled or contaminated while being carried to the Metallurgical Laboratory.
3 The HIRA was completed for the task of filtering samples using a laboratory-scale pressure filter.
4 A labelled piece of filter paper was positioned and secured on the base of the pressure filter. Each sample bucket was filtered separately to ensure that the filter cake was not too big, as this would hamper the drying time of the sample. The filtered samples were placed in sample dishes and placed in the oven to be dried at 60°C.
5 Once dried and cooled, the individual dried filter cakes were weighed before being blended. The blending was done to ensure a homogenous sample, since the recovery of

minerals in a laboratory-scale or plant-scale flotation cell is dependent on the feed grade to the process. The blended sample was then split by means of a 10-way rotary splitter.

6 Since the original mass of sample was approximately 7.0kg, each of the 10 sample beakers would contain approximately 0.7kg. This implies that two (2) of the sample beakers were sufficient to make up the feed for one (1) repeatability flotation test and, hence, five (5) representative samples were prepared. When mixing sample beakers to make up a single sample, it was important to use beakers that are directly opposite each other on the turntable.

4.5.2.3 *Reagent make-up*

Due to the fact that Copper Tails Thickener underflow sample contained no reagents, reagents had to be added before the test was formally started, i.e. before air was dispersed into the flotation cell. The method of preparing the reagent solutions is listed below.

1 The batch flotation standard operating procedure (SOP) of the Metallurgical Laboratory prescribes the use of 1% mass/mass concentration solutions for particular reagents. These reagents are sodium cyanide, zinc sulphate and sodium ethyl xanthate (S.E.X.) for lead flotation tests.

2 The batch flotation SOP specifies that a drop of frother, in concentrated form, should be added in the conditioning stage of the test. However, this is based on 1kg of solids sample used and the volume of the drop was assumed. As mentioned above, 1.4kg of solids was used in the repeatability tests and, therefore, the frother dosage would have had to be scaled up to 1.4 drops of frother. It was, therefore, decided to dilute the frother solution to 1% mass/mass concentration and the frother was added in line with the dosage rate of the Concentrator on a g/t basis.

3 Glass beakers were cleaned and placed on the bench-top scale. The scale was zeroed such that the mass of the contents placed in it could be measured.

4 1.0g of reagent was added to the glass beaker. Water was added to the raw reagent, whether in powder, liquid or pellet form, such that the solution mass equalled 100g.

5 Due to the temperature requirements to optimally slake lime, the lime solution was collected from the Lime Slaking plant of the Concentrator. Lime solution was added to the pulp during the flotation tests until the desired pH of 7.8 was reached. This justified the use of obtaining the lime solution from the Lime Slaking plant where the exact solution concentration was unknown as it was not necessary to add an exact amount, rather to monitor and control the pH by adding as much lime as necessary.

4.5.2.4 *Repeatability batch flotation test procedure*

The steps followed to conduct the repeatability tests using the batch flotation procedure are listed below.

1 An empty bucket was cleaned and placed on the bench-top scale. The scale was zeroed such that the mass of the contents placed in it could be measured. The prepared repeatability test feed sample, as described above in Section 4.5.2.2, was deposited into the bucket. The mass of the feed sample was recorded and the scale was zeroed.

2 Since the percent solids required for the repeatability flotation tests was set at 35%, the required mass of water was 2.7kg.

3 Approximately 2.0L of the water was added to the bucket and the solids and water were mixed to form a dense slurry mixture. The slurry was then transferred to the 3L bench-scale flotation cell. Generally, a small amount of solids was not transferred and was washed out of the bucket using the remaining 700ml, which made up the total feed water for the repeatability test.

4 Steps outlined in Section 4.5.1.2, i.e. slurry agitation and test feed sample collection, were followed before reagents were added. The reagents were added in the sequence outlined and were allowed to condition for various times as shown in Table 4.2.

Table 4.2: Dosage rates and conditioning times used for repeatability tests

Addition sequence	Reagent	Test dosage (g/t)	Conditioning time (mins)
1	Lime solution	To pH 8	N/A
2a	NaCN	100	2
2b	ZnSO4	200	
3a	SEX	48	3
3b	Frother	68	

5 Once the pH of the pulp was at approximately 7.8, the sodium cyanide and zinc sulphate solutions were added simultaneously and allowed to condition for two (2) minutes. S.E.X. and frother solutions were then added simultaneously and allowed to condition for three (3) minutes. The reagents were added using individual syringes that were placed next to the agitator to allow for maximum mixing in the cell.

6 When conducting the test and collecting concentrates, all steps outlined in Section 4.5.1.3 were followed.

7 After the flotation test was completed, i.e. 20 minutes flotation time had elapsed, the steps listed in Section 4.5.1.4 were followed to prepare the test samples, i.e. the feed, concentrate and tailings samples, for assay analysis.

4.5.3 Experimental procedure for hot batch flotation tests

As mentioned previously, in order to quantify and understand the minerals' floatability down the flotation bank, rate tests were conducted on "hot" samples of specific streams and the results thereof were indicative of the floatability of the minerals. This section describes how the hot float test differs from the standard laboratory batch flotation test used for the repeatability analysis.

The samples used to conduct the hot batch flotation test were collected from flotation streams in the Concentrator in the form of conditioned slurry samples using the samplers and method as described in Sections 4.3 and 4.4.

In order to ensure that the floatability of the minerals in the sample was not compromised, samples were not collected and stored. Therefore, only one (1) sample was collected for hot batch flotation tests at any given time. The way these samples were taken is described below.

1 While standing at the sampling point, numerous cuts were taken of the stream that was going to be tested until the volume of sample deposited in the sample bucket was approximately 3L. This was done such that the majority of the slurry characteristics were maintained when the sample was transferred to the flotation cell, i.e. no additional water was required to fill the Leeds flotation cell volume.

2 The lid was placed on the bucket to ensure that the sample was not spilled or contaminated while being carried to the Metallurgical Laboratory.

Since the sample used in the hot batch flotation test procedure was in slurry form, the test was started immediately once the slurry sample was transferred to the Leeds flotation cell. All steps listed in 4.5.1.2, 4.5.1.3 and 4.5.1.4 were followed.

As part of this study, the effect of allowing a slurry sample to age was tested, i.e. stored for a certain period of time before being floated in the batch flotation cell. In order to do this, a total of four (4) individual samples were collected as per the method described in Section 4.4. One (1) sample was floated "hot" and the remaining three (3) samples were stored for varying periods of time.

4.6 Data reconciliation and processing

Although circuit surveys are planned such that it is conducted when the flotation circuit is relatively stable, running optimally and under normal operating conditions, some error is associated with sampling as well as the various tests and analyses that are conducted on the collected samples. Therefore, data reconciliation and mass balancing is required before modelling of the flotation circuit is conducted. For this study, the circuit feed, i.e. Rougher feed stream, was pegged as the basis for the mass balancing and modelling process. This was due to the confidence assigned to the data obtained from this stream as a result of the sampling point, sampling method and because some historical data pertaining to this stream was available at BMM.

The methodology for the mass balancing was to adjust the enhancement factor of each species in each flotation cell for which experimental data was obtained such that the error between the experimental data and calculated data was minimised.

The methodology used for model fitting was similar in that the enhancement factor was adjusted in order to minimise the difference between the model predicted and the mass balanced data. However, in model fitting the enhancement factor was calculated using various model parameters (Equations 2.15 and 2.16 shown in Section 2.6) and so the algorithm actually adjusted these parameters and the enhancement factor was calculated as a result.

As previously mentioned, by using the matrix method outlined by Woodburn and Wallin (1984), the mass balancing and model fitting of the flotation circuit can be achieved using a single MS Excel spreadsheet. The process of how this was done for this study is outlined in this section.

4.6.1 Mass balancing procedure

In order to conduct a full mass balance of the flotation circuit, data pertaining to various parameters were collected. These included the percent solids and the slurry mass flowrate of particular streams as well as the assay analysis of all the valuable species, i.e. chalcopyrite, galena, sphalerite and silver, in all accessible streams.

4.6.1.1 *Experimental data required for mass balancing*

Table 4.3 summarises the experimental data that was required from the circuit survey for the nine (9) streams and the unit of measurement used for each.

Table 4.3: Experimental data required for mass balancing

Type of data	Units
Slurry flow	tph
%Solids	%
Copper assay	%
Lead assay	%
Zinc assay	%
Silver assay	ppm
Relative Standard Deviation (SD)	%

An example of the experimental data shown in Table 4.3 is the metal assay. The metal assay describes the mass percentage a specific metal makes up of the total stream. The metal assay for all the flotation streams was derived by ICP Mass Spectroscopy (ICP-MS).

4.6.1.2 *Assigning the relative standard deviation for mass balancing*

During the circuit survey, samples were collected in triplicate for assay and for the three (3) samples collected, they were weighed before and after filtration and drying. Therefore, the assay analysis samples were able to give additional information regarding the percent solids of the various streams as well as the relative standard deviation of percent solids for the streams.

Furthermore, mass flows of certain streams were determined by sampling the same stream every 30 minutes, as described in Section 4.4.2, and in so doing it was possible to determine the relative standard deviation for the mass flows of these streams.

Lastly, the assignment of the relative standard deviation for the assay analyses values was based on the confidence level assigned to the sample, with reference to the sampling point and sampling method that was used. Table 4.4 shows the relative standard deviation for the percent solids, assay analysis of the various streams and mass flows.

Table 4.4: Relative standard deviation (%) used for mass balancing

Stream Number	Solids mass flow		%Solids		Chalc*	Galena	Sphal*	Silver
	Calc'd	Assigned	Calc'd	Assigned	Assigned	Assigned	Assigned	Assigned
Rougher Feed	-	5	-	5	15	10	15	15
1st Ro Conc	33	35	19	20	10	8	10	12
2nd Ro Conc	5	10	14	15	10	8	10	12
3rd Ro Conc	12	15	17	20	10	8	10	12
Scav Conc	67	100	72	-	10	8	10	12
1st Ro Tail	-	-	-	-	20	15	20	20
2nd Ro Tail	-	-	-	-	20	15	20	20
3rd Ro Tail	-	-	-	-	20	15	20	20
Ro Tail	-	-	-	-	20	15	20	20

where Calc'd denotes calculated, Chalc* denotes chalcopyrite and Sphal* denotes sphalerite

The relative standard deviation of the solids mass flow and percent solids of the Rougher and Scavenger concentrate streams were calculated from the raw experimental data. The calculated relative standard deviation was then rounded up to the nearest multiple of 5, and was assigned accordingly. However, for the Scavenger concentrate the 100% relative standard deviation assigned for the solids mass flow was as a result of the significant fluctuation observed from the raw experimental data. Based on the significant scatter in experimental data of the percent solids of the Scavenger concentrate stream, it was not taken into account in the error calculation and no relative standard deviation was assigned.

Since the galena was the mineral of interest in the Lead flotation circuit, the assigned relative standard deviations for the assays were lower than the other species. Galena is upgraded significantly in the Lead flotation circuit and the large differences in grade between the concentrate and tailings products from each cell allow the data reconciliation to be done with greater confidence using this species to drive the mass split across the cell.

Due to concerns about the experimental percent solids highlighted when analysing the data obtained for the tailings stream, and specifically the intermediate tailings streams, no relative standard deviations were assigned. Some more detail regarding the inconsistencies of the percent solids for these streams will be discussed in Section 6.2.2.

4.6.1.3 *Calculating the experimental mass flow*

The experimental mass flow of slurry for certain streams, as described in Section 4.4.2.2, was obtained during the circuit survey. Based on the experimental slurry mass flow and percent solids, the experimental mass flow of the solids was calculated using Equations 4.1 and the

mass flow of water was calculated by difference, i.e. the mass of water was determined using the slurry mass flow and the mass flow of solids for the particular stream. The 1st Rougher concentrate stream is used as an example.

Equation 4.1: Calculate the experimental mass flow of solids

$$Solids_{R1C} = Slurry_{R1C} \times \%Solids_{R1C}$$

where: $Solids_{R1C}$ is the mass flow of solids in the 1st Rougher concentrate stream $(e.g. \frac{kg}{hour} \text{ or } \frac{t}{hour})$

$Slurry_{R1C}$ is the mass flow of slurry in the 1st Rougher concentrate stream $(e.g. \frac{kg}{hour} \text{ or } \frac{t}{hour})$

$\%Solids_{R1C}$ is the percent solids in the 1st Rougher concentrate stream (fractional)

At the BMM Analytical Laboratory, samples are not analysed for the minerals, viz. chalcopyrite, galena and sphalerite, but rather for their respective metals, i.e. copper, lead and zinc. Using the calculated experimental mass flow of solids and the metal assays, as well as the chemical formula for the mineral, the experimental mass flows of the various mineral species were calculated. Equation 4.2 shows, for example, how the experimental mass flow of chalcopyrite was calculated in the Rougher feed stream.

Equation 4.2: Calculate the experimental mass flow of mineral species

$$Chal_{Feed} = \frac{\%Cu_{Feed} x Solids_{Feed}}{\frac{Copper}{Chalcopyrite}}$$

where: $Chal_{Feed}$ is the mass flow of chalcopyrite in the Rougher feed stream $(e.g. \frac{kg}{hour} \text{ or } \frac{t}{hour})$

$\%Cu_{Feed}$ is the assay of copper in the Rougher feed stream (fractional)

$Solids_{Feed}$ is the mass flow of solids in the Rougher feed stream $(e.g. \frac{kg}{hour} \text{ or } \frac{t}{hour})$

Copper is the atomic mass of copper (grams)

Chalcopyrite is the atomic mass of chalcopyrite (grams)

The empirical formula and atomic mass of the sulphide minerals considered in this study are as follows:

Chalcopyrite: $CuFeS_2$ and the atomic mass of the mineral is 183.5g

Galena: PbS and the atomic mass of the mineral is 239.3g

Sphalerite: ZnS and the atomic mass of the mineral is 97.5g

It was assumed that the solids in a particular stream was made up of the valuable minerals, i.e. chalcopyrite, galena, sphalerite and silver, and the remainder of the solids was made up of non-sulphide gangue. All gangue was, therefore, described by the term remainder. Therefore, by using the information pertaining to the experimental mass flow of solids and valuable mineral species, the mass flow of the remainder, for example in the Rougher feed stream, was calculated using Equation 4.3.

Equation 4.3: Calculate the experimental mass flow of remainder

$$Rem_{Feed} = Solids_{Feed} - Chal_{Feed} - Gal_{Feed} - Sphal_{Feed} - Silver_{Feed}$$

where: Rem_{Feed} is the mass flow of the remainder in the Rougher feed stream

$Solids_{Feed}$ is the mass flow of solids in the Rougher feed stream

$Chal_{Feed}$ is the mass flow of chalcopyrite in the Rougher feed stream

Gal_{Feed} is the mass flow of galena in the Rougher feed stream

$Sphal_{Feed}$ is the mass flow of sphalerite in the Rougher feed stream

$Silver_{Feed}$ is the mass flow of silver in the Rougher feed stream

All parameters in Equation 4.3 are given as mass per time, e. $g. \frac{kg}{hour}$ or $\frac{t}{hour}$.

4.6.1.4 *Calculating the balanced mass flows*

The mass balanced flow of species within the concentrate and tailings streams were determined by simultaneously adjusting the enhancement factors of the various species that make up these stream viz. the solids, water, chalcopyrite, galena, sphalerite and silver. The mass balanced mass flow of the remainder was calculated by difference, as shown in Equation 4.3.

As previously mentioned, the enhancement factor is a ratio of the mass of a species in the concentrate stream relative to the mass of the same species in the tailings stream. The simultaneous equations that were used are shown below:

Equation 2.13: Enhancement factor

$$g_{ijA} = \frac{C_{ij,A}}{T_{ij,A}}$$

where: g_{ijA} is the enhancement factor of sub-class i of species j for the flotation cell A (dimensionless)

$C_{ij,A}$ is the mass flow of sub-class i of species j exiting flotation cell A in the concentrate stream $(e.g. \frac{kg}{hour}\ or\ \frac{t}{hour})$

$T_{ij,A}$ is the mass flow of sub-class i of species j exiting flotation cell A in the tailings stream $(e.g. \frac{kg}{hour}\ or\ \frac{t}{hour})$

Equation 4.4: Tailings mass flow as a function of the connection matrix

$$T_{j,A} = -F_j f_A X_{j,A}{}^{-1}$$

where: $T_{j,A}$ is the mass flow of species j in the tailings stream exiting flotation cell A$(e.g. \frac{kg}{hour}\ or\ \frac{t}{hour})$

F_j is the mass flow of species j in the feed to the circuit, i.e. Rougher feed stream $(e.g. \frac{kg}{hour}\ or\ \frac{t}{hour})$

f_A is the fraction of the feed entering the flotation cell A (dimensionless)

$X_{j,A}{}^{-1}$ is the inverse of the connection matrix for species j (dimensionless)

For this study, the entire Rougher feed stream entered the 1st Rougher flotation cell and hence f_A was 1 and could be omitted from the calculation. Hence Equation 4.4 could be reduced to:

$$T_{j,A} = -F_j X_{j,A}{}^{-1} \qquad \text{Equation 4.4}$$

4.6.1.5 *Calculating the balanced percent solids and assay of the flotation streams*

Based on the balanced data calculated for the solids and water mass flow, the balanced percent solids of the flotation streams were determined.

Similar to the balanced percent solids, the balanced assay of the flotation streams was calculated using the balanced mass flow of the mineral species and solids. The mineral assay was converted to the elemental assay, by means of Equation 4.2 (cf. Section 4.6.1.3), in order to compare the experimental and mass balanced elemental assay.

4.6.1.6 *Calculating the mass balanced recovery for all species*

The mass balanced recovery for the species indicates the distribution of the particular species in the various flotation streams with reference to the feed stream, i.e. Rougher feed. The equation used to calculate this is shown in Equation 4.5 with reference to chalcopyrite in the 1st Rougher concentrate stream.

Equation 4.5: Calculate the mass balanced recovery for all species

$$\%R\_Chal_{R1C} = \frac{Chal_{R1C}}{Chal_{Feed}} x\ 100$$

where: $\%R\_Chal_{R1C}$ is the recovery of chalcopyrite in the 1st Rougher concentrate stream (%)

$Chal_{R1C}$ is the mass flow of chalcopyrite in the 1st Rougher concentrate stream $\left(e.g. \frac{kg}{hour}\ or\ \frac{t}{hour}\right)$

$Chal_{Feed}$ is the mass flow of chalcopyrite in the Rougher feed stream $\left(e.g. \frac{kg}{hour}\ or\ \frac{t}{hour}\right)$

4.6.1.7 *Minimising the mass balancing error*

Ideally the mass balanced data and the experimental data would be identical. However, this is typically not the case due to propagation of error as a result of fluctuations in the system, sampling error, bias associated with analytical methods, etc. As mentioned above, the enhancement factors for the species were adjusted such that the total error between the experimental data and mass balanced data was minimised. For the mass balancing process, the error of the valuable mineral species, i.e. chalcopyrite, galena, sphalerite and silver, was based on the metal assays.

The weighted sum of squared errors between the experimental and balanced data was calculated as shown in Equation 4.6. As an example, Equation 4.6 is based on the mass flow of solids in the 1st Rougher concentrate stream.

Equation 4.6: Weighted sum of squared error for mass balancing

$$Error_{Sol,R1C} = \left[\frac{R1C\_Sol_{exp} - R1C\_Sol_{MB}}{R1C\_Sol_{exp} x R1C\_Sol_{SD,MB}}\right]^2$$

where: $Error_{Sol,R1C}$ is the weighted error of the solids mass flow for the 1st Rougher concentrate stream

$R1C\_Sol_{exp}$ is the experimental mass flow of solids in the 1st Rougher concentrate stream

$R1C\_Sol_{MB}$ is the mass balanced mass flow of solids in the 1st Rougher concentrate stream

$R1C\_Sol_{SD}$ is the assigned relative standard deviation for the mass balancing process, as a fraction, for the mass flow of solids in the 1st Rougher concentrate stream

The unit of measure for the weighted error of all the parameters is dimensionless. The weighted errors for all species in all streams were combined and this total error was minimised by adjusting the enhancement factors of the species. It was assumed that a weighted sum of squared error equal to or lower than five (5) showed strong correlation between the balanced and experimental data.

4.6.2 Modelling procedure

When modelling the flotation circuit, the mass balanced data from the circuit survey as well as the hot batch flotation tests were used. As mentioned previously, the model fitted parameters were adjusted which thereby adjusted the enhancement factor of the species such that the error between the mass balanced and modelled data was minimised.

Similarly to the mass balancing procedure discussed in Section 4.6.1, equations were solved simultaneously and these equations are outlined in Chapter 2 (cf. Sections 2.4, 2.5 and 2.6). Further to the method discussed in Section 4.6.1, during the modelling process the species were also divided into sub-classes. The process for model fitting the Lead flotation circuit is detailed in this section.

4.6.2.1 *Defining the sub-classes of mineral species*

As mentioned in Section 2.5, for all species, floatability is not described by a single value but rather by a distribution. This was the assumption used for the valuable minerals, and the remainder was assumed to be completely non-floating. Therefore, a particular valuable

mineral species in the feed stream could be sub-divided into various sub-classes and the summation of the mass fractions for the various sub-classes would equate to 1 or 100%, since mass is conserved. For example, in the case of galena, the feed stream was sub-divided into fast, slow and non-floating galena. This is quantified in Equation 4.7.

Equation 4.7: Defining the sub-classes of mineral species

$$Gal_{Feed} = Gal_{Feed}m_{F,Gal} + Gal_{Feed}m_{S,Gal} + Gal_{Feed}m_{NF,Gal}$$

where: Gal_{Feed} is the mass flow of galena in the Rougher feed stream $(e.g. \frac{g}{min} or \frac{t}{hour})$

$m_{F,Gal}$ is the fast floating mass fraction of galena (dimensionless)

$m_{S,Gal}$ is the slow floating mass fraction of galena (dimensionless)

$m_{NF,Gal}$ is the non-floating mass fraction of galena (dimensionless)

Each sub-class of species has its own floatability constant. That is, the fast floating fraction will have a floatability constant that is different to the slow and non-floating floatability constants.

In order to constrain the model using the data that was available, the mass fraction of the non-floating sub-class of valuable mineral species was set to be equal to the portion of that species that did not float in the hot batch flotation test of the Scavenger tailings stream. Using galena as an example, the non-floating fraction was calculated as follows in Equation 4.8.

Equation 4.8: Assigning the non-floating mass fraction

$$m_{NF,Galena} = (100\% - Rec_{Galena,HB\_RT}) \times Loss_{Galena,Circuit\_RT}$$

where: $m_{NF,Galena}$ is the non-floating mass fraction of galena (fractional)

Rec_{Galena,HB_RT} is the experimental cumulative recovery of galena for the hot batch flotation test conducted on the Scavenger tailings sample (fractional)

$Loss_{Galena,Circuit\_RT}$ is the mass balanced percentage of galena exiting the circuit in the Scavenger tailings stream (fractional)

As an initial estimate of the fast floating mass fraction of each of the valuable mineral species, the mass fraction was set to be that of the experimental recovery of the first concentrate collected in the hot batch flotation of the Rougher feed sample, i.e. the 30 second concentrate. Using galena as an example, the initial estimate of the fast floating fraction was 29,0%.

4.6.2.2 *Assigning the relative standard deviation for modelling*

Due to the simultaneous modelling of the circuit and batch flotation test data, relative standard deviations were assigned to both sets of data.

Circuit:

Due to the increased confidence in the balanced water mass flow data compared to the experimental data of water, the relative standard deviations assigned to the water flow in the modelling process were reduced compared to those assigned for the mass balancing process. Furthermore, since there were mass balanced assays of the remainder for all streams, these were assigned with relative standard deviations as well.

Apart from the assignments mentioned above, the assignment of the relative standard deviations of chalcopyrite, galena, sphalerite and silver were as per the mass balancing process, shown in Table 4.4. The assigned relative standard deviations for the modelling process are shown in Table 4.5

Table 4.5: Relative standard deviation (%) used for circuit modelling

Stream Number	Water	Chalc*	Galena	Sphal*	Silver	Remainder
Rougher Feed	5	15	10	15	15	10
1st Ro Conc	5	10	8	10	12	10
2nd Ro Conc	5	10	8	10	12	10
3rd Ro Conc	5	10	8	10	12	10
Scav Conc	5	10	8	10	12	10
1st Ro Tail	5	20	15	20	20	15
2nd Ro Tail	5	20	15	20	20	15
3rd Ro Tail	5	20	15	20	20	15
Ro Tail	5	20	15	20	20	15

where Chalc* denotes chalcopyrite and Sphal* denotes sphalerite

Batch flotation tests:

For all tests, a higher relative standard deviation was assigned to the first two (2) concentrates since it was assumed that there was likely more error at the start of the test, for example it was difficult to accurately maintain the pulp-froth interface. The experimental batch recovery of all species for certain tests conducted had a high degree of inconsistency in terms of the recovery achieved during the hot batch flotation test. For these specific tests the assigned relative standard deviations were such that the predicted batch recovery of these tests was

allowed to vary significantly more during model fitting. The assigned relative standard deviation table can be found in Appendix C.

4.6.2.3 *Assigning the parameter starting values for the modelling process*

The starting point for the floatability constants (P) of each species used in Equation 2.12 was set such that the modelled recovery for the first concentrate (30 seconds) and last concentrate (20 minutes) for the hot batch flotation test conducted on the Rougher feed sample was similar to the experimental recovery.

The floatability of the fast floating fraction was set to be an order of magnitude higher than for the slow floating fraction, and the floatability of the non-floating fraction was set to be zero. Since the study was conducted in the Lead flotation circuit, the initial estimate of the fast and slow floating galena was set to be an order of magnitude higher than that of the other floating species.

A degree of entrainment parameter was assigned to the gangue, i.e. the remainder, such that the total mass recovered was the same order of magnitude as the mass balanced values.

The residence time, used in Equation 2.12 (cf. Section 2.5.3) was initially calculated using the volume of the flotation cells and the mass balanced slurry volumetric flow of the various tailings streams. After an iteration of the model fitting algorithm, the residence time was recalculated using the predicted volumetric flow.

Similarly, the water recovery, used in Equation 2.6 (cf. Section 2.4.5.5) was calculated using the mass balanced water recovery per flotation cell, which was then recalculated during model fitting. Starting estimates for the water recovery model parameters "a" and "b" were calculated by fitting an exponential trendline to a plot of Q_w versus F_s.

4.6.2.4 *Model fitting the froth recovery per species*

Froth recovery is influenced by a number of parameters including characteristics of the minerals, such as degree of liberation and degree of hydrophobicity, as well as the operating conditions of the flotation cell, such as froth depth and aeration rate. Since the operating conditions of the cell should affect all mineral species equally, the characteristics of the minerals play a significant role in the froth recovery of the species in the flotation bank.

Since the feed to the Lead flotation circuit consisted of three (3) naturally floating sulphide minerals, i.e. chalcopyrite, galena and sphalerite, it was assumed that each of these would have varying degrees of hydrophobicity. As previously mentioned, the hydrophobicity of galena was enhanced by the addition of sodium ethyl xanthate (S.E.X.) collector, while

depressant was added to render the sphalerite hydrophillic. Along with other factors, the degree of liberation would influence the reagent coverage of the mineral surface and, therefore, the overall floatability of the species. Therefore, all species could not be assigned the same froth recovery and the froth recovery of each species per flotation cell was model fitted such that the error between the predicted and balanced data was minimised.

4.6.2.5 *Calculating the mass flows*

Using the initial estimates as per Section 4.6.2.3, the mass flows of the various sub-classes were calculated. The solids mass flow was calculated by the summation of the sub-classes for each of the valuable species and the remainder, and is shown in Equation 4.9 using the Rougher feed stream as an example

Equation 4.9: Calculate the modelled mass flow of solids

$$Solids_{\text{Feed}} = \sum_{i=1}^{3} \text{Chal}_{Feed} + \sum_{i=1}^{3} \text{Gal}_{Feed} + \sum_{i=1}^{3} \text{Sphal}_{Feed} + \sum_{i=1}^{3} \text{Silver}_{Feed} + \sum_{i=1}^{1} \text{Remainder}_{Feed}$$

where: $\text{Solids}_{\text{Feed}}$ is the mass flow of the solids in the Rougher feed stream

$\sum_{i=1}^{3} \text{Chal}_{Feed}$ is the mass flow of chalcopyrite in the Rougher feed stream based on the three (3) sub-classes

$\sum_{i=1}^{3} \text{Gal}_{Feed}$ is the mass flow of galena in the Rougher feed stream based on the three (3) sub-classes

$\sum_{i=1}^{3} \text{Sphal}_{Feed}$ is the mass flow of sphalerite in the Rougher feed stream based on the three (3) sub-classes

$\sum_{i=1}^{3} \text{Silver}_{Feed}$ is the mass flow of silver in the Rougher feed stream based on the three (3) sub-classes

$\sum_{i=1}^{1} \text{Remainder}_{Feed}$ is the mass flow of the remainder in the Rougher feed stream based on the one (1) sub-class

All parameters in Equation 4.9 are given as mass per time, e.$g. \frac{kg}{hour}$ or $\frac{t}{hour}$.

By means of Equation 4.4, which incorporates the connection matrix of the considered flotation circuit, the tailings mass flow was calculated and the resulting modelled tailings volumetric flow was used to recalculate the residence time. Equation 2.15, which is the enhancement factor of the sub-class of species in terms of the mineral floatability (P), bubble surface area flux of the flotation cell (S_b) and the froth recovery (R_f), was used to calculate the

concentrate mass flow. The water recovery was calculated using the relationship between water and solids recovery, i.e. Equation 2.6.

The above-mentioned procedure was iterated until there was convergence of the residence time and water recovery to four (4) decimal places.

The batch recovery was calculated using the cumulative flotation time and the parameters for the floatability constants and sub-class mass fractions.

Solver was used to find the best set of parameters to equate the modelled data to the mass balanced data for the circuit and batch simultaneously.

4.6.2.6 *Calculating the model predicted percent solids of the flotation streams*

The percent solids of the flotation streams for the model predicted data was calculated using the model predicted water and solids mass flows.

4.6.2.7 *Calculating the model predicted assay of the flotation streams*

The assays of the flotation streams for the modelled data was determined using Equation 4.2 (cf. Sections 4.6.1.1 and 4.6.1.3), where the experimental and mass balanced data was replaced by mass balanced data and modelled data respectively.

4.6.2.8 *Calculating the model predicted circuit recovery for all species*

As with the mass balanced recovery, the modelled recovery for the species indicates the distribution of the particular species in the various flotation streams with reference to the feed stream, i.e. Rougher feed, using the modelled data. The equation used was Equation 4.5 (cf. Section 4.6.1.6) where the experimental and mass balanced data was replaced by mass balanced data and modelled data respectively.

4.6.2.9 *Calculating the model predicted batch flotation recovery for all species*

By using Equation 4.10, the batch recovery per flotation time for each sub-class of each valuable mineral species was predicted. The total batch recovery per species for each flotation time was, therefore, calculated by the summation of the individual sub-class recoveries at that flotation time. Equation 4.10 is shown using chalcopyrite as an example.

Equation 4.10: Overall batch flotation recovery for species in terms of sub-classes

$$R\_Chal_{1min} = R\_Chal_{F,1min} + R\_Chal_{S,1min} + R\_Chal_{NF}$$

where: R_Chal_{1min} is the total batch recovery of chalcopyrite after one (1) minute flotation time (%)

$R\_Chal_{F,1min}$ is the predicted batch recovery of fast floating chalcopyrite after one (1) minute flotation time (%)

$R\_Chal_{S,1min}$ is the predicted batch recovery of slow floating chalcopyrite after one (1) minute flotation time (%)

$R\_Chal_{NF,1min}$ is the predicted batch recovery of non-floating chalcopyrite after one (1) minute flotation time (%)

4.6.2.10 *Minimising the modelling error*

Since the FCM approach was used in modelling the Lead flotation circuit, both circuit and laboratory-scale data was used. The parameters that influence the enhancement factors of the sub-classes of the species were adjusted simultaneously until the error between the modelled and balanced circuit data as well as the modelled and experimental batch flotation data was minimised. As previously mentioned in Section 4.6.1.7, it was assumed that a weighted sum of squared error equal to or lower than five (5) showed strong correlation between the model predicted and balanced data.

In terms of model fitting the circuit data, the weighted sum of squared error calculation was based on the mass flow of the valuable mineral species, i.e. chalcopyrite, galena, sphalerite and silver. Therefore, the error between the balanced and modelled mass flow of the species was minimised. In terms of model fitting the batch data, the weighted sum of squared error calculation was based on the cumulative batch recovery of the valuable mineral species.

To calculate the error of modelling the circuit, the weighted sum of squared error calculation is used and is based on mass balanced data and modelled data. As an example, Equation 4.11 is based on the mass flow of solids in the 1st Rougher concentrate stream.

Equation 4.11: Weighted sum of squared error for model fitting

$$Error_{Sol,R1C} = \left[\frac{R1C\_Sol_{MB} - R1C\_Sol_{Mod}}{R1C\_Sol_{MB} x R1C\_Sol_{SD}}\right]^2$$

where: $Error_{Sol,R1C}$ is the error of the solids mass flow for the 1st Rougher concentrate stream

$R1C\_Sol_{MB}$ is the mass balanced mass flow of solids in the 1st Rougher concentrate stream

$R1C\_Sol_{Mod}$ is the modelled mass flow of solids in the 1st Rougher concentrate stream

$R1C\_Sol_{SD}$ is the assigned relative standard deviation for the mass flow of solids for the modelling process, as a fraction, in the 1st Rougher concentrate stream

The unit of measure for the error of all the parameters is dimensionless. The error for all species in all streams was combined and this total error was minimised.

As mentioned above, the error between the predicted and experimental batch recovery was minimised simultaneously along with that of the circuit error. Equation 4.12 was used to calculate the weighted sum of squared error for the batch flotation test modelling. The equation uses chalcopyrite as an example.

Equation 4.12: Weighted sum of squared error for modelling the batch data

$$Batch\_Error_{Chal,Feed\_1min} = \left[\frac{Feed\_Chal_{exp,1min} - Feed\_Chal_{Mod,1min}}{Feed\_Chal_{Mod,1min} x Feed\_Chal_{SD}}\right]^2$$

where: $Batch\_Error_{Chal,Feed\_1min}$ is the error of the chalcopyrite recovery after one (1) minute flotation time for the test conducted on the Rougher feed sample

$Feed\_Chal_{exp,1min}$ is the experimental batch flotation test recovery of chalcopyrite after one (1) minute flotation time for the Rougher feed sample

$Feed\_Chal_{Mod,1min}$ is the modelled batch flotation test recovery of chalcopyrite after one (1) minute flotation time for the Rougher feed sample

$Feed\_Chal_{SD}$ is the assigned relative standard deviation for the recovery of chalcopyrite for the modelling process, as a fraction, using the sample from Rougher sample stream

5 RESULTS

The results obtained from the validation testwork (Phase One) as well as the circuit survey and hot batch flotation tests (Phase Two) will be presented in this chapter.

5.1 Validation of batch flotation test procedure

As mentioned in Chapter 4, validation of the batch flotation test procedure and the conservation of floatability in the Lead flotation circuit were required before the circuit survey was conducted. This was done in Phase One of the study. The validation ensured that the outputs from the hot batch flotation tests would be as representative as possible and could be used for modelling the Lead flotation circuit.

Furthermore, due to the fact that numerous samples had to undergo hot batch flotation tests during the circuit survey, it was necessary to confirm whether or not storing the samples for an extended period of time after sample collection would result in oxidation or other ageing phenomena that would negatively affect the floatability results obtained. This would also confirm whether oxidation was likely to occur in the residence time of the Lead flotation circuit.

Some key findings from Phase One, which will be presented in this chapter and are later discussed in Chapter 6, were that the methodology used for the batch flotation tests produced repeatable results, ageing of samples occurred after a certain storage period and that a strong correlation was observed between lead and silver recovery.

5.1.1 Repeatability of batch flotation test procedure

In order to ensure that results obtained from a singular hot batch flotation test were accurate, the repeatability of testwork had to be ascertained as well as the cumulative flotation time required for the test. This was done using the method described in Section 4.5.2 where a bulk sample was taken in the Concentrator, dried in the oven and thereafter the same procedure, i.e. reagent addition, air addition, scraping of concentrate as well as maintaining the level of the pulp-froth interface, was followed when conducting the batch flotation test in triplicate. The results of the repeatability tests for lead and silver as well as the test used to confirm the required cumulative flotation time are shown below.

5.1.1.1 *Measured feed and reconciled feed grades*

The measured and reconciled lead and silver feed grades are shown in Table 5.1. The methodology to carry out these calculations is shown in Appendix D.

Table 5.1: Measured and reconciled feed grades of repeatability batch flotation tests

Feed grade	Test 1		Test 2		Test 3		Average	
	Lead (%)	Silver (ppm)	Lead (%)	Silver (ppm)	Lead (%)	Silver (ppm)	Lead (%)	Silver (ppm)
Measured	6.4	32.0	6.1	33.0	6.2	33.0	6.2	32.7
Reconciled	6.7	39.1	6.6	38.6	6.7	39.5	6.7	39.0
Relative Error (%)	3.6	22.1	8.7	16.8	8.5	19.5	6.9	16.3

Table 5.1 shows that for lead, the relative error of the feed grade for the three (3) tests was below 10%. However, the relative error of the silver feed grade was above the 10% guideline for the three (3) tests, with the highest error for Test 1 at 22.1% and the lowest error for Test 2 at 16.8%. Although the error in the reconciled feed grade of silver was fairly high, i.e. above the guideline of 10%, it was in line with the tolerance of propagated error based on the BMM Analytical Laboratory standard. More detail will be given in Chapter 6.

5.1.1.2 *Cumulative solids recovery for repeatability tests*

The cumulative solids recovery versus flotation time results of the triplicate batch flotation tests are shown in Figure 5.1.

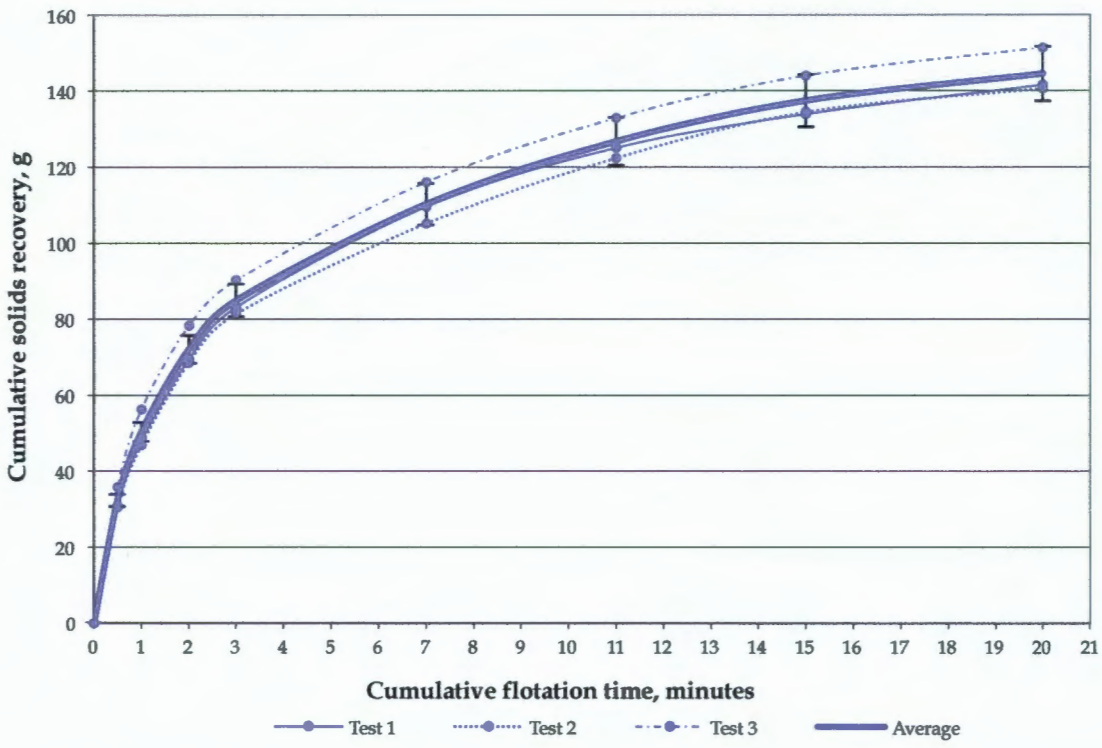

Figure 5.1: Cumulative solids recovery (g) versus flotation time (minutes) with error bars showing 95% confidence level

Figure 5.1 shows that the cumulative solids recovery versus flotation time curves for the three (3) tests conducted was mostly within the 95% confidence level of the average, but at the start of the test the errors were marginally higher. The average total solids recovered after 20 minutes cumulative flotation time was 144,5g, with a relative standard deviation of 4,1%.

5.1.1.3 *Cumulative lead recovery for repeatability tests*

The results of the three (3) repeatability batch flotation tests that were conducted are shown in Figure 5.2 with reference to lead recovery.

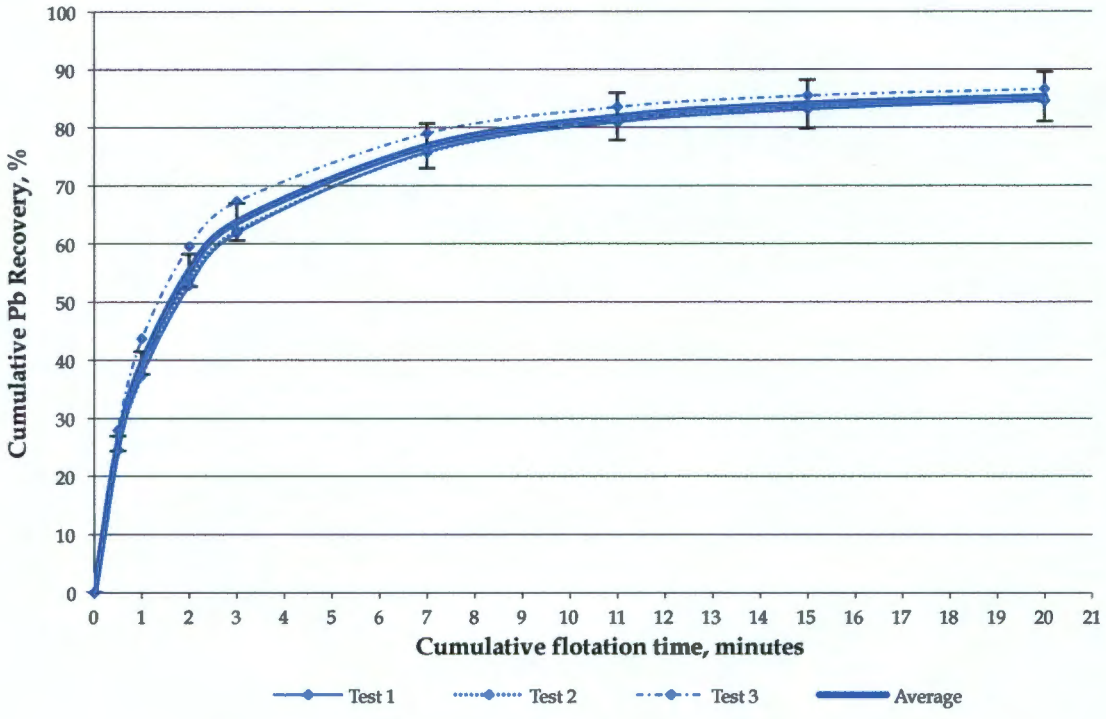

Figure 5.2: Cumulative lead recovery (%) versus flotation time (minutes) with error bars showing 95% confidence level

As with the total solids, the lead recovery results obtained were consistently within the 95% confidence limits after three (3) minutes of flotation time, with slightly higher deviations at the start of the test. The average total lead recovered after 20 minutes flotation time for the three (3) tests was 85,3%, where the lowest and highest recoveries obtained were 84,6% and 86,6% respectively. The relative standard deviation of the cumulative lead recovered was 1,4%.

5.1.1.4 *Cumulative silver recovery for repeatability tests*

The results of the three (3) repeatability batch flotation tests that were conducted with respect to silver recovery are shown in Figures 5.3.

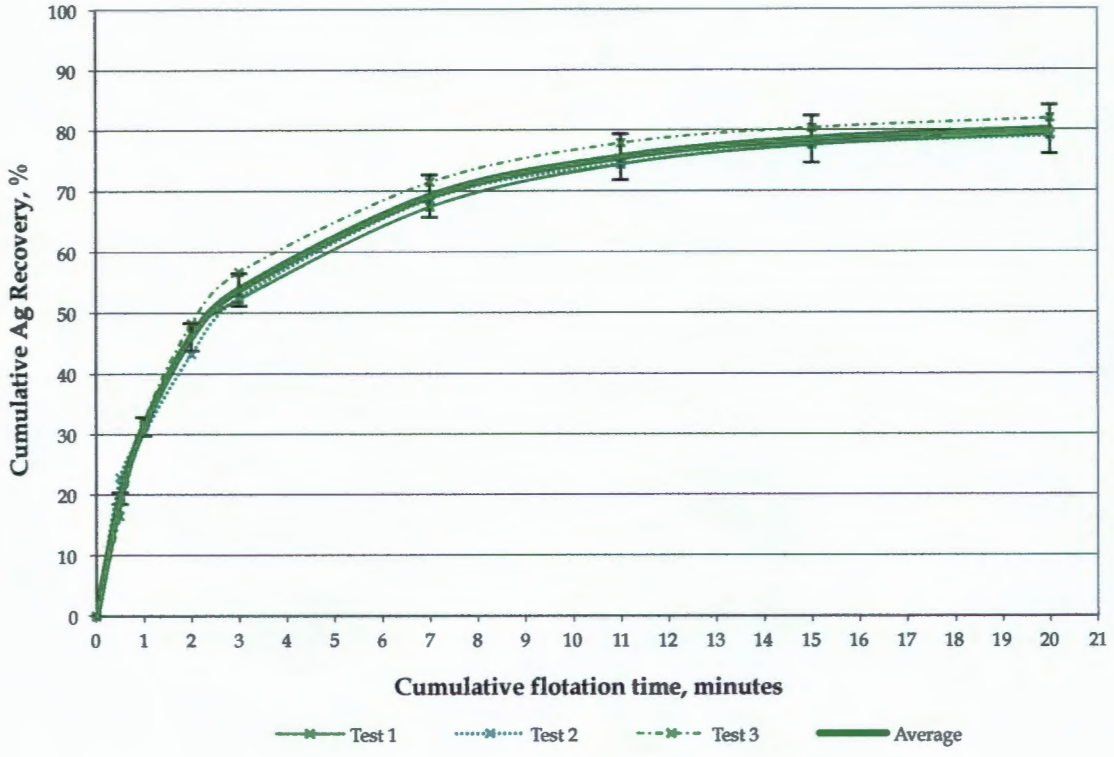

Figure 5.3: Cumulative silver recovery (%) versus flotation time (minutes) with error bars showing 95% confidence level

The silver recovery results obtained were consistently within the 95% confidence limits after seven (7) minutes of flotation time, with slightly higher deviations at the start of the test. For the three (3) tests the average total silver recovered was 80,1% and the relative standard deviation of the total silver recovered was 2,0%.

5.1.1.5 *Maximum flotation time for batch flotation tests*

When conducting batch flotation tests, it is observed that after a certain flotation time, the increase in metal recovery is negligible, i.e. the recovery reaches an asymptote. The time to reach the asymptote varies based on the nature of the material being floated, for example the feed grade, reagent dosage, mineral type, etc. Hence, the total flotation time allotted to a test must be established by conducting scoping batch flotation tests to determine the maximum flotation time required, i.e. when no more metal is recovered into the concentrate.

When using the Klimpel model, as cited by Saleh (2010) and Brezani (2010) for the batch tests conducted as part of this section, the maximum lead recovery for infinite flotation time was 87,6%, which was 2,3% greater than the 85,3% recovered after 20 minutes flotation time, but was within the 95% confidence level of the repeatability tests. The BMM standard operating procedure (SOP) for lead Rougher batch flotation tests is seven (7) minutes. If the repeatability batch flotation tests were stopped after seven (7) minutes as per BMM SOP, the

10% below the infinite time recovery. Hence 20 minutes flotation time adequately represented the infinite time recovery and the BMM SOP should be adjusted accordingly.

5.1.2 The effect of ageing on metal recovery

In the Lead flotation circuit, galena is the target mineral and by mineral association silver metal is also recovered. In order to use the FCM approach, the conservation of floatability, particularly for galena, had to be validated. The aim of the series of tests discussed in this section was to determine whether significant oxidation occurred within the residence time of the circuit as well as whether keeping slurry samples for a certain period of time, e.g. one (1) hour, before carrying out a hot batch flotation test, would have any effect on the mineral floatability as a result of oxidation of the sample, reactions between reagents, etc.

Four (4) feed samples were collected at the Rougher feed sump in a randomised manner in order to minimise variation in feed grade, specifically of lead. These were used to test the effect of ageing, by allowing the sample to stand for a certain period of time before performing a batch flotation test. The effect which ageing may have had on mineral floatability and recovery was then determined.

The four (4) feed samples collected were floated in the following order:

- Immediately – Test 1
- After one (1) hour of standing time – Test 2
- After three (3) hours of standing time – Test 3
- After 24 hours of standing time – Test 4

The lead and silver recoveries achieved in the hot batch flotation test, i.e. Test 1, were the reference recoveries.

5.1.2.1 *Cumulative lead recovery*

The results of the four (4) batch flotation tests that were conducted are shown in Figure 5.4 with respect to lead recovery.

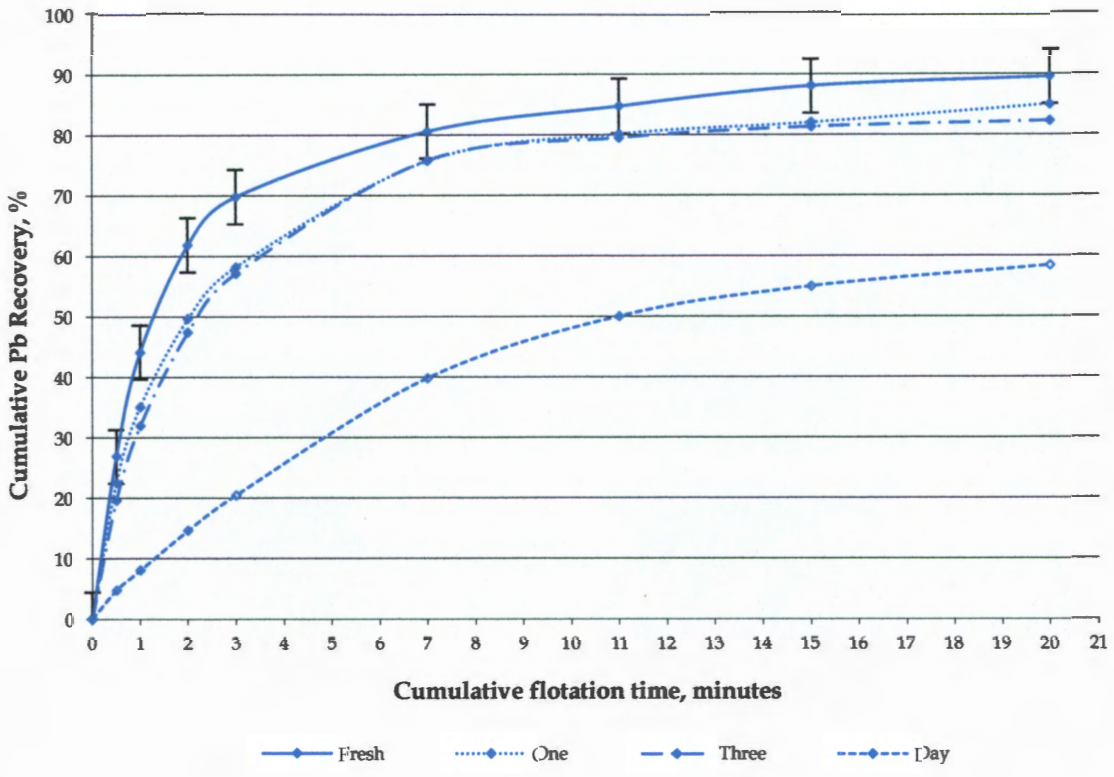

Figure 5.4: Cumulative lead recovery (%) versus flotation time (minutes) of ageing tests with error bars showing 95% confidence level for the reference test

Figure 5.4 shows that the cumulative lead recovery decreased gradually with standing time. The reference cumulative lead recovery, for the fresh sample, was approximately 89,5%. The lead recovery results obtained in Tests 2 and 3, i.e. one (1) hour and three (3) hours standing time respectively, were very similar to each other. The results also show that after seven (7) minutes cumulative flotation time, the cumulative recovery of the one (1) and three (3) hour standing time tests did not deviate significantly from the reference test, i.e. fresh sample test, and were almost within the standard deviation limits of the fresh sample test. The cumulative lead recovery of the test conducted after a day standing time, i.e. Test 4, was significantly different to the reference test, which indicated the floatability was negatively affected.

5.1.2.2 *Cumulative silver recovery*

The results of the four (4) batch flotation tests that were conducted are shown in Figure 5.5 with respect to the silver recovery.

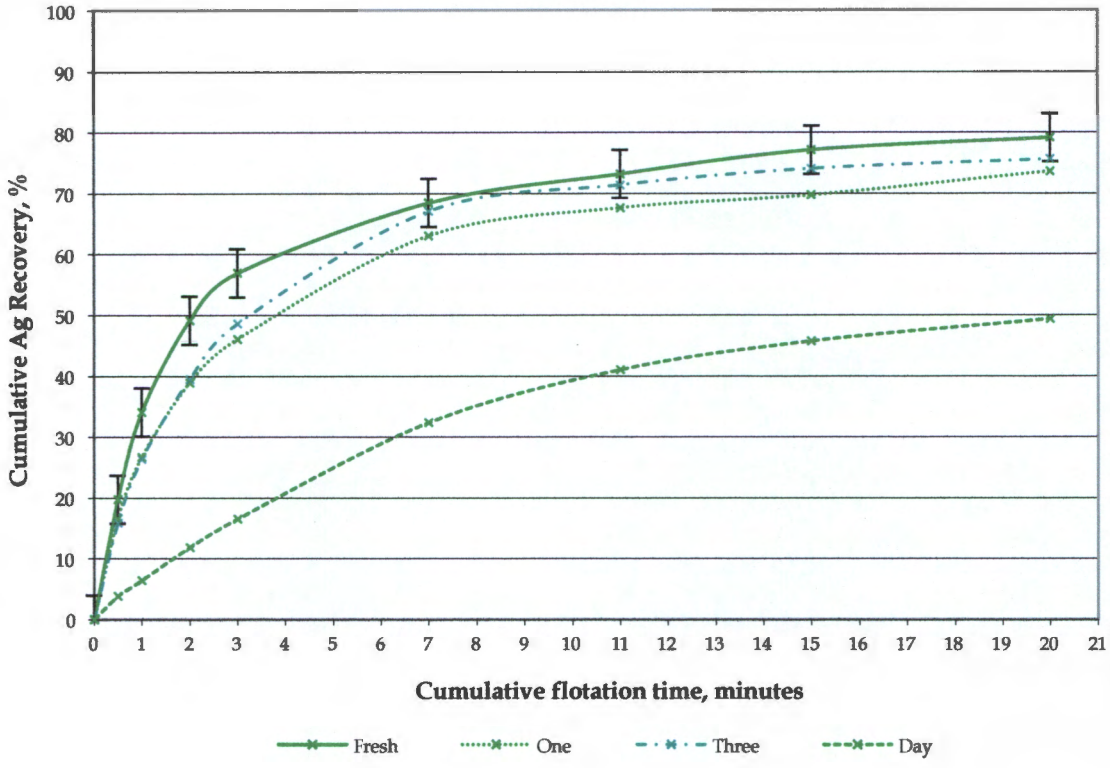

Figure 5.5: Cumulative silver recovery (%) versus flotation time (minutes) of ageing tests with error bars showing 95% confidence level for the reference test

As with the lead recovery results, the cumulative silver recovery showed a gradual decrease with standing time when compared to the reference batch flotation test, i.e. Test 1. The reference total silver recovered was 79,1% and that of Test 4, i.e. after a day standing time, was 49,4%. The silver recovery was, therefore, significantly reduced and the test results indicated that the floatability of silver metal was negatively impacted by prolonged standing time.

5.1.3 Relationship between lead and silver recovery

As mentioned previously, silver metal was mainly associated with galena in the BMM ore. It was observed in plant-scale operation that the recovery of silver metal strongly correlated with the recovery of galena in the Lead flotation circuit. This relationship was observed for the testwork conducted as part of Phase One. Figure 5.6 shows the relationship between silver recovery and lead recovery for the seven (7) tests that were discussed in Sections 5.1.1 and 5.1.2.

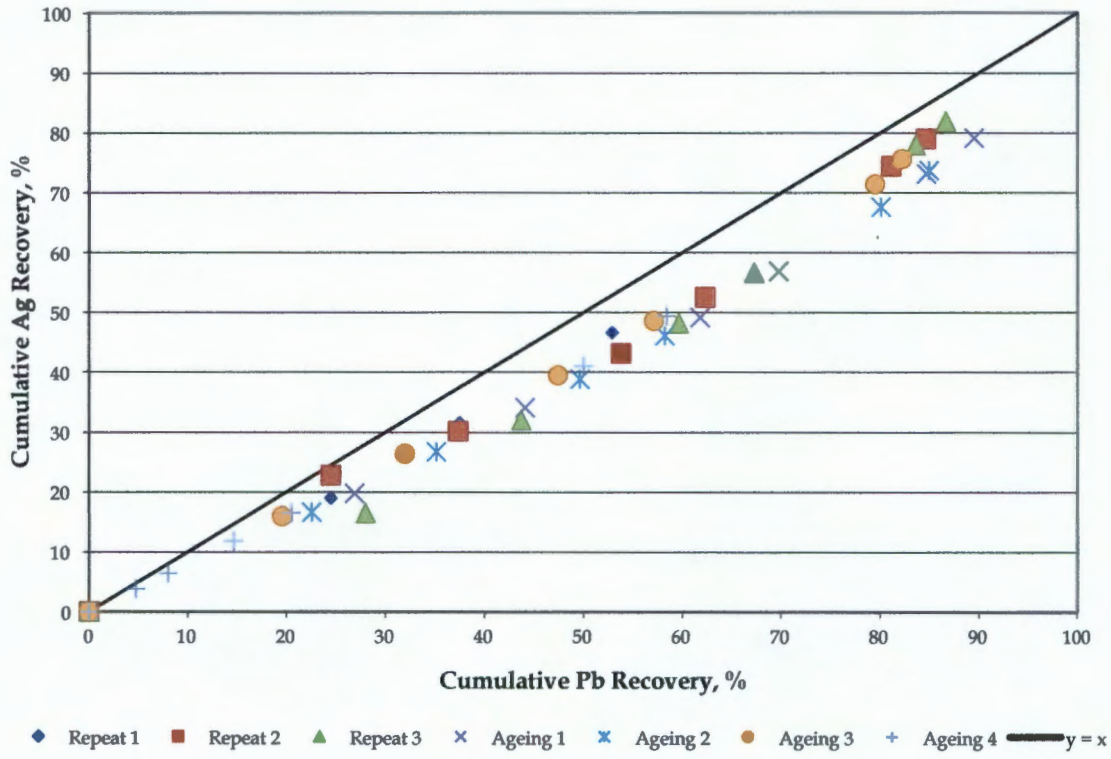

Figure 5.6: Cumulative silver recovery (%) versus lead recovery (%) for Phase One tests

Figure 5.6 shows that there was indeed a strong relationship between the silver and lead metal recovered for the tests discussed in Sections 5.1.1 and 5.1.2. From the data obtained from these tests, it was observed that the relationship was not linear and the ratio of lead recovered versus silver recovered decreased from the start to the end of the test. This relationship will be explored in more detail in the subsequent chapters.

5.2 Data analysis of circuit survey and hot batch flotation tests

Based on the data collected in the circuit survey, the mass balancing and modelling of the Lead flotation circuit at BMM was conducted, which made up Phase Two of this study. This chapter presents these results.

Some key findings from Phase Two, which will be presented in this chapter and are discussed in Chapter 6, were that the circuit data could be reconciled, that the model predicted data strongly correlated with the balanced data, that the relationship between silver and lead found in Phase One was observed but not for all streams, and that there was a lack of stream representivity for samples collected using a dip sampler.

5.2.1 Experimental data from circuit survey

During the circuit survey, various samples were collected and for ease of referencing they are shown in Figure 4.4.

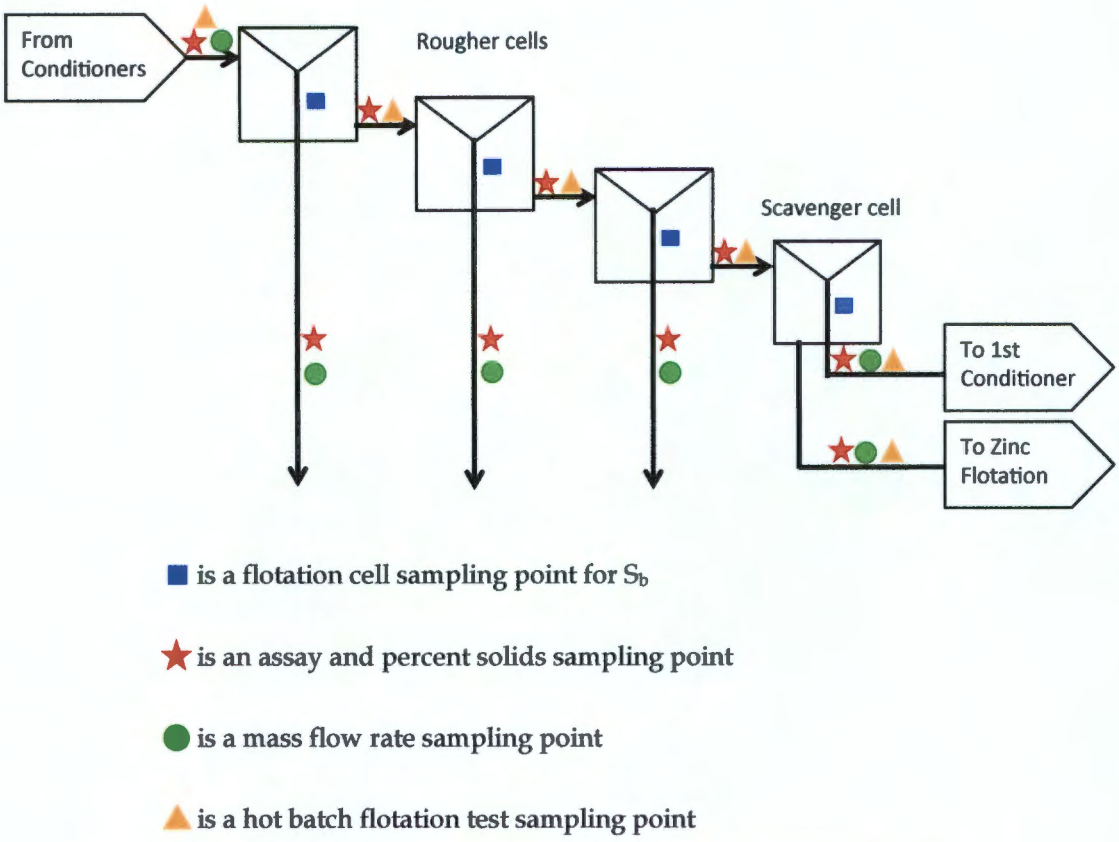

Figure 4.4: Lead flotation circuit considered in this study showing sampling points

Figure 4.4 shows the nine (9) streams that were sampled and the properties that were measured for each sample.

5.2.1.1 *Stability of the lead flotation circuit during the circuit survey*

Before discussing any of the data obtained from the circuit survey in detail, this section highlights the stability of the circuit over the duration of the circuit survey. As mentioned in Section 4.4.1, a total of three (3) samples were taken per stream for composite assay and percent solids determination, and a further six (6) samples were taken of selected streams to determine the mass flow. The average percent solids was calculated separately for the composite sample and the mass flow samples. The results of the individual samples as well as the two averages for the Rougher concentrate streams are shown below in Table 5.2.

Table 5.2: Experimental percent solids for concentrate streams showing stability of circuit

Sample Number	1st Rougher concentrate	2nd Rougher concentrate	3rd Rougher concentrate
	(%)	(%)	(%)
Comp 1	37.8	37.9	30.9
Comp 2	46.9	39.6	28.7
Comp 3	38.6	39.3	31.3
Comp Avg	*41.1*	*38.9*	*30.3*
Comp Standard Error	*2.9*	*0.5*	*0.8*
Mass flow 1	33.1	30.2	33.2
Mass flow 2	45.0	37.2	28.0
Mass flow 3	40.4	37.6	37.2
Mass flow 4	37.8	40.6	26.6
Mass flow 5	38.1	40.1	25.3
Mass flow 6	55.7	46.1	25.4
Mass flow Avg	*41.7*	*38.6*	*29.3*
Mass flow Standard Error	*3.2*	*2.1*	*2.0*
Overall Avg	**41.5**	**38.7**	**29.6**
Overall Standard Error	**2.2**	**1.4**	**1.3**

where Comp denotes composite

The percent solids of the three (3) concentrate streams show that over the duration of the circuit survey, the Lead flotation circuit was adequately stable as the standard error of all nine (9) samples was below 5%. The methodology used to calculate the percent solids and the standard error are shown in Appendix D.

5.2.1.2 *Experimental data obtained from the circuit survey*

As mentioned in Section 4.4.2, six (6) samples were collected to determine the mass flow of the concentrate streams. These six (6) samples were also used to calculate the percent solids of the concentrate streams. The percent solids for the remaining streams, i.e. the Rougher feed, intermediate tailings streams as well as the Scavenger tailings stream, was obtained from the average of the three (3) composite samples collected over the duration of the circuit survey. The composite samples were also used to obtain the assay data for all the flotation streams considered in this study. The average of the experimental data obtained from the circuit survey is shown in Tables 5.3 and 5.4.

Table 5.3: Experimental data obtained from the circuit survey

Stream Name	Slurry	%Solids	Copper assay	Lead assay	Zinc assay	Silver assay
	(kg/h)	(%)	(%)	(%)	(%)	(ppm)
Rougher Feed	450 675.6	54.7	0.1	2.2	2.5	38
1st Ro Conc	14 622.7	41.7	1.1	68.1	3.1	654
2nd Ro Conc	6 794.2	38.6	3.2	52.7	6.6	649
3rd Ro Conc	6 903.9	29.3	4.2	34.0	11.3	575
Scav Conc	3 410.8	3.4	4.7	27.1	13.6	523
1st Ro Tail	-	22.9	0.2	3.0	4.0	34
2nd Ro Tail	-	18.1	0.2	2.0	4.8	32
3rd Ro Tail	-	36.1	0.1	0.7	3.2	14
Ro Tail	-	45.9	0.1	0.2	2.7	18

The grade of the feed and tails streams obtained from the samples collected during the circuit survey were within the limits of the normal operating conditions of the BMM Concentrator. Table 5.3 shows some inconsistency in the percent solids and the assay data, for example the assay of lead in the 1st Rougher tailings stream was greater than that of the Rougher feed stream. The possible reasons for the inconsistency observed, specifically of the intermediate tailings streams, will be explored in more detail in later sections of this chapter.

Please refer to Appendix B for all the raw experimental data pertaining to mass flows, assay analysis and percent solids.

Table 5.4: Experimental bubble surface area flux (S_b) data

Cell name	S_b
	(sec^{-1})
1st Rougher	15.6
2nd Rougher	16.1
3rd Rougher	17.0
Scavenger	18.1

As mentioned in Section 4.4.2.3, although the raw data pertaining to the superficial gas velocity (J_g) and Sauter mean bubble size (d_{32}) measurements could have given significant insight to the operating conditions of the circuit, the data was not recorded by the metallurgical assistant during the circuit survey. The calculated bubble surface area flux (S_b) values are shown in Table 5.4, which shows that the bubble surface area flux increased down the bank of the Rougher flotation cells with the lowest being 15.6 sec^{-1} in the 1st Rougher flotation cell and the highest being 18.1 sec^{-1} in the Scavenger flotation cell. The S_b results

obtained for the Lead flotation circuit were significantly lower than those observed previously for a similar sized flotation cell, i.e. OK38, where the values obtained from the study conducted by Deglon and co-workers (2000) ranged between 43 and 63 sec^{-1}. However, it is important to note that the study reported by Deglon and co-workers in 2000 was conducted on flotation cells used in the platinum industry, where the operating density of the cells was significantly lower than that of the BMM Lead flotation circuit. The mineralisation of the ore was also significantly different whereby the ore fed to the platinum concentrators consisted of sparse minerals (i.e. overall concentration of sulphides in the feed less than 5%) and for BMM the sulphide mineral concentration was significantly higher. However, the S_b data obtained for the BMM Rougher and Scavenger flotation cells compared well to that of the Elura Lead flotation circuit in a study conducted by Grano (2006), where the S_b for the first Rougher cell was in the range of 14 – 33 sec^{-1} with the feed to the circuit being 55% percent solids.

It is important to note that although the cell used in the Grano (2006) study was approximately a quarter of the size of the BMM Lead Rougher flotation cells, the mineralisation and pulp characteristics, specifically the percent solids, were very similar.

The results obtained from the hot batch flotation tests conducted in Phase Two are shown in Figures 5.7 through 5.10.

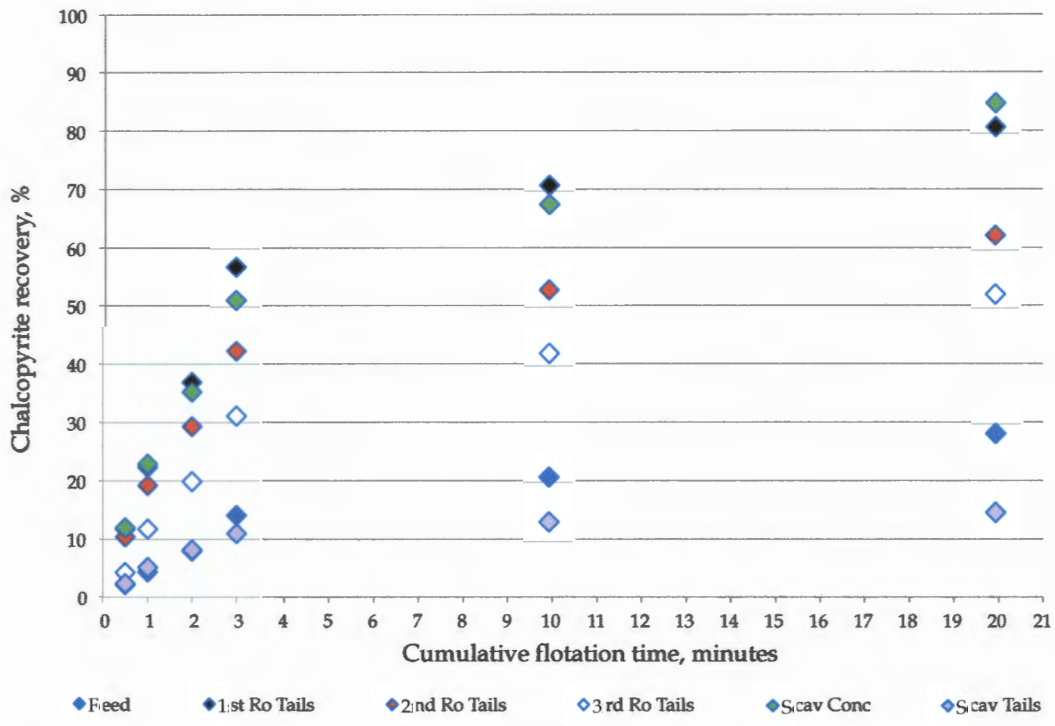

Figure 5.7: Cumulative chalcopyrite recovery (%) versus flotation time (minutes) for hot batch flotation tests conducted

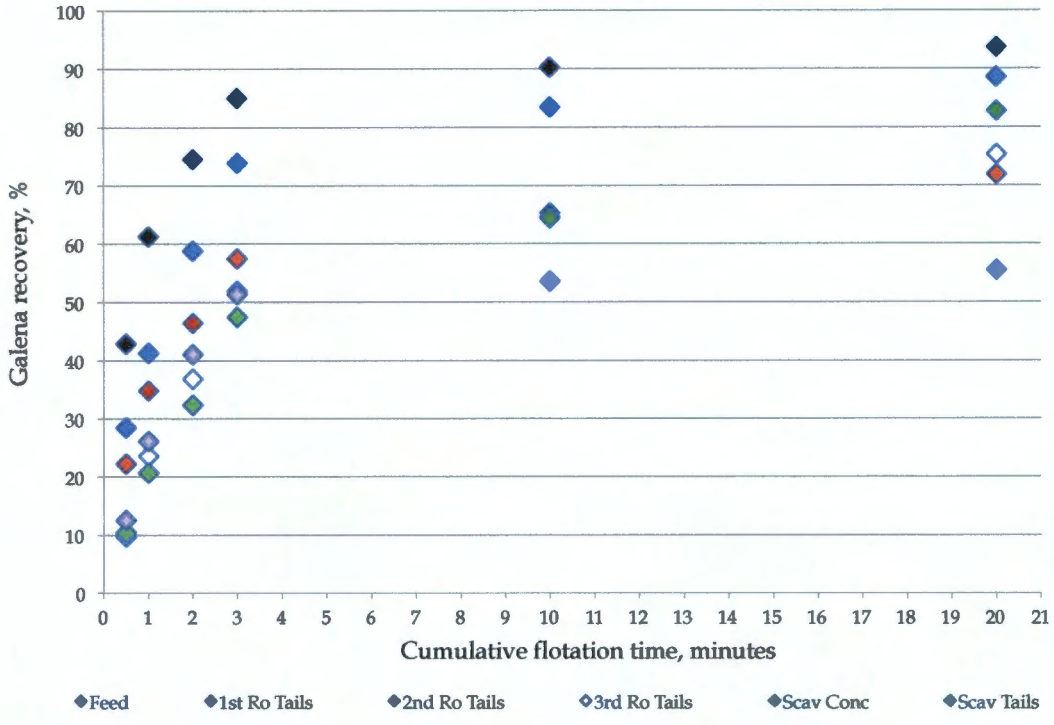

Figure 5.8: Cumulative galena recovery (%) versus flotation time (minutes) for hot batch flotation tests conducted

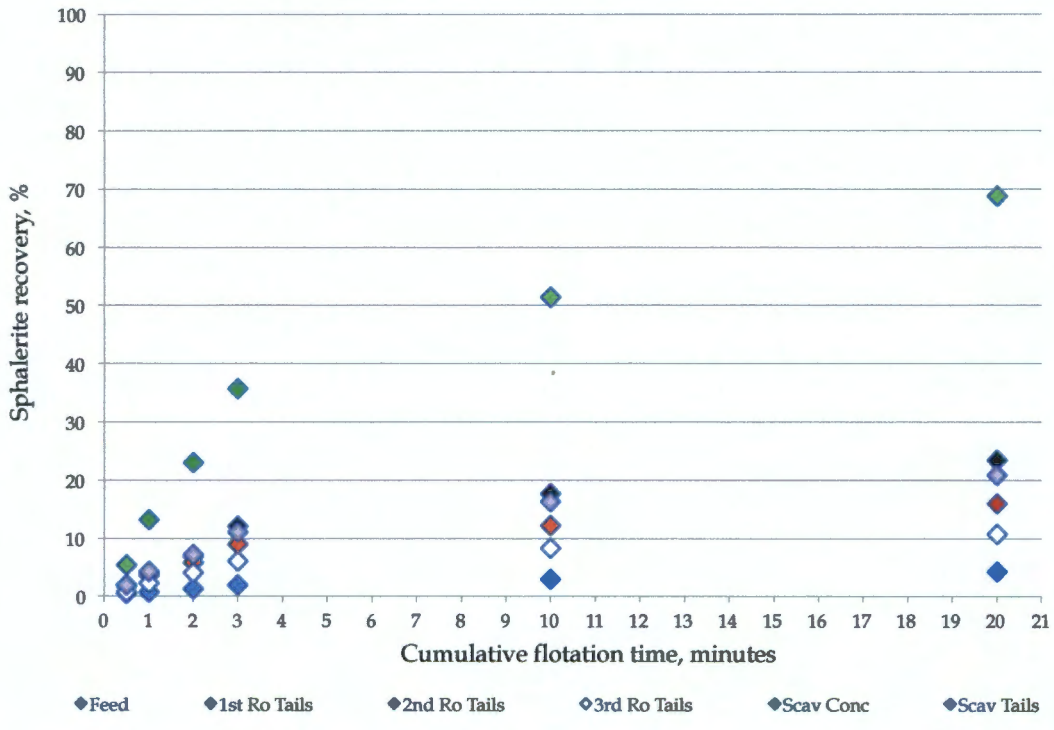

Figure 5.9: Cumulative sphalerite recovery (%) versus flotation time (minutes) for hot batch flotation tests conducted

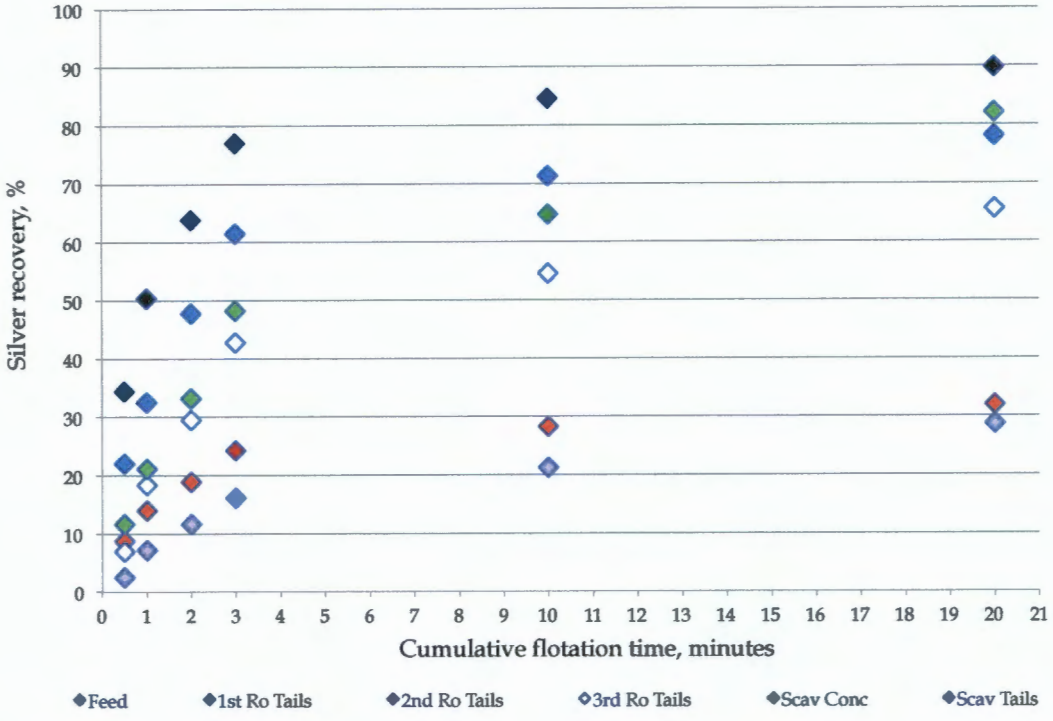

Figure 5.10: Cumulative silver recovery (%) versus flotation time (minutes) for hot batch flotation tests conducted

Inconsistencies in the results obtained from the hot batch flotation tests were observed when analysing the data. These will be discussed in Chapter 6.

5.2.2 Experimental stream properties calculated using circuit survey data

Table 5.5 shows all the mass flows of the various species considered for mass reconciliation in the Lead flotation circuit.

Table 5.5: Calculated species mass flows using experimental data

Stream Name	Solids (kg/h)	Water (kg/h)	Chalc* (kg/h)	Galena (kg/h)	Sphalerite (kg/h)	Silver (kg/h)
Rougher Feed	246 564.6	204 111.0	911.5	6 309.4	9 106.4	9.37
1st Ro Conc	6 094.1	8 527.1	193.4	4 795.2	277.9	3.99
2nd Ro Conc	2 624.4	4 169.3	244.3	1 596.8	257.7	1.70
3rd Ro Conc	2 021.1	4 883.9	246.7	792.8	341.0	1.16
Scav Conc	114.6	3 296.7	15.5	35.9	23.2	0.06

where Chalc* denotes chalcopyrite

Table 5.5 shows that the mass flow of chalcopyrite in the Rougher feed was significantly less than that of the galena and sphalerite minerals. This was due to the fact that the majority of the chalcopyrite minerals fed to the Concentrator were recovered in the Copper flotation

circuit, which preceded the Lead flotation circuit. It is important to note the low mass flows in the Scavenger concentrate for all species.

5.2.3 Results obtained from reconciling the data

The results obtained from the mass balancing process are outlined in this section.

5.2.3.1 *Quality of mass balance using parity charts*

Figure 5.11 shows the parity chart of the mass balanced assays versus experimental assays and Figure 5.12 shows the parity chart of the mass balanced flows of solids and water versus the experimental flows of solids and water. In both cases, it was assumed that the correlation between data was strong when the weighted sum of squared error was below or equal to five (5).

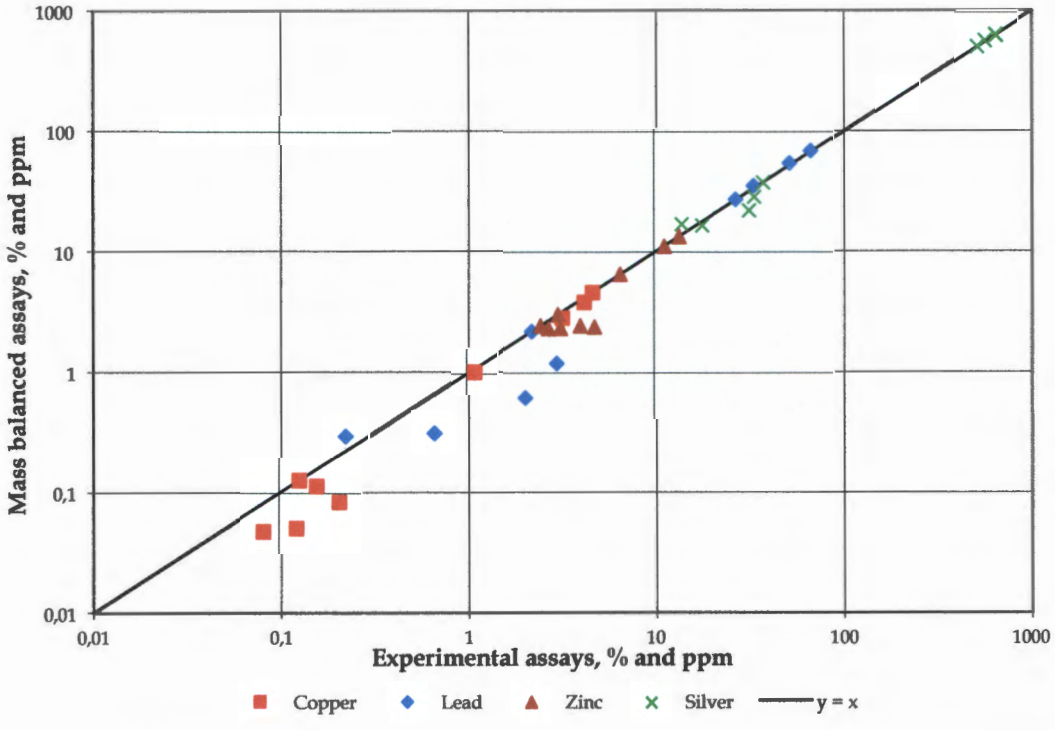

Figure 5.11: Parity chart of mass balanced assays versus experimental assays

Figure 5.11 shows that there was an overall strong correlation between the balanced and experimental data. However, when looking at the correlation of assays in more detail, i.e. looking at how the mineral assays in each of the streams compared, it was found that the Rougher feed, Rougher concentrates, Scavenger concentrates as well as the Scavenger tailings streams had strong correlations and that of the intermediate tailings streams did not. For the intermediate tailings streams the correlation of galena was strongest (R^2 of 0,927) and

chalcopyrite was weakest (R^2 of 0,187). These are indicated by the data points which deviated significantly below the y = x line in Figure 5.7.

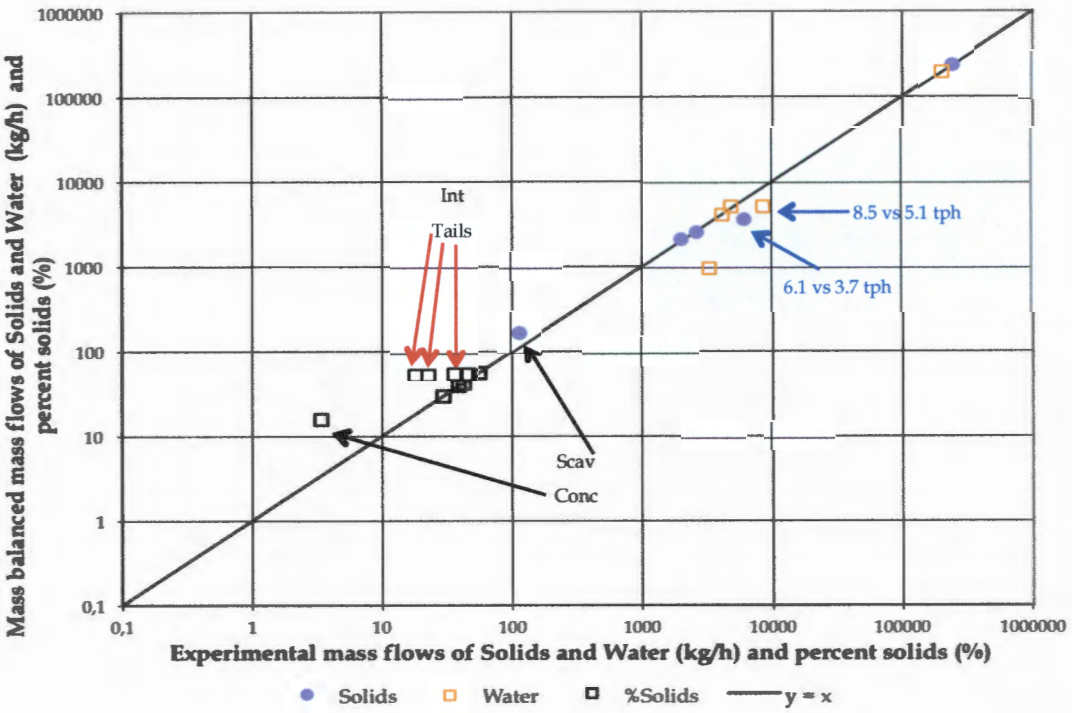

Figure 5.12: Parity chart of mass balanced flows (kg/h) versus experimental flows (kg/h)

Figure 5.12 shows that the overall correlation between the balanced and experimental solids and water flows was strong. Although not very clear from Figure 5.12, the correlation of solids and water flows in the 1st Rougher concentrate stream was weak and the balanced solids and water flows were only 60% of their respective experimental value (values shown in blue text in Figure 5.12). These data points are highlighted with the blue arrows.

The percent solids of the streams, and more specifically the percent solids of the intermediate and Scavenger tailings streams, was the most difficult to reconcile. When looking at the percent solids of the Rougher feed and concentrate streams, the streams were strongly correlated. However, the correlation of the Scavenger concentrate, intermediate tailings and Scavenger tailings streams was weak as seen by the significant deviation from the diagonal in Figure 5.12. The data points of the percent solids of the intermediate tailings streams, i.e. 1st through 3rd Rougher tailings streams, are highlighted in Figure 5.8 with the term "Int Tails" and red arrows and that of the Scavenger concentrate are highlighted with the term "Scav Conc" and black arrows.

The experimental percent solids data obtained from the circuit survey was not consistent with the law of conservation of mass, i.e. the percent solids of the feed to the circuit should have

been between that of the concentrate and tailings streams. For example, the percent solids of the Rougher feed was higher than that of the 1st Rougher concentrate and tailings streams. As the concentrate streams contained more water than solids (percent solids less than 50%) one would also expect that the percent solids of the tailings streams should have increased down the bank of the flotation cells since water was gradually removed from the system throughout the bank. The circuit feed and concentrate percent solids values correlated with typical Concentrator values but the intermediate tailings streams did not.

As mentioned in Section 4.4.2, the Rougher feed sample and Rougher concentrate samples were collected using a pelican sampler and the concentrate samples were collected by sampling at the respective cell lip. The intermediate tailings streams, i.e. 1st Rougher, 2nd Rougher and 3rd Rougher tailings streams, were sampled using a dip sampler. The inconsistency observed was possibly due to the sampler used for these intermediate tailings streams. More detail pertaining to the inconsistencies observed will be discussed in Chapter 6. Figure 5.13 shows the balanced stream data for the Lead flotation circuit considered in this study.

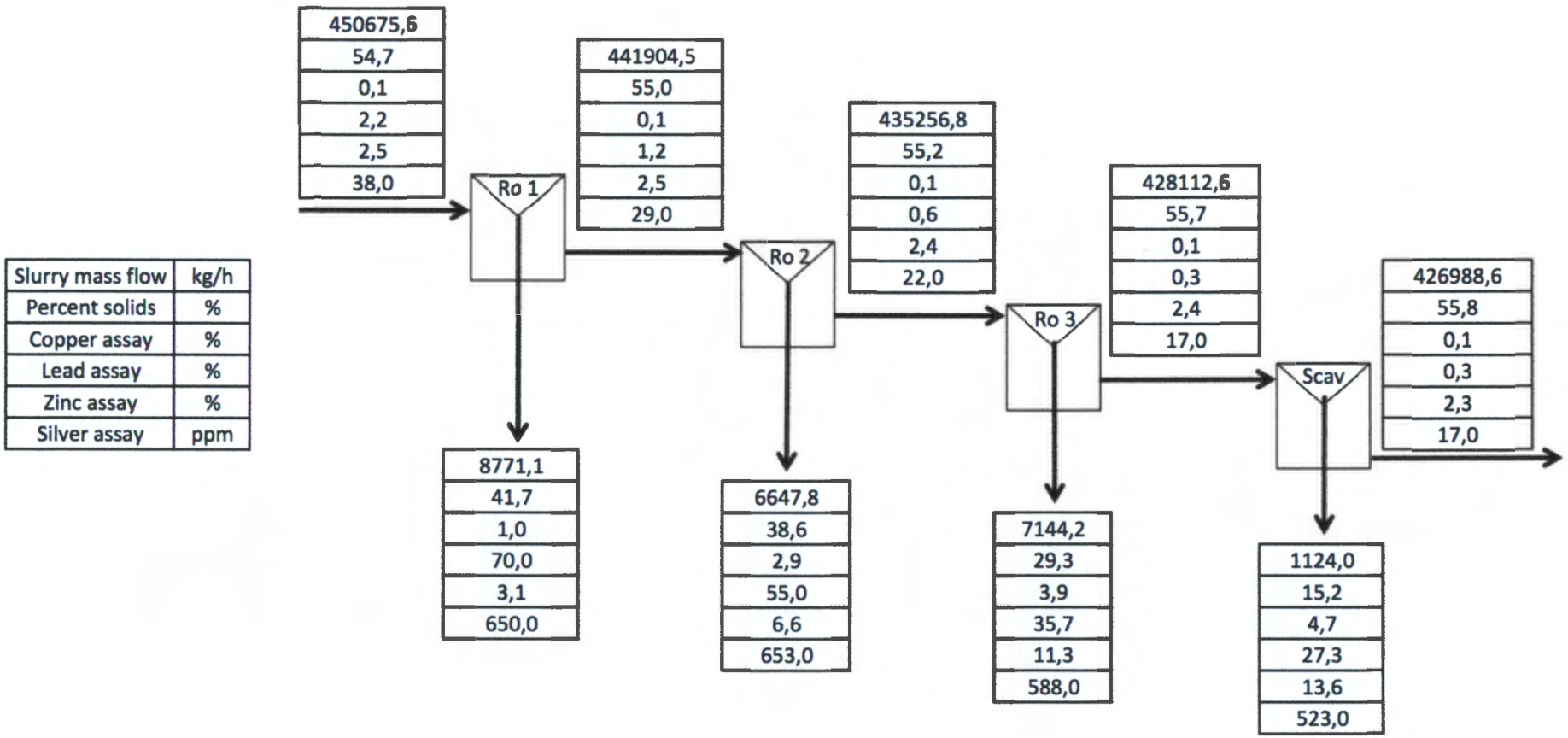

Figure 5.13: Circuit flowsheet showing stream properties

5.2.3.2 *Mass balanced recovery for all species*

Using the mass balanced data, the balanced recovery of the species was calculated across the Lead flotation circuit. It is important to note that the Rougher feed stream, which included the Cleaner tailings and Scavenger concentrate recycled streams, was considered as the feed to the part of the Lead flotation circuit under investigation and was, therefore, the basis for the mass recovery of the overall circuit. The balanced mass recovery for all species is shown in Table 5.6.

Table 5.6: Cell-by-cell recovery of the Lead flotation circuit using balanced data

Flotation Cell	Solids (%)	Water (%)	Chalc* (%)	Galena (%)	Sphal* (%)	Silver (%)	Remainder (%)
1st Rougher	1.5%	2.5%	12.0%	46.6%	1.8%	25.4%	0.2%
2nd Rougher	1.1%	2.1%	26.6%	48.4%	2.8%	24.0%	0.2%
3rd Rougher	0.9%	2.6%	39.4%	49.6%	4.0%	23.1%	0.3%
Scavenger	0.1%	0.5%	6.5%	6.2%	0.4%	2.2%	0.0%
Circuit recovery (balanced data)	**3.4**	**7.4**	**63.4**	**87.0**	**8.8**	**57.3**	**0.7**

where Chalc* denotes chalcopyrite and Sphal* denotes sphalerite

Based on the mass balanced data, the overall circuit recovery of galena and silver was 87.0% and 57.3% respectively. Table 5.6 also shows that the unit recovery was very low in the Scavenger flotation cell for all species. This will be discussed in some more detail in the sections.

5.2.3.3 *Error associated with the mass balanced data*

Using the method described in Section 4.6.1.7, the total weighted sum of squared error for the mass balancing process was 98.7. Table 5.7 shows the total contribution per stream towards the overall error. As previously mentioned in Section 4.6.1, it was assumed that a weighted sum of squared error equal to or lower than five (5) showed strong correlation between the balanced and experimental data.

Table 5.7: Weighted sum of squared error per species for mass balancing

Stream Name	Solids	%Solids	Chalc*	Galena	Sphalerite	Silver	Contribution (%)
Rougher Feed	0.0	0.0	0.0	0.0	0.0	0.0	0.0
1st Ro Conc	1.3	0.0	0.4	0.1	0.0	0.0	1.8
2nd Ro Conc	0.0	0.0	1.2	0.3	0.0	0.0	1.6
3rd Ro Conc	0.1	0.0	0.8	0.4	0.0	0.0	1.3
Scav Conc	0.2	-	0.0	0.0	0.0	0.0	0.3
1st Ro Tail	-	-	1.9	16.1	3.8	0.6	22.7
2nd Ro Tail	-	-	8.8	21.4	6.1	2.4	39.1
3rd Ro Tail	-	-	8.5	12.2	1.6	1.3	23.8
Ro Tail	-	-	4.3	4.4	0.5	0.1	9.5
Total	**98.7**						

where Chalc* denotes chalcopyrite

Table 5.7 shows that the error associated to the galena mineral was significantly higher than any other species. This was due to the galena being assigned the lowest relative standard deviation, as mentioned in Section 4.6.1.2, which constrained the mass balancing for galena significantly more than the other species.

It is important to note that the streams, which contributed the most error to the overall mass balancing error, were the intermediate tailings streams. As mentioned in Section 5.2.2.1, the mass balanced assays of all species, solids and water mass flows as well as the percent solids for these streams, i.e. the 1st through 3rd Rougher tailings streams, had a poor correlation with the experimental data. As previously mentioned, this will be discussed in some more detail in Chapter 6.

5.2.4 Results obtained from model fitting the circuit and batch testwork data

The modelling of the Lead flotation circuit was done using the FCM approach, which entailed simultaneously model fitting the data obtained from the circuit survey and the hot batch flotation tests.

As mentioned in Section 4.6.2, the methodology used for model fitting was to adjust the parameters of the enhancement factor equation in order to minimise the difference between the model predicted and the balanced data. Since the enhancement factor per species was obtained by combining the mineral floatability (P), bubble surface area flux (S_b) and the froth

recovery per flotation cell (R_f), the enhancement factor, and indirectly the flotation rate constant and recovery of the species, was adjusted by model fitting the mineral floatability and froth recovery parameters. The S_b of the flotation cells was measured experimentally and was shown in Table 5.4 (cf. Section 5.2.1.2). Similarly, for the recovery of the remainder, the enhancement factor was adjusted by model fitting the degree of entrainment of the gangue (ENT_{gangue}).

Based on the model predicted flow of species, the flow of the concentrates and tailings streams were determined, as well as the residence time of the flotation circuit (by means of the tailings flows). The results obtained from the model fitting process are outlined in this section.

5.2.4.1 *Model fitted parameters*

The mass fractions per sub-class, floatability constants per sub-class, froth recovery values, degree of entrainment and water recovery parameters ("a" and "b" in Equation 2.6) were obtained as described in Section 4.6.2.3. The sub-class mass fractions, or mass distributions, in the circuit feed are shown in Table 5.8 and the floatability constants per sub-class are shown in Table 5.9.

Table 5.8: Feed mass distribution for the sub-classes of mineral species

Mineral Species	Fast	Slow	Non-floating
Chalcopyrite	0.0%	40.3%	59.7%
Galena	21.0%	73.2%	5.8%
Sphalerite	4.8%	23.0%	72.2%
Silver	28.6%	40.9%	30.4%
Remainder	0.0%	0.0%	100.0%

Using the criteria outlined in Section 4.6.2.1, 5.8% of the galena was found to be non-floating. The model fit resulted in 21.0% of the galena being considered as fast floating and 73.2% as slow floating. It is important to note that although silver has been found to be associated mostly with galena in the BMM ore, with reference to the results shown in Section 5.1.3, this correlation was not observed from the floatability sub-classes for silver. More specifically, there was significantly more non-floating silver than non-floating galena. The implication of this will be discussed later.

It is also important to note the mass distribution of chalcopyrite and sphalerite. There was no fast floating chalcopyrite in the Lead flotation circuit as it had all been recovered in the Copper flotation circuit. But 40.3% of the chalcopyrite in the Lead flotation circuit feed could

still be classified as slow floating. Although sphalerite was actively depressed in the Lead flotation circuit, a small portion of the sphalerite, i.e. 4.8%, was fast floating and 23.0% was slow floating. However, the majority of the mineral at 72.2% was non-floating. As mentioned, it was assumed that all the remainder was recovered by entrainment and, therefore, it was considered entirely non-floating.

Table 5.9 Floatability constants per sub-class of species

Mineral Species	Fast	Slow	Non-floating
Chalcopyrite	0.0	1.3×10^{-4}	0.0
Galena	2.8×10^{-2}	2.4×10^{-4}	0.0
Sphalerite	1.3×10^{-4}	1.4×10^{-6}	0.0
Silver	2.0×10^{-3}	1.6×10^{-4}	0.0
Remainder	0.0	0>0	0.0

Table 5.9 shows the highest floatability constant was 2.8×10^{-2} for fast floating galena and the lowest floatability constant was 1.4×10^{-6} for slow floating sphalerite. The fast floating galena was approximately 10 times higher than its closest competitor, i.e. fast floating silver, and 100 times higher than the slowest fast floating sulphide gangue mineral, i.e. sphalerite. When looking at the floatability constants of the slow floating species, the floatability of galena was only somewhat higher than the chalcopyrite and silver, with the same order of magnitude, and it was 100 times higher than sphalerite.

Table 5.10 shows the model fitted froth recovery for each of the flotation cells. It is important to note that it was not possible to model the Lead flotation circuit with a single froth recovery value per flotation cell, i.e. one (1) froth recovery for all species in each flotation cell.

Table 5.10: Model fitted froth recovery for the flotation cells

Flotation Cell	Chalc*	Galena	Sphalerite	Silver
	(%)	(%)	(%)	(%)
1st Rougher	22.6	22.9	31.5	12.8
2nd Rougher	28.8	45.5	46.0	29.8
3rd Rougher	49.8	47.6	90.3	52.9
Scavenger	19.5	4.2	33.6	5.9

The model fitted froth recovery tabulated in Table 5.10 shows that all of the species showed similar behaviour in the froth zone, i.e. for all species the froth recovery increased from the 1st to the 3rd Rougher flotation cell and reduced significantly in the Scavenger flotation cell. It is important to note the exceptionally high froth recovery of sphalerite in the 3rd Rougher flotation cell, which does not seem realistic. This was primarily due to the fact that the experimental zinc assay, and hence sphalerite mass flow, in the 3rd Rougher concentrate was significantly higher than the preceding cells. The froth recovery results obtained will be discussed in more detail in Chapter 6.

Based on the solids flow in the concentrate streams, the water recovered into the concentrate streams was calculated using Equation 2.6 (cf. Section 2.4.5.5). The model fitted "a" value was 2.4 and "b" value was 0.6.

Using the calculated water recovery, the recovery of entrained gangue (remainder) was calculated using Equation 2.5 (cf. Section 2.4.5.4) by model fitting the degree of entrainment parameter for the remainder. The degree of entrainment of the remainder was 0.07.

5.2.4.2 *Model predicted outputs*

Based on the model predicted flow of water and solids, the water recovery was calculated from the feed and concentrate streams of each flotation cell. Furthermore, using the water and solids flows of the tailings streams the residence time for each flotation cell was calculated. The model predicted and balanced water recovery and residence times per flotation cell are shown in Table 5.11.

Table 5.11: Model predicted and balanced water recovery (%) and residence time (minutes) for the flotation cells of the Lead flotation circuit

Flotation Cell	Balanced R_w	Predicted R_w	Relative error for R_w	Balanced res. time	Predicted res. time	Relative error for res. time
	(%)	(%)	(%)	(minutes)	(minutes)	(%)
1st Rougher	2.5	2.5	1.0	9.2	9.2	0.0
2nd Rougher	2.1	1.9	7.3	9.4	9.4	0.2
3rd Rougher	2.6	1.4	44.6	9.6	9.5	1.2
Scavenger	0.5	0.5	8.9	7.2	7.2	1.2

Table 5.11 shows that the model predicted water recovery decreased down the flotation bank and that the balanced and model predicted water recovery of the 1st and 2nd Rougher flotation cells as well as the Scavenger flotation cell correlated, i.e. the relative error was below 10% and the R^2 for these data points was 0,997. However, the relative error of the balanced and

model predicted water recovery for the 3rd Rougher flotation cell was significant at 44.6%. The reasons for this will be explained later in the section.

In terms of the residence time of the circuit and flotation cells, the model predicted data strongly correlated with the balanced data as shown in Table 5.11. The model predicted residence time increased down the bank from the 1st to the 3rd Rougher flotation cell. The values were, however, fairly similar as the volume of the concentrate removed in each cell was small. Since the Scavenger flotation cell was smaller in size compared to the three (3) preceding flotation cells, i.e. 30m^3 versus 40m^3, the residence time of the Scavenger flotation cell was significantly shorter.

5.2.4.3 *Galena recovery by floatability class*

Although it is important to look at the overall mass flow of each stream and the grade and recovery of the various species in the stream, it is also important to analyse the composition of the stream based on the floatability parameters. Simply put, determine how the portion of each sub-class is distributed based on recovery into the various streams and how much each sub-class, i.e. fast, slow and non-floating, contributes to the overall species mass flow of the particular stream. Figure 5.14 shows the floatability distribution of galena in the flotation streams in this study. The magnitude of the bars represents the mass flow of galena of that floatability class in that particular stream with reference to the Rougher feed stream.

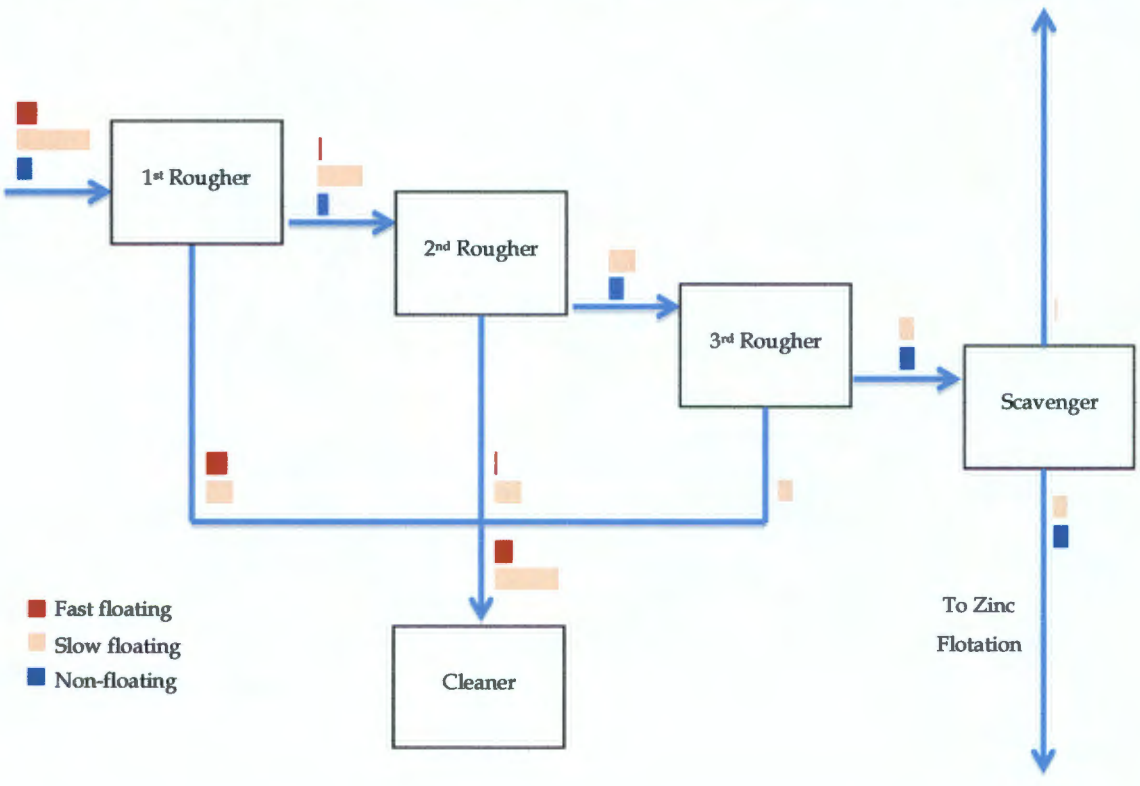

Figure 5.14: Floatability distribution of fast, slow and non-floating galena in circuit streams

Figure 5.14 shows that the majority of the fast floating fraction was recovered in the 1st Rougher concentrate stream, i.e. 98.2%, and the remaining fast floating galena was recovered in the 2nd Rougher concentrate stream. With respect to galena, the 3rd Rougher and Scavenger concentrate streams were made up entirely of slow floating material. A total of 85.4% of the slow floating galena was recovered across the flotation circuit, with the 1st and 2nd Rougher flotation cells recovering almost equal proportions (32.7% and 33.9% respectively). Only 1.2% of the slow floating galena was recovered into the Scavenger concentrate resulting in 14.6% of the slow floating fraction lost to the Scavenger tailings stream. All non-floating galena entering the Lead flotation circuit exited in the Scavenger tailings stream and was fed to the Zinc flotation circuit. The galena in the Scavenger tailings stream was made up of 64.8% slow floating and 35.2% non-floating galena by mass.

5.2.4.4 *Correlation of model predicted data*

Since the connection matrix and enhancement factors predicted the mass flows of the species across the circuit, the error between the balanced and model fitted mass flows was minimised during the model fitting process, as mentioned in Section 4.6.2. Figure 5.15 shows the parity chart of the predicted mass flows for all species and the percent solids versus the mass balanced mass flows of all species.

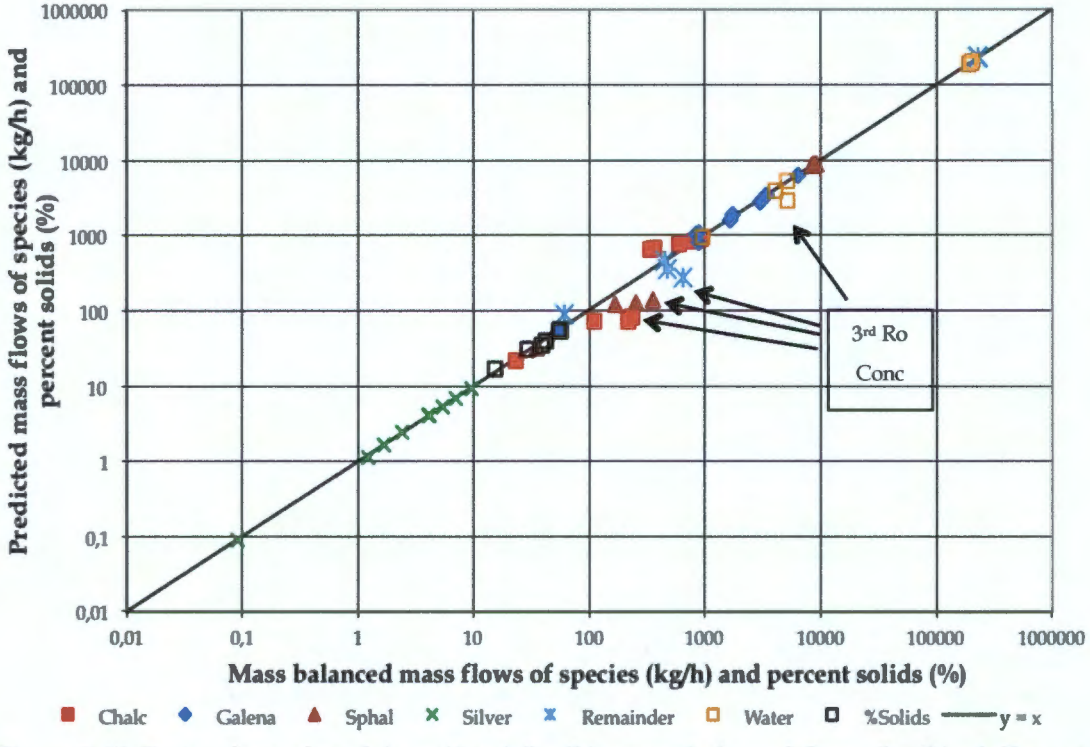

Figure 5.15: Parity chart of model predicted (kg/h) versus balanced flows (kg/h) of all species

Figure 5.15 shows that there was good correlation, in general, between the predicted and mass balanced data. The stream which showed the weakest correlation for multiple species

was the 3rd Rougher concentrate where the water, chalcopyrite, sphalerite and remainder mass flows deviated significantly from the y = x line, highlighted by the black arrows in Figure 5.15. It is important to note that the correlation of chalcopyrite was weak for the Rougher concentrate streams, i.e. 1st through 3rd Rougher concentrate, which was influenced by the model fitting of the hot batch flotation test data. This will be discussed in some more detail in Chapter 6.

5.2.4.4.1 Predicted concentrate quality based on modelled data

Table 5.12 shows the predicted assay of the concentrate streams as well as the average BMM assay of the final lead concentrate based on historical data, i.e. 2013 financial year. The galena assay of the combined Rougher concentrates, i.e. 1st through 3rd Rougher concentrate streams, predicted by the model was 76.8% compared to the mass balanced value of 65.4%.

Table 5.12: Model predicted and historical average assay of the concentrate streams

Stream Name	Chalcopyrite (%)	Galena (%)	Sphalerite (%)	Silver (ppm)	Remainder (%)
1st Ro Conc	2.1	82.3	3.5	708	12.0
2nd Ro Conc	3.5	75.6	5.9	796	14.9
3rd Ro Conc	6.6	64.2	10.8	893	18.4
Scav Conc	12.2	29.5	18.0	500	40.3
Combined Ro Conc	3.4	76.8	5.6	770	14.1
Avg BMM Final Conc	2.8	81.6	4.8	656	10.8

It is important to note that the average BMM concentrate assay was based on the final product from the Lead flotation circuit, i.e. the Cleaner concentrate. Therefore, from Table 5.12 it was observed that only the 1st Rougher concentrate was at a final concentrate grade and the remaining individual concentrates, i.e. 2nd Rougher, 3rd Rougher and Scavenger concentrate streams, would require additional upgrading in a Cleaning stage.

5.2.4.4.2 Predicted circuit recovery for all species

The circuit recovery of the species was predicted across the Lead flotation circuit using the model parameters as described in Section 4.6.2. As with the mass balanced data, it is important to note that the Rougher feed stream, which included the recycled Lead flotation circuit streams, was used as the basis for the mass recovery calculations of the circuit and the unit recovery for each flotation circuit was based on the feed to the specific flotation cell. The predicted mass recovery for all species per flotation cell is shown in Table 5.13.

Table 5.13: Cell-by-cell recovery of the Lead flotation circuit using modelled data

Flotation Cell	Solids (%)	Water (%)	Chalc* (%)	Galena (%)	Sphal* (%)	Silver (%)	Remainder (%)
1st Rougher	1.4	2.5	7.9	44.5	1.3	25.8	0.2
2nd Rougher	0.9	1.9	8.7	45.4	1.4	24.1	0.1
3rd Rougher	0.5	1.4	10.9	42.8	1.6	21.6	0.1
Scavenger	0.1	0.5	3.2	4.9	0.4	2.2	0.0
Circuit recovery (modelled data)	**2.8**	**6.1**	**27.5**	**83.5**	**4.5**	**56.8**	**0.5**

where Chalc* denotes chalcopyrite and Sphal* denotes sphalerite

Based on the output of the model, the overall circuit recovery of galena and silver was 83.5% and 56.8% respectively. Table 5.13 also shows that the unit recovery was significantly lower for the Scavenger flotation cell compared to the preceding Rougher flotation cells.

When comparing the predicted recovery of galena with actual historical data from the BMM metallurgical reports, it shows that the model predicted galena recovery was very comparable with what has been achieved by BMM. For the financial year of 2013, there were 10 instances, three (3) of which were in the month the circuit survey was conducted, when the lead assay of the Copper flotation circuit tailings stream was in the range of 2.2%to 2.3% lead. The average galena recovery for these instances was 83.1%. Therefore, the model predicted recovery was within a 99% confidence level of the average historical galena recovery observed at BMM. Although lower recoveries have been reported, typically the silver recovery achieved at BMM was above 60.0% for the Lead flotation circuit. The predicted silver performance was, therefore, not consistent with what was achieved at the BMM Concentrator during the period the circuit survey was conducted and the possible reasons for this will be discussed in later sections.

Figure 5.11 shows the model predicted chalcopyrite, galena and sphalerite recovery as a function of the circuit's residence time. In order to get an understanding of the effect on mineral recovery if the residence time of the circuit was extended to 60 minutes, it was assumed that the increase in residence time could be achieved by the addition of another Scavenger flotation cell to the circuit or increasing the cell volume of the existing Scavenger flotation cell. It was also assumed that the froth recovery (R_f) and bubble surface area flux (S_b) of the additional cell or the bigger Scavenger flotation cell was the same as that found for the existing Scavenger flotation cell in this study, e.g. 4.2% froth recovery for galena and S_b of 18.1 sec^{-1}. The predicted chalcopyrite, galena and sphalerite recovery for the increased circuit recovery is also shown in Figure 5.16. Figure 5.17 shows the model predicted chalcopyrite and sphalerite recovery as a function of water recovered into the concentrates.

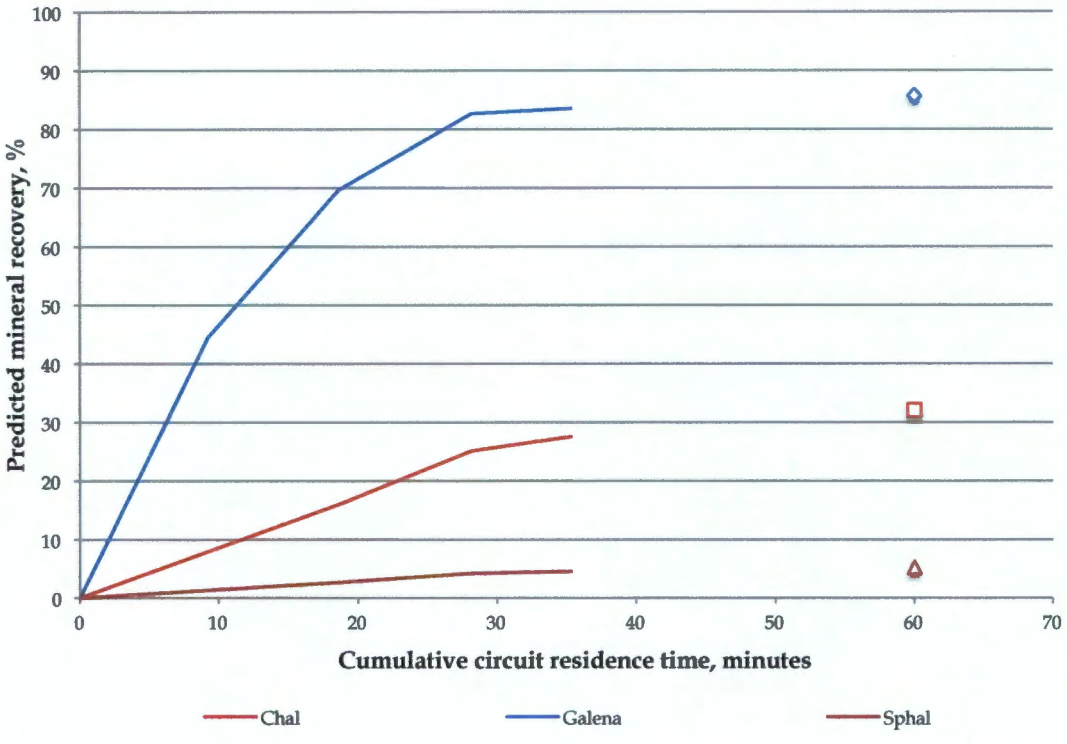

Figure 5.16: Model predicted recovery (%) versus cumulative residence time (minutes) of chalcopyrite, galena and sphalerite

Figure 5.16 shows the mineral recovery increases with residence time for all sulphide species. Furthermore, Figure 5.16 shows that an increase in residence time to 60 minutes (markers with white fill) will result in an increase in galena recovery, which is desired, as well as the undesired increase in sulphide gangue minerals, i.e. chalcopyrite and sphalerite.

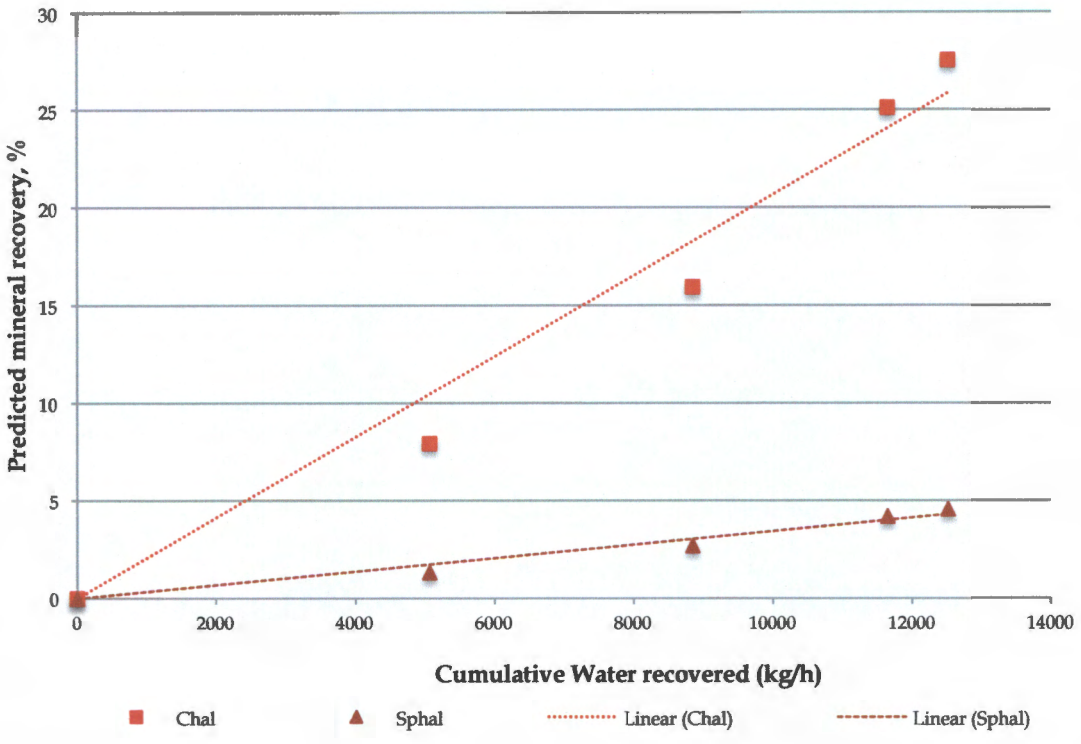

Figure 5.17: Model predicted cumulative recovery (%) versus water recovery (minutes) of chalcopyrite and sphalerite

The trendlines of chalcopyrite and sphalerite recovery versus water recovery in Figure 5.17 passed through the origin and showed a linear correlation which could suggest that some of the chalcopyrite and sphalerite that was recovered (possibly the ultrafine particles) may have been as a result of entrainment. However, since detail pertaining to the size-by-size recovery of minerals was not available for this study, this could not be validated.

5.2.4.5 *Error associated with the model fit*

As mentioned in Section 4.6.2, the circuit and batch flotation test data were model fitted simultaneously and the model parameters that influence the enhancement factors were adjusted in order to minimise the overall error, i.e. the error associated with the circuit data as well as the batch flotation test data. This section highlights the error contributions for both of these.

5.2.4.5.1 Error contributions for model fitting the circuit data

Table 5.14 shows the total contribution per species, per stream to the overall error.

Table 5.14: Weighted sum of squared error per species for modelling the circuit

Stream Name	Water	Chalc*	Galena	Sphalerite	Silver	Remainder	Contribution (%)
Rougher Feed	0.0	0.0	0.0	0.0	0.0	0.0	0.0%
1st Ro Conc	0.0	11.3	0.3	7.8	0.0	0.3	5.4%
2nd Ro Conc	2.1	43.3	0.1	25.4	0.0	11.3	22.6%
3rd Ro Conc	79.5	41.1	0.4	37.4	0.4	40.3	54.7%
Scav Conc	3.2	0.2	0.0	0.4	0.0	5.3	2.5%
1st Ro Tail	0.0	0.1	0.1	0.0	0.0	0.0	0.0%
2nd Ro Tail	0.0	2.2	0.4	0.0	0.0	0.0	0.7%
3rd Ro Tail	0.1	20.8	2.7	0.1	0.0	0.0	6.5%
Ro Tail	0.1	23.9	3.1	0.1	0.0	0.0	7.5%
Total	**363.8**						

Based on the relative standard deviation information supplied in Table 4.5, the total sum of squared errors for modelling the circuit was 363.8. Table 5.14 shows that the stream that contributed most significantly to the error was the 3rd Rougher concentrate stream. This reinforces the poor correlation noted between the species in this stream in the parity chart (cf. Figure 5.10). It is important to note that the model fit of the galena and silver data was good, as seen by the small error contribution of these species in all streams.

5.2.4.5.2 Error contributions for model fitting the batch flotation test data

Based on the relative standard deviation information supplied in Appendix C the total sum of squared errors for the model fitting of the batch flotation test was 472.1. Table 5.15 shows the total contribution per species, per test to the overall error.

Table 5.15: Weighted sum of squared error per species for modelling the batch flotation tests

Stream Name	Chalc*	Galena	Sphalerite	Silver	Contribution (%)
Rougher Feed	57.8	7.1	30.1	20.1	24.4
1st Ro Tail	0.8	0.3	1.1	0.4	0.6
2nd Ro Tail	0.8	0.1	1.1	0.1	0.5
3rd Ro Tail	0.7	0.1	1.2	0.6	0.5
Scav Conc	29.4	88.7	10.6	32.0	34.0
Ro Tail	49.7	56.4	58.4	24.5	40.0
Total	**472.1**				

As previously mentioned, the results from the tests conducted on samples collected from the intermediate tailings streams showed significant inconsistency. These streams were assigned a very high relative standard deviation and, therefore, had a low contribution to the overall weighted sum of squared error.

5.2.4.6 *Relationship between silver and galena in hot batch flotation tests*

As highlighted in Section 5.1 (Phase One of this study), a strong relationship was observed between the silver and lead (or galena) recovery. This section compares the results obtained from the hot batch flotation tests conducted during the circuit survey with those obtained during the validation testwork, and they are shown in Figure 5.18.

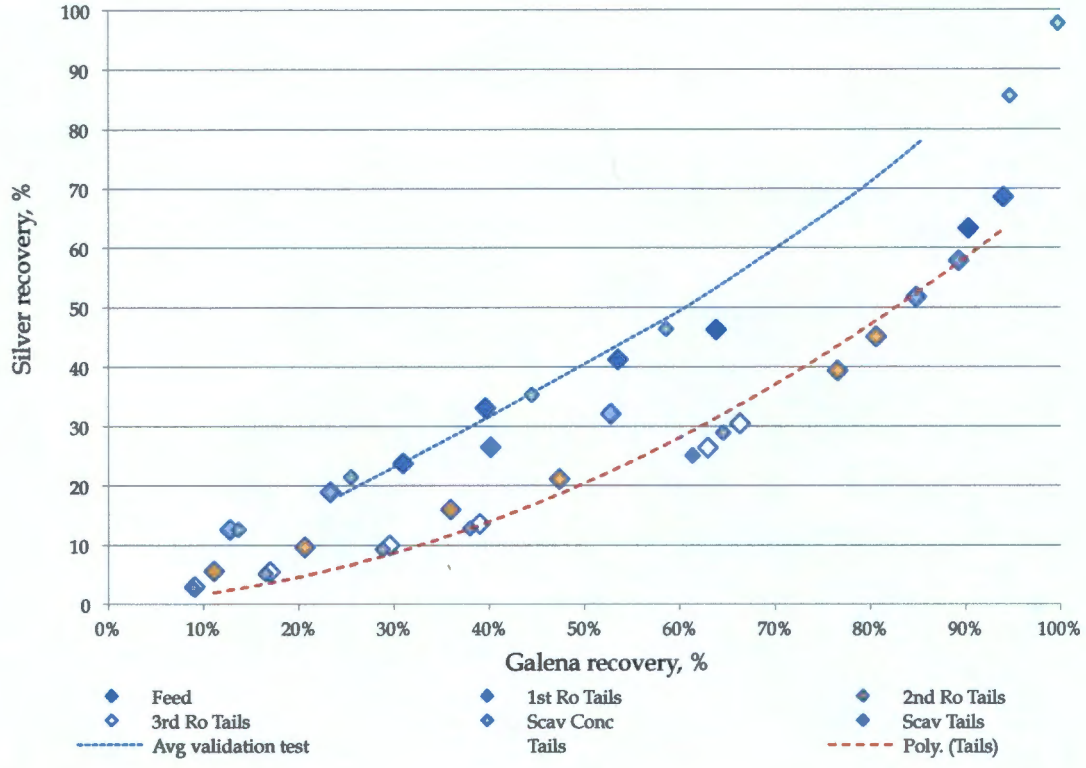

Figure 5.18: Cumulative silver recovery (%) versus galena recovery (%) for the batch flotation tests in Phase One and Phase Two

Figure 5.18 shows the relationship observed between silver and galena in the batch flotation tests conducted during Phase One (dashed blue line), and the results obtained from the hot batch flotation tests in Phase Two (diamond markers). When looking at the predicted silver recovery relative to the predicted galena recovery for the Phase Two hot batch flotation tests conducted, it was apparent that there were two bands of results. The streams that showed the best correlation to the Phase One results were the Rougher feed and Scavenger concentrate streams, even though the last two data points of the Rougher feed stream deviated somewhat from the relationship. Figure 5.18 also shows that the data points from the 2nd Rougher, 3rd Rougher and Scavenger tailings streams appeared to follow a separate trendline, highlighted by the dashed red line. The upper band (blue dashed line) appears to represent samples where the proportion of floating material outweighed non-floating material for these streams, whereas the lower band (red dashed line) represent the streams which contained predominantly non-floating material. This will be discussed in more detail in Chapter 6.

5.3 Summary of results

This section gives a summary of the results obtained in this study.

5.3.1 Repeatability of batch flotation test procedure

The results obtained from the tests conducted to determine the repeatability of the batch flotation test procedure showed that the recovery of solids, lead and silver were sufficiently consistent for all three (3) tests. The infinite recovery (R_{inf}), determined using the Klimpel model, for the repeatability tests was 87.6%. Although the average cumulative lead recovery achieved after a cumulative flotation time of 20 minutes was below the infinite recovery (97.3% of R_{inf}), it was significantly better than what would have been achieved if the flotation tests were conducted for seven (7) minutes, as per the BMM SOP. Hence the flotation time of 20 minutes adequately represented infinite time recovery.

5.3.2 The effect of ageing on metal recovery

The results obtained from the four (4) tests conducted showed that there was a gradual decrease in lead and silver metal recovery when the samples were floated after different periods of storage time. However, the reduction in recovery for the one (1) and three (3) hour tests was not significant. The results obtained for the sample that was allowed to age for a day show that the kinetics of lead and silver were nearly half that of the reference test. The lead and silver cumulative recovery of Test 4 were 58.4% and 49.4% compared to 89.5% and 79.1% for the reference test respectively. Hence, it was decided that it was imperative to carry out the batch tests immediately after the sample had been collected or no longer than 1 – 3 hours after collection.

5.3.3 Silver-galena relationship for batch flotation tests

In Phase One, the batch flotation tests conducted using the Copper Tails Thickener underflow and Rougher feed showed that there was a strong correlation between silver and lead metal. However, for the hot batch flotation tests conducted as part of Phase Two, the relationship was not observed for all tests. The tests conducted on the samples collected from the Rougher feed and Scavenger concentrate streams showed the best correlation to the tests conducted during Phase One.

5.3.4 Circuit data reconciliation

5.3.4.1 *Stability of the Lead flotation circuit*

The percent solids of the nine (9) individual samples collected from the Rougher concentrate streams during the circuit survey had a standard error of only 2.2%, 1.4% and 1.3% for the 1st

Rougher concentrate, 2nd Rougher concentrate and 3rd Rougher concentrate streams respectively demonstrating that the circuit was sufficiently stable for the duration of the circuit survey.

5.3.4.2 *Inconsistency in data obtained from the intermediate tailings streams*

The experimental data obtained from the intermediate tailings streams showed inconsistencies in terms of the percent solids, assays as well as the results obtained in the hot batch flotation tests. The intermediate tailings samples were collected from the flotation cells using a dip sampler and it is possible that the sampling procedures were a factor in contributing to the inconsistencies.

5.3.4.3 *Quality of mass balance and error associated with reconciliation*

The mass balanced data showed good correlation with the experimental data, apart from the intermediate tailings streams that were more difficult to reconcile. The intermediate tailings streams, therefore, contributed the most to the overall error for the mass balancing process. The error contribution of galena was significantly higher than the other species and this was due to the low relative standard deviations that were assigned. The assignment of low relative standard deviations was such that the data reconciliation was done with greater confidence by using galena to drive the mass split across the cell.

5.3.5 Characterising the Lead flotation circuit

5.3.5.1 *Cell characteristics*

The bubble surface area flux values determined in the flotation cells increased down the bank and ranged from 15.6 sec^{-1} in the 1st Rougher flotation cell to 18.1 sec^{-1} in the Scavenger flotation cell. The values obtained for the BMM Concentrator were consistent with studies conducted at the Elura Lead Concentrator (Grano, 2006).

The froth recovery values for all species increased down the bank from the 1st through 3rd Rougher flotation cell. The froth recovery for Sphalerite in the 3rd Rougher flotation cell was unrealistically high (90.3%), especially when compared to the other species. The froth recovery of all species in the Scavenger flotation cell was significantly lower than the preceding 1st, 2nd and 3rd Rougher flotation cells.

5.3.5.2 *Ore characteristics*

Galena was classified into three (3) sub-classes with majority of the galena being slow floating. The silver sub-class distribution did not correlate with galena, specifically for the slow and non-floating fractions. Chalcopyrite did not demonstrate any fast floating

characteristics and was, therefore, classified into two (2) sub-classes, i.e. slow and non-floating. Sphalerite was made up of three (3) sub-classes with the majority being non-floating and a moderate amount, i.e. 23.0%, slow floating.

As expected the fast floating galena had the highest floatability constant, which was 10 times higher than silver and 100 times higher than sphalerite. The floatability constants of slow floating chalcopyrite, galena and silver were of the same order of magnitude. The floatability constant of the slow floating sphalerite was 100 times lower than the other valuable minerals. This was likely the result of the depression in the Conditioning stage.

5.3.5.3 *Adequacy of the model predictions*

A key finding from this study was that the FCM approach was able to adequately predict the performance of the Lead flotation circuit and the overall correlation between model predicted and balanced data was strong. There were some deviations from the diagonal in parity charts for chalcopyrite, sphalerite and the remainder in certain streams. The stream that showed poorest prediction was the 3rd Rougher concentrate and chalcopyrite was not well predicted in the Rougher concentrates streams, i.e. 1st through 3rd Rougher concentrate.

5.3.5.4 *Efficiency of the flotation units in terms of mineral recovery*

The unit recoveries of the 1st, 2nd and 3rd Rougher flotation cells showed that they were operating efficiently with respect to mineral recovery since they recovered more than 40% of the galena to each of their respective concentrate streams. However, the Scavenger flotation cell had a very low recovery for all species, including water.

5.3.5.5 *Galena recovery by floatability class*

The majority of the fast floating galena was recovered in the 1st Rougher flotation cell with the rest of the fast floating galena being recovered by the 2nd Rougher flotation cell. With respect to galena, the 3rd Rougher and Scavenger concentrate streams consisted of entirely slow floating material. A total of 85.5% of the slow floating galena fed to the Lead flotation circuit was recovered in the bank, although the Scavenger flotation cell contributed only 1.2% to this. All non-floating galena entering the Lead flotation circuit exited in the Scavenger tailings stream and was fed to the Zinc flotation circuit.

6 DISCUSSION

This chapter focuses on the discussion of results presented in Chapter 5.

6.1 Validation of batch flotation test procedure

This section discusses the results obtained from the validation testwork that was conducted prior to the circuit survey. The testwork included the validation of the batch flotation test procedure that would be used for hot batch flotation tests as well as the validation that floatability of minerals would be conserved during the circuit survey.

6.1.1 Validation of batch flotation test procedure

The plot of the cumulative solids recovery (Figure 5.1) and lead recovery (Figure 5.2) versus flotation time show that the results of the three (3) tests were repeatable. The results of the individual tests lay within a 95% confidence level, as can be seen by the error bars in the respective figures. Furthermore, the relative standard deviation for the average solids and lead recovery were both below 5% and the error of the reconciled feed grade for lead was below 10%, as per the guidelines set out in Section 4.5.2.

For silver the relative error of the average reconciled feed grade was above the limit of 10% at 16.3%, but the relative standard deviation for the total silver recovered of three (3) tests was 2.0%, which was below the 5% guideline. The standard deviation of the ICP-MS method used to analyse silver in high and low grade samples at BMM is 9.2% for low grade and 6.3% for high grade samples. The propagated error for the reconciled feed grade was, therefore, based on eight (8) high grade samples and one (1) low grade sample. The calculated propagated error was 20.2% and, therefore, the error between reconciled and measured feed grade of silver was within the tolerance of BMM standards. The methodology used to calculate the propagated error is shown in Appendix D. Furthermore, the average measured silver feed grade for the tests and the average reconciled grade was approximately 33 ppm and 39 ppm respectively. The average BMM circuit data, based on a three (3) month average, showed that the silver feed grade to the Lead flotation circuit was approximately 39 ppm. The reconciled feed grade was, therefore, in line with the average observed at BMM and this further validated that batch flotation test procedure was found to give repeatable results.

Using the Klimpel model, the R_{inf} for lead from the batch flotation tests was found to be 87.6%. After 20 minutes flotation time the average experimental cumulative lead recovery was 85.3%, equating to 97.3% of R_{inf}. If the test were only seven (7) minutes long, as per the BMM SOP, the average experimental cumulative lead recovery would have only been 87.7%

of R_{inf}. The flotation time was, therefore, set to be 20 minutes since the flotation time was practical and the cumulative lead recovery results obtained was adequate and as close as necessary to the infinite time recovery.

6.1.2 The effect of ageing on metal recovery

The results obtained showed that the samples could be left for up to three (3) hours without the recovery of lead and silver being significantly reduced. It is interesting to note, though, that even with one (1) hour standing time there was some reduction in cumulative lead and silver recovery. This could have been due to a number of reasons including a certain degree of oxidation or possible reactions between reagents. It is important, therefore, in carrying out such investigations on the performance of the circuit that the batch flotation tests are done as soon as possible after the sample is collected. The cumulative lead and silver recovery results from Test 4, which was conducted after a day standing time, showed that the rate of flotation of the lead and silver metal were significantly slower and the floatability of the lead and silver were negatively impacted. In order to prevent any possible ageing of the sample, it was decided that when conducting the hot batch flotation tests during the circuit survey, the sample would be floated immediately, i.e. while the sample was "hot".

6.2 Circuit survey data reconciliation

As mentioned previously, the first step in modelling a flotation circuit is reconciling the experimental data obtained. This section looks at the stability of the circuit during the circuit survey, the quality of the experimental data obtained from the circuit survey as well as the quality of the mass balanced or reconciled data.

6.2.1 Stability of the Lead flotation circuit

The Lead flotation circuit was found to be sufficiently stable throughout the circuit survey, as shown in the experimental percent solids data obtained for the Rougher concentrate streams (cf. Section 6.1.1). The standard error of the nine (9) individual 1st Rougher concentrate, 2nd Rougher concentrate and 3rd Rougher concentrate samples were 2.2%, 1.4% and 1.3% respectively.

6.2.2 Quality of the experimental data and reconciled data

The overall mass balance was found to be satisfactory since there was good correlation between most of the experimental and balanced assay data, i.e. of the 36 data points regarding the assay of the flotation streams, only six (6) data points had a weighted sum of squared error greater than five (5). The data of the intermediate tailings streams, i.e. assay, percent solids and mass flow data, were more difficult to reconcile which could be seen from

the deviation of points from the diagonal of the parity plot in Figures 5.11 and 5.12. It is thought that the sample integrity or representivity of the intermediate tailings samples was compromised due to the method of sampling, i.e. using a dip sampler. For example, the percent solids was significantly lower in the intermediate tailings streams than it should have been based on the principle of conservation of mass, i.e. since water was removed in the concentrate streams the percent solids of the tailings streams should have been greater than that of the feed to that flotation cell. The lower experimental percent solids could have been as a result of a leak in the sampler while extracting the sampler from the flotation cell or sampling in the incorrect zone in the flotation cell. By application of the principle of conservation of mass, the reconciled percent solids and assay for all species was found to be better aligned to what is observed at the BMM Concentrator, i.e. the percent solids of the intermediate tailings streams increased down the bank while the assay of the mineral species gradually decreased down the bank.

The assumption of compromised sample integrity was further substantiated by the results obtained from the hot batch flotation tests, which showed significant inconsistency in results. The inconsistencies of the hot batch flotation test results, as shown in Figures 5.7 through 5.10, were as follows:

1 The cumulative recovery of all species for the 1st Rougher tailings hot batch flotation test hot batch flotation test was consistently higher than that achieved for the Rougher feed hot batch flotation test. This was observed for all the individual concentrates recovered.
2 Although the cumulative recovery of chalcopyrite, galena and sphalerite was lower for the 2nd Rougher tailings hot batch flotation test compared to the 1st Rougher tailings hot batch flotation test, the recovery was still higher than that achieved for the Rougher feed hot batch flotation test. The silver recovery in the 2nd Rougher tailings hot batch flotation test was significantly lower, i.e. 32.0%, compared to the Rougher feed (78.1%) and 1st Rougher tailings (89.8%) hot batch flotation tests. Although the recovery of silver in the 2nd Rougher tailings hot batch flotation test was expected to be lower than that achieved in the 1st Rougher tailings hot batch flotation test, the significant reduction was unexpected since the recovery of the other minerals, specifically galena, did not show such a significant reduction.
3 For the 3rd Rougher tailings hot batch flotation test the cumulative recovery of chalcopyrite and sphalerite reduced in line with the reduction observed from the 1st to the 2nd Rougher tailings hot batch flotation test, e.g. chalcopyrite reduced from 81.2% to 62.5% to 52.4%. However, the cumulative recovery of galena and silver for the 3rd Rougher tailings hot batch flotation test was greater than that achieved for the 2nd Rougher tailings hot batch flotation test. This is not the typical trend observed in batch flotation tests since the amount of floatable valuable minerals decreases down the bank,

i.e. the Rougher feed hot batch flotation test should have the highest mineral recovery and the Scavenger tailings hot batch flotation test should have the lowest mineral recovery.

4 The cumulative recovery of chalcopyrite, galena and silver was lowest for the hot batch flotation test conducted on the Scavenger tailings sample. However, the sphalerite recovery of 20.8% was greater than that achieved for the Rougher feed, 2nd Rougher tailings and 3rd Rougher tailings hot batch flotation tests.

In summary, the results obtained for the Rougher feed, Scavenger concentrate and Scavenger tailings hot batch flotation tests were consistent and appeared to be representative, while the results from the hot batch flotation tests conducted on the intermediate tailings samples were not consistent with what is observed in practice, i.e. the cumulative recovery achieved for tests conducted on samples obtained down the flotation bank should show a gradual decrease in mineral recovery since there would be less recoverable metal down the flotation bank. However, this was not observed from the hot batch flotation test data.

6.3 Characterising the Lead flotation circuit

As mentioned in Chapter 3, this study was concerned with the modelling of the Lead flotation circuit using the Floatability Component Model (FCM) approach implemented in MS Excel with the Woodburn and Wallin (1984) matrix algorithm to reconcile the circuit mass balance. Using this modelling approach, all species were divided into sub-classes based on their floatability. Therefore, each species was assumed to consist of portions of the three (3) floatability classes, i.e. fast, slow and non-floating. Furthermore, based on previous work done by Gorain and co-workers (1998), it was found that the flotation rate constant (k) could be defined by the combination of the mineral floatability constant (P), bubble surface area flux of the flotation cell (S_b) as well as the froth recovery of the mineral in the flotation cell (R_f). Since the S_b and R_f of each flotation cell was assumed to remain constant, the floatability or hydrophobicity of the mineral was directly proportional to the floatability constant (P), i.e. a high floatability constant indicated fast kinetics and highly hydrophobic particles while a lower floatability constant (for slow floating material) indicated slower kinetics and moderately hydrophobic particles. It is important to note that the terms fast and slow floating were relative to each of the species or minerals themselves and not to all the floating species present in the circuit, i.e. although sphalerite was observed to consist of two floating classes defined as fast and slow floating sphalerite, the kinetics of sphalerite were found to be much slower relative to galena, chalcopyrite and silver.

The Floatability Component Model requires several parameters to be fitted that are related to the ore (floatability and amount of material in each floatability class, as well as the degree of entrainment), the flotation cell (froth recovery) and the circuit ("a" and "b" model fitted

parameters used to calculate the water recovery per flotation cell). In order to constrain the model, the data obtained from hot batch flotation tests were used since they gave additional data pertaining to the kinetics of the minerals (based on the inherent mineral floatability) in the various flotation streams and allowed for a more robust fit.

Typically, hot batch flotation tests are conducted on samples of the feed stream to the circuit and as many other streams as it is possible to access, or that are required to complete a nodal balance. Rougher or Cleaner concentrate stream samples would generally contain large amounts of fast floating material, which would cause significant difficulty for the batch flotation cell operator to control the scraping of froth and could cause inaccurate results. Tailings streams or Scavenger concentrate streams, on the other hand, contain smaller amounts of fast floating material and, therefore, makes it easier to perform the hot batch flotation test accurately. Using this guideline, the hot batch flotation tests conducted in this study were only done for the Rougher feed, intermediate tailings, Scavenger concentrate and Scavenger tailings streams. However, it was found after processing the data from the intermediate tailings streams that those tests were not representative, as discussed in Section 6.2.2, and the results from the intermediate tailings tests were, therefore, not used to constrain the model. Therefore, only the results from the Rougher feed, Scavenger concentrate and Scavenger tailings hot batch flotation tests were used to constrain the model by means of assigning lower relative standard deviations to the mineral recovery data. The Rougher feed and Scavenger tailings hot batch flotation tests were used to assign the initial estimates of the mass fractions (fast and non-floating) and floatability constants per sub-class (fast and slow).

6.3.1 Ore floatability component parameters

6.3.1.1 *Galena*

The overall correlation of balanced and model predicted mass flow of galena was strong. The behaviour of the galena in the flotation circuit was characterised in terms of three (3) sub-classes, i.e. fast, slow and non-floating. About one fifth of the galena in the Rougher feed was found to be fast floating, with a floatability constant 10 times higher than the fast floating silver. The entire fast floating galena was recovered in the circuit (cf. Figure 5.14). Only 5.8% was found to be non-floating, which was comparable with results obtained from a mineralogy study conducted by Anglo Research Mineralogical Research Department (ARMRD) in 2008 (Bramdeo et al., 2008). In the ARMRD study it was determined that of the feed to the Lead flotation circuit, 5.2% of the galena minerals were locked and associated with gangue. Furthermore, that study highlighted the fact that 84% of the galena in the feed to the Lead flotation circuit was well liberated, i.e. more than 80% of the particle was the mineral of interest.

The floatability constant of the slow floating fraction of the galena in the Rougher feed was the same order of magnitude as the slow floating fraction of chalcopyrite and silver, and 100 times higher than slow floating sphalerite. It was also found in the mineralogical study (Bramdeo et al., 2008), that the high and medium grade middlings (where 30% to 80% of the particle was the mineral of interest, i.e. galena) of the Lead flotation circuit feed consisted of galena minerals that were associated with sphalerite. The high grade middlings made up 9% of the feed to the Lead flotation circuit while the medium grade middlings made up 2% of the feed.

Assuming a portion of the slow floating fraction of galena was made up of these middlings, if the residence time of the circuit was increased in order to recover additional slow floating galena, there would be a resulting increase in recovery of sulphide gangue minerals, i.e. chalcopyrite and sphalerite. The increase in chalcopyrite recovery would be as a result of the recovery of slow floating chalcopyrite, since this was found to have a floatability constant of the same order of magnitude as slow floating galena, and the increase in sphalerite recovery would be as a result of mineral association with galena, i.e. high grade middlings. The same was observed in Figure 5.16, which showed that with an increase in residence time there would be an increase in the recovery of all sulphide minerals, i.e. chalcopyrite, galena and sphalerite. Since the Zinc flotation circuit followed on from the Lead flotation circuit, the recovery of sphalerite in the Lead flotation circuit was seen as a loss of payable zinc metal to the Zinc flotation circuit. Furthermore, the increased recovery of both chalcopyrite and sphalerite would not be desirable in the Lead flotation circuit since this would reduce the grade of the lead Rougher concentrate recovered.

The BMM Lead flotation circuit configuration at the time of the circuit survey, as shown in Figure 2.1 (cf. Section 2.3), had the 1st through 3rd Rougher concentrate streams mixed in a sump to form the combined Rougher concentrate that was pumped to a Cleaner for upgrading. The Scavenger concentrate was recycled to the Conditioning stage where it was combined with the Copper Tails Thickener underflow stream. When looking at the distribution of the floatability classes of galena, shown in Section 5.2.3.3, it was observed that the Rougher feed stream comprised of fast, slow and non-floating galena. It was also observed that the 1st and 2nd Rougher concentrate streams comprised of fast and slow floating galena while the 3rd Rougher concentrate and Scavenger concentrates streams comprised of only slow floating galena. Ideally streams should be combined based on their composition of floatability classes since this influences the rate at which they would be recovered in the bank and, therefore, the Lead flotation circuit configuration at the time of the circuit survey was not ideal. A recommended configuration is discussed in later sections.

6.3.1.2 *Silver*

The overall correlation of balanced and model predicted mass flow of silver was strong. Similar to galena, the majority of the silver metal in the Rougher feed stream was found in the slow floating fraction, although the amount of slow floating galena significantly outweighed that of silver, i.e. 73.2% slow floating galena versus 40.9% slow floating silver in the Rougher feed. It was also observed that more than five (5) times the amount of silver was classified as non-floating compared to galena in the Rougher feed stream. The exact cause for the lack of association between silver and galena was not clear from this study since no mineralogical data pertaining to the circuit survey was available. However, it was interesting to note that a correlation between silver metal and galena minerals was observed from the hot batch flotation tests for streams that contained significantly more floating material (i.e. Rougher feed and Scavenger concentrate) and a different correlation was observed for streams that contained more non-floating material (i.e. intermediate and Scavenger tailings). The floatability of silver was 10 times slower than galena for the fast floating fraction and of the same order of magnitude as galena for the slow floating fraction. This suggests that some of the silver was associated with non-floating minerals, resulting in its slower kinetics for the fast floating fraction and larger amount of non-floating silver. As mentioned in Section 2.2, silver was also found to be associated with chalcopyrite in the Deeps ore. It is possible that the large amount of non-floating silver and the slower kinetics of silver flotation, relative to galena, were as a result of its association with chalcopyrite.

In summary, it was observed that the flotation response of silver metal did not strongly correlate to the response of galena minerals in the Lead flotation circuit and could not be characterised solely by its association with galena.

6.3.1.3 *Chalcopyrite*

Only two (2) sub-classes were observed for chalcopyrite, i.e. slow and non-floating, and 40,3% of the chalcopyrite was floatable. The sub-class distribution of chalcopyrite was consistent with what would be expected since the Copper flotation circuit preceded the Lead flotation circuit where most, if not all, of the fast floating chalcopyrite would be removed in the former circuit. Since the floatability constant of slow floating chalcopyrite was similar to that observed for slow floating galena, these minerals were recovered in similar proportions.

The BMM Concentrator average copper recovery into the final copper concentrate, based on the 2013 financial year, was approximately 66.5%. Therefore, the 40.3% slow floating chalcopyrite in the feed to the Lead flotation circuit (Copper flotation circuit tailings) represented 13.5% of the Copper flotation circuit feed (i.e. 40.3% of the 33.5%). Although the recovery of chalcopyrite to the lead concentrates does not pose a problem in terms of

penalties incurred with the sale of lead concentrate, the results obtained from this study indicate that there was an opportunity for BMM to improve the chalcopyrite recovery in the Copper flotation circuit.

The overall model prediction of chalcopyrite deportment in the Lead flotation circuit was weak and was exacerbated by the weak correlation of the data for the Rougher concentrate streams. It is important to note that the model predicted and balanced chalcopyrite data were strongly correlated when model fitting the circuit survey data on its own. The correlation was weakened when model fitting the circuit survey and hot batch flotation test data simultaneously. This was mostly as a result of the low recovery obtained in the Rougher feed hot batch flotation test, i.e. for the circuit survey the cumulative recovery was 63.4% while the cumulative recovery from the Rougher Feed hot batch flotation test was only 28.5% after 20 minutes flotation time. As mentioned in the introduction of this section, the data from the hot batch flotation tests were used to constrain the model by means of the additional information pertaining to the mineral floatability.

It was also observed that when plotting the model predicted cumulative chalcopyrite recovery versus water recovery, an almost linear correlation was observed with the trendline passing through the origin. This suggested that the bulk of the chalcopyrite recovery may have been due to entrainment. However, since no size-by-size data was available, this could not be validated.

6.3.1.4 *Sphalerite*

The balanced and model predicted sphalerite data was strongly correlated. Sphalerite was characterised into three (3) floatability sub-classes. The majority of the sphalerite was non-floating, at 72.2%, but there was a fair amount of fast and slow floating sphalerite.

When looking at the mass balanced recovery of sphalerite and the hot batch flotation tests, similarly to chalcopyrite, the balanced circuit data showed higher recovery compared to the hot batch flotation tests and the correlation of the balanced and model predicted data was weakened when simultaneously model fitting the hot batch flotation and circuit data.

Since the Zinc flotation circuit followed on from the Lead flotation circuit, it would have been ideal if all sphalerite entering the Lead flotation circuit was non-floating in order to minimise the recovery of zinc metal in the Lead flotation circuit. In order to minimise sphalerite recovery, sphalerite was actively depressed in the Conditioning stage by means of sodium cyanide (NaCN) and zinc sulphate ($ZnSO_4$) addition. However, it is possible that the depression of sphalerite was not sufficient since almost 28% of the sphalerite fed to the Lead flotation circuit was characterised as floatable. Two possible causes for this could have been

residence time for conditioning or the dosage rate of the depressant. For example, it is possible that the residence time for conditioning of the NaCN and $ZnSO_4$ was not sufficient to render the entire mineral surface hydrophillic, or there was under-addition of the reagent solutions based on the amount of sphalerite entering the Lead flotation circuit. At the time of the circuit survey, based on the BMM reagent report of the 2013 financial year, the target dosage of NaCN was 240 g/t and that of $ZnSO_4$ was 48 g/t.

Furthermore, as with chalcopyrite, the almost linear correlation found between the cumulative recovery of sphalerite and water recovery of the circuit suggested that recovery could have been due to entrainment. However, since no size-by-size data was available, this could not be validated.

6.3.1.5 *Gangue*

The remainder, which made up the non-sulphide gangue, was classified as being entirely non-floating and the predicted recovery was, therefore, as a result of entrainment. The model predicted degree of entrainment of the remainder was 0.07 and the overall circuit (Rougher and Scavenger) recovery was 0.5%. Based on the lower recovery of the remainder, it suggests that the determination of the concentrate quality was highly dependent on the undesired recovery of sulphide gangue minerals, i.e. chalcopyrite and sphalerite.

6.3.2 Parameters related to flotation cells and circuit

6.3.2.1 *Experimental bubble surface area flux (S_b)*

As highlighted in Section 5.2.1.2, the S_b for the flotation cells increased from the head to the end of the flotation bank with the Scavenger flotation cell having the highest S_b of 18.1 sec^{-1}. As previously mentioned, the raw data pertaining to the aeration rate (J_g) and bubble size (d_{32}) was not recorded during the circuit survey and, hence, no insight with respect to these parameters was available. Although the S_b values found for the Lead flotation circuit were found to be significantly lower than that measured in industrial platinum flotation cells, of similar size, the S_b data was comparable with the study conducted by Grano (2006) at the Elura Lead Concentrator. The S_b measured at the first Rougher cell of the Elura Concentrator, operated at similar percent solids, was in the range of 14 – 33 sec^{-1} when operated at the various conditions investigated, i.e. changing the impeller rotational speed and the gas rate to the flotation cells. The S_b data obtained from BMM was, therefore, found to be consistent with values observed on other Lead flotation circuits.

6.3.2.2 *Model predicted water recovery and residence time*

Based on the model predicted solids and water mass flows, the residence time and water recovery of each flotation cell were calculated. The model predicted residence times were used in the true flotation recovery equation (Equation 2.12) for the valuable species, i.e. chalcopyrite, galena, sphalerite and silver. The residence times of the 1st through 3rd Rougher flotation cell were fairly similar but showed a slight increase down the flotation bank and the residence time of the Scavenger flotation cell was lower than the Rougher flotation cells, due to its smaller volume, and was found to be 7.2 minutes versus 9.2 - 9.5 minutes obtained for the Rougher flotation cells. Overall, the model predicted residence time was well matched to the residence time calculated using the balanced circuit data, and the relative error between the balanced and model predicted residence time ranged from 0.0% to 1.2%.

The water recovery was found to decrease down the flotation bank and the Scavenger flotation cell was significantly lower compared to the preceding Rougher flotation cells, due to the low mass recovery of the cell. The overall model predicted water recovery for the Lead flotation circuit was 6.1%. The model predicted water recovery of the 1st Rougher, 2nd Rougher and Scavenger flotation cells strongly correlated the balanced data, i.e. the relative error for these was below 10%. However, the relative error of the model predicted and balanced water recovery of the 3rd Rougher flotation cell was significant at 44.6%. As previously mentioned, the water recovery was calculated using Equation 2.6, which incorporates the flow of solids ($Q_W = aF_S{}^b$). Since the correlation of mineral species was weak in the 3rd Rougher concentrate stream, particularly chalcopyrite and sphalerite as discussed in Section 6.3.2, the correlation of model predicted water recovery was affected, i.e. the model predicted Solids flow was 816.2 kg/h lower than the balanced data resulting in a lower corresponding model predicted water recovery.

6.3.3 Model fitted froth recovery

The froth recovery for each of the flotation cells was model fitted based on the balanced circuit data. In certain cases, particularly when modelling the flotation of sparsely mineralised ores, the behaviour of multiple floating species in a particular flotation cell can be defined by a single froth recovery. That is, all floating species demonstrate the same behaviour in the froth phase of the flotation cell and hence a global froth recovery for the flotation cell is used for all species. However, in the case of the Lead flotation circuit considered in this study it was not possible to define the behaviour of all the floating species with a global froth recovery and this was most likely influenced, to a large extent, by the amount of each floating species in the circuit feed (measured in percent rather than ppm). Furthermore, the sulphide minerals all had varying degrees of hydrophobicity, i.e. galena was significantly faster floating and, in effect, had a higher degree of hydrophobicity than chalcopyrite, silver and

sphalerite which would influence their behaviour in the froth. Therefore, the approach used to model fit the froth recovery in the Lead flotation circuit, which resulted in the best correlation between balanced and model predicted data, was to fit separate froth recoveries for each of the floating species for each of the four (4) flotation cells.

The model fitted froth recovery of all species increased along the flotation bank with the 1st Rougher flotation cell having the lowest froth recovery. As cited by Ata and co-workers (2003), Johansson and Pugh (1992) showed that highly hydrophobic particles destabilise the froth, and in effect would result in a lower froth recovery, while moderately hydrophobic particles have a stabilising effect on the froth. It is probable that the 1st Rougher concentrate consisted of large amounts of highly hydrophobic galena and silver since 98.2% of the fast floating galena and 69.1% of fast floating silver was recovered in this cell. This would have resulted in a less stable froth in the 1st Rougher flotation cell and, therefore, a lower froth recovery. Since most of the fast floating galena and silver were recovered by the 1st Rougher flotation cell, when moving down the Lead flotation bank the degree of hydrophobicity, as well as the amount of the sulphide minerals present (i.e. chalcopyrite, galena and sphalerite) decreased, which would have resulted in the stabilisation of the froth. It is also important to note that general visual observation of the froth in the Lead flotation circuit supports these findings, i.e. that the froth stabilises down the bank, since the 1st Rougher flotation cell typically consisted of smaller bubbles with some of them bursting before collection in the launder and the 3rd Rougher flotation cell would have larger bubbles at the top of the froth that would not easily burst before collection in the launder.

It was observed that the calculated froth recovery of sphalerite in the 3rd Rougher flotation cell was exceptionally high, and unrealistic (90.3%). It is important to note that the mass recovery of sphalerite in the Lead flotation circuit was significantly lower than the other species and the floatability constants of the fast and slow floating fraction of sphalerite were also lower than the other species. As mentioned in Section 6.3.1.4, the recovery of sphalerite in the Rougher feed hot batch flotation test was lower than that observed from the balanced circuit data, i.e. 4.2% versus 8.8% respectively. The FCM approach assumes that the material collected from the plant streams has the same floatability in the Concentrator as in the batch flotation cell and that the difference in performance in bench-scale versus plant-scale is due to the hydrodynamics (S_b) and the froth performance (R_f). The measured batch cell and plant S_b were similar and the batch cell was operated with a shallow froth to prevent drop-back to ensure 100% froth recovery. Therefore, the Concentrator cell froth recovery is essentially a fraction of the batch cell froth recovery. The model fitted R_f value of 90.3% for sphalerite in the 3rd Rougher cell is most likely indicative that the froth recovery of sphalerite in the batch flotation cell was not 100%, as shown by the lower than expected recovery from the Rougher feed hot batch flotation test compared to the balanced data. Although the froth recovery of

chalcopyrite in the 3rd Rougher flotation cell was not as high as that of sphalerite, it was found to be higher than that of galena in the 3rd Rougher flotation cell. Furthermore, similarly to sphalerite, the lower than expected recovery of chalcopyrite in the Rougher feed hot batch flotation test could be due to a lower froth recovery of chalcopyrite in hot batch flotation tests, i.e. not 100%.

Lastly, it was observed that the low froth recovery of all species in the Scavenger flotation cell resulted in low mass recovery of all species. This will be discussed in some more detail in Section 6.3.4.

6.3.4 Insight into the Lead flotation circuit performance

The grade of the 2nd Rougher, 3rd Rougher and Scavenger concentrates were not high enough to be considered final concentrate, specifically for galena. However, the grade of the 1st Rougher concentrate, i.e. 82.3%, was above the target Lead final concentrate. Therefore, it is possible that the 1st Rougher concentrate could be pumped directly to the Lead Concentrate Thickener while the other concentrates would require additional upgrading in a Cleaner stage.

In terms of the species recovery from the individual flotation cells, it was observed that the 1st, 2nd and 3rd Rougher flotation cells operated fairly consistently and the Scavenger flotation cell was not performing optimally, e.g. the Scavenger unit recovery with respect to galena was only 4.9% compared to the unit recovery of the preceding Rougher flotation cells each being over 40%. It is important to note that the Scavenger flotation cell was historically not always operational, i.e. it was often on standby and was typically only put online when the feed grade to the Lead flotation circuit was higher than the normal operating range or when the production team had difficulty with achieving the target galena recovery.

It was also observed that sphalerite in the Lead flotation circuit exhibited some degree of floatability even though it had been actively depressed and was recovered in the Lead flotation circuit resulting in a predicted loss of 4.5% payable zinc metal to the Zinc flotation circuit. Since active depression of sphalerite took place in the Conditioning stage, no fast or slow floating material should have been present. As previously mentioned, the presence of fast and slow floating sphalerite suggests that the depression was not sufficient and could have been as a result of insufficient residence time for conditioning or under-addition of the reagents with respect to the mass of sphalerite entering the Lead flotation circuit.

It was seen that froth recovery for all species was significantly lower in the Scavenger flotation cell. The flotation process was modelled as a first order rate process, and the flotation rate was directly proportional to the froth recovery. As previously mentioned in

Section 2.4.5.1, the froth recovery was related to various parameters including the mineralisation of the froth, the hydrophobicity of minerals as well as the operating conditions of the cell in terms of aeration rate and froth depth. Unfortunately, information pertaining to the operational froth depth of the Lead flotation cells during the circuit survey was not available. However, the bubble surface area flux information (cf. Section 5.2.1.2) indicated that the gas dispersion of the Scavenger cell was not problematic.

The sub-optimal performance of the circuit noted during the circuit survey, with reference to the significant amount of slow floating galena (14.6%) not recovered in the circuit, was supported by a mineralogy report compiled by Anglo Research Mineralogical Research Department (Bramdeo et al., 2008). In the study conducted by Bramdeo and co-workers it was found that the Lead flotation circuit tailings contained liberated galena, i.e. where 80% of the particle was the mineral of interest, which made up 25% of the total galena in the tailings stream. Of the 25% portion of liberated galena, 15% was below 20 μm and the remaining 10% was within the size range 20 – 160 μm. In 1980 Jowett showed, using data from Trahar (not referenced), that in a batch system the optimal size range for flotation of galena particles is 20 - 80 μm (as cited by Jameson and co-workers (2007)). Relating the findings of this study to the study conducted by ARMRD and literature, it is possible that a portion of the slow floating galena lost in the Scavenger tailings stream was made up of fine mineral particles (< 20μm) and was, hence, not recovered. Unfortunately no size-by-size data was available from this study and the exact cause for the loss of slow floating galena could not be determined. However, it is evident that the Lead flotation circuit was not performing to its potential, since liberated material had been previously found to exit the circuit, and it is postulated that this could be as a result of the poor Scavenger flotation cell performance as indicated by the low froth recovery.

As previously mentioned, ideally streams should be combined based on the composition of floatability classes within the circuit streams rather than just considering the grade of the valuable mineral. With respect to the distribution of floatability classes of galena in the Lead flotation circuit and the circuit configuration at the time of the study, the 3rd Rougher concentrate and Scavenger concentrate streams (which contained only slow floating material, with reference to galena) were mixed with streams that contained other floatability classes of galena as well. That is, the 3rd Rougher concentrate was mixed with the 1st and 2nd Rougher concentrate streams as part of the Cleaner feed although the 1st and 2nd Rougher concentrates contained fast and slow floating galena, and the Scavenger concentrate was recycled to the Rougher feed to join the Copper Tails Thickener underflow stream which contained all three of the floatability classes.

As mentioned in Section 5.2.3.4.1, as well as earlier in this section, the grade of the 2nd Rougher, 3rd Rougher and Scavenger concentrate streams were not high enough to be considered final concentrate, specifically for galena, and required additional upgrading in a Cleaner stage. It is important to note that although the mixing of concentrate streams as per the flowsheet at the time of this study was not ideal, with respect to the composition of floatability classes in the streams, a single Cleaner flotation cell was available in the Lead flotation circuit, as mentioned in Section 2.3, which limited the possible re-routing of the Rougher and Scavenger concentrate streams. Possible re-routing of the concentrate streams based on floatability composition will be discussed in Section 6.3.5.

6.3.5 Using the model for circuit improvement

Since the FCM approach allows the flotation process to be decoupled into the pulp zone and froth zone, the effect of a specific parameter which influences the flotation response can be investigated and the model predicted response could be easily determined.

An example would be when reagent screening is done on site. As highlighted in Section 2.4.2.3, the floatability of minerals is affected by various parameters including the particle hydrophobicity, which is as a result of liberation and reagent coverage. In the event that a new collector is tested on site, for example, the effect this has on floatability can be isolated by means of conducting hot batch flotation tests. It is unlikely that a collector will change the proportion of material that is fast, slow or non-floating but more likely that the floatability will be changed. Using the model parameters previously calculated in this study, the resultant new floatability constant could be determined. Based on the new floatability constants for the mineral(s) investigated, the model predicted recovery could be determined.

Alternatively, the model could be used to identify improvement areas. Figure 6.1 shows the model predicted cumulative recovery of galena, for the circuit and batch data, as a function of residence time.

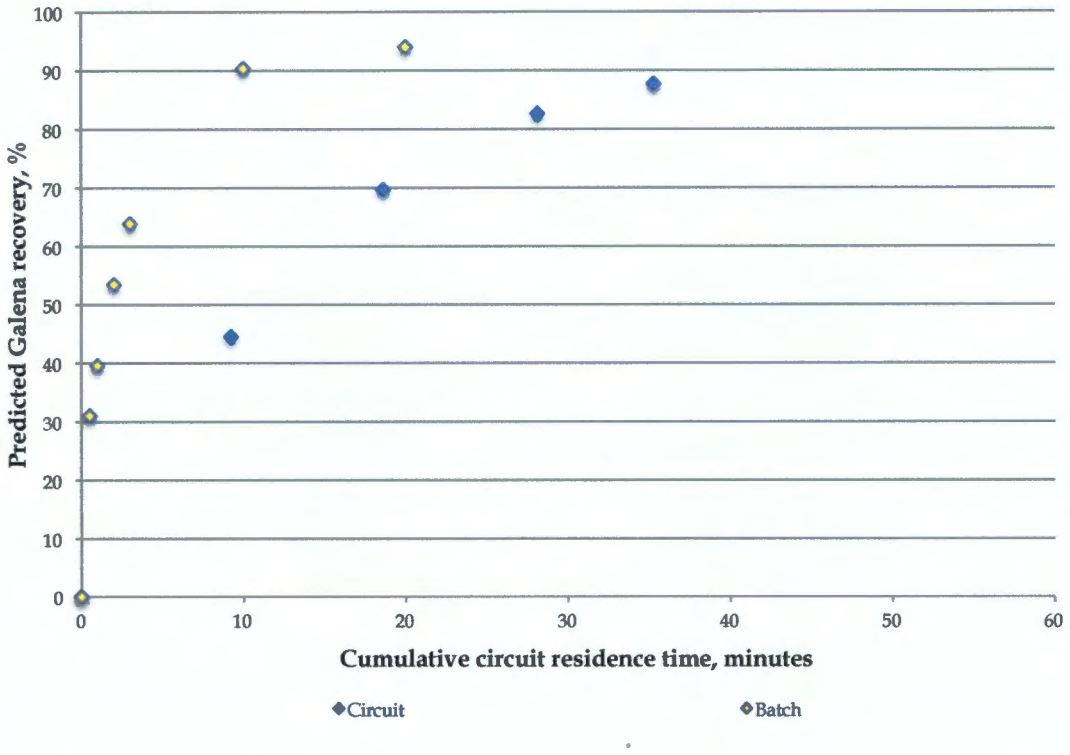

Figure 6.1: Model predicted circuit and batch cumulative galena recovery (%) versus residence time (minutes)

Figure 6.1 shows that the kinetics of the galena flotation in the circuit (markers with blue fill) was significantly slower compared to that in the batch flotation tests (markers with white fill). Since mineral floatability (P) remains unchanged for the circuit and the batch, the only parameters that could have reduced the kinetics of galena in the circuit were the bubble surface area flux (S_b) and the froth recovery (R_f) of the flotation cells.

As previously mentioned, the 1st through 3rd Rougher flotation cells were found to be performing well and the bubble surface area flux that was measured in the circuit was comparable with data obtained from another lead concentrator (Grano, 2006). However, a simple desktop simulation was done using the spreadsheet on which the model was developed, which looked at the effect of altering the S_b in all the flotation cells. In practice, a change in the S_b could be achieved by increasing the aeration rate or by changing, for example, the impeller speed of the agitators. In order to only consider the effect the change in S_b would have on the flotation process, it was assumed that the froth recovery of the flotation cells would remain unchanged for this simple simulation, although in practice increasing the aeration rate would reduce the froth stability and, hence, the froth recovery. In the simulation the S_b of all the flotation cells in the bank were made equal to the upper end of the S_b range measured at the Elura Concentrator (Grano, 2006), i.e. 33 min^{-1}. The results of this simulation are shown in Figure 6.2.

Alternatively, the effect of an improved froth recovery in only the Scavenger flotation cell was also simulated. In this simulation it was assumed that the S_b of all the flotation cells did not change, i.e. would remain as was measured during the circuit survey at BMM, and the froth recovery of only the Scavenger flotation cell was increased from 4.2% (model predicted) by reducing the operational froth depth. Since the composition of the 3rd Rougher tailings and 3rd Rougher concentrate streams were similar, i.e. almost equal amounts of slow floating galena with respect to mass flow, it is probable that the behaviour and stability of the froth in the Scavenger flotation cell would be similar to that of the 3rd Rougher flotation cell. Assuming the froth recovery of the Scavenger flotation cell could be increased, by decreasing the operational froth depth of the cell, to be approximately the average of the froth recovery predicted for the three (3) Rougher flotation cells, i.e. 40%, the simulated effect on galena recovery is also shown in Figure 6.2.

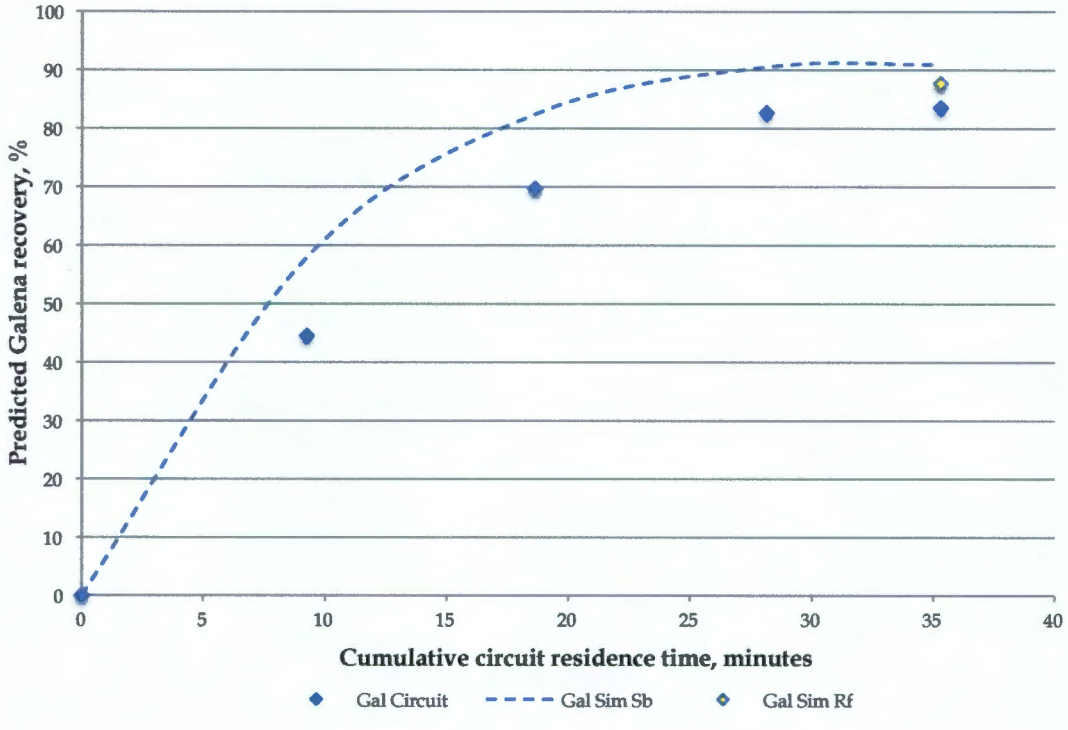

Figure 6.2: Model predicted and simulated circuit cumulative galena recovery (%) versus residence time (minutes)

Figure 6.2 shows that if the S_b of all the flotation cells was increased, as expected the overall kinetics and recovery of galena (dashed line) would increase significantly (since $k = PS_bR_f$) and the possible galena recovery within the residence time of the circuit would increase from 83.5% to 91.0%. Alternatively, if the froth recovery of only the Scavenger flotation cell was improved (marker with yellow fill), the possible galena recovery would improve by approximately 4.1%, i.e. increase to 87.7%.

Another example of how the model could be used for future circuit improvement would be to determine the optimal flotation cell volume for the Cleaner stage in the event BMM Concentrator considered re-routing the Rougher and Scavenger concentrate streams. Currently the Rougher concentrate streams are mixed in a way that does not take into account the composition of the floating classes in the flotation streams. Using the information shown in Figure 5.14 (cf. Section 5.2.3.3), ideally the 1st Rougher concentrate stream should be pumped directly to the Lead Concentrate Thickener since the grade of the stream is above final concentrate quality, i.e. 82% galena. Furthermore, since the 2nd Rougher concentrate stream contained fast and slow floating galena it should ideally be fed to a Cleaner flotation cell, e.g. "high grade Cleaner", and the 3rd Rougher and Scavenger concentrate streams, which contained only slow floating galena, should be combined and fed to a separate Cleaner flotation cell, e.g. "low grade Cleaner". However, ince the 2nd Rougher concentrate stream contained such a small amount of fast floating galena, i.e. 1.5 % by mass, it does not validate the capital and operating cost required and instead the 2nd Rougher, 3rd Rougher and Scavenger concentrate streams should be combined and upgraded in a single Cleaner flotation cell. The proposed flowsheet is shown in Figure 6.3.

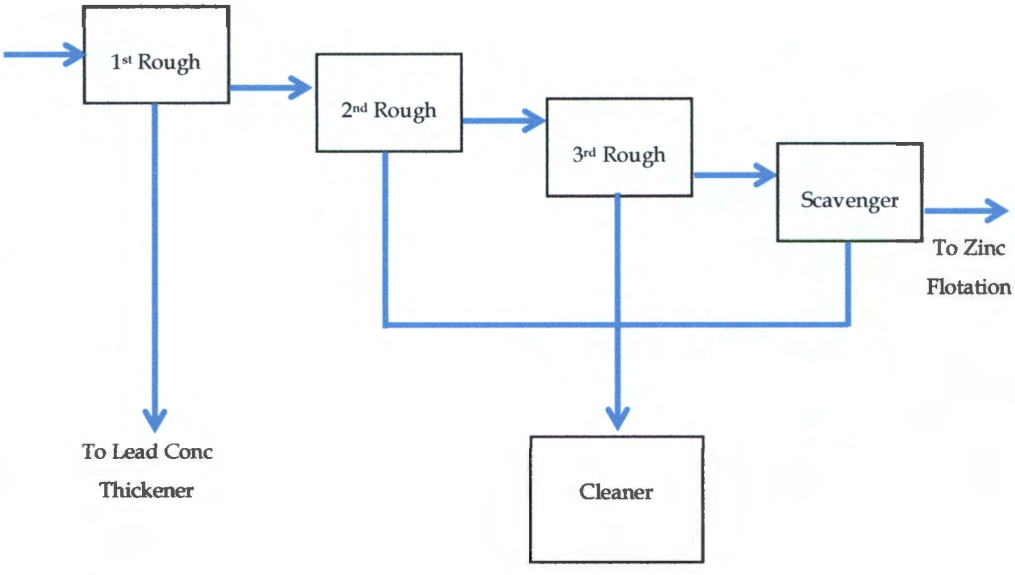

Figure 6.3: Flowsheet showing proposed changes to the Lead flotation circuit

Assuming the percent solids of the feed to the Cleaner flotation cell was reduced by 5% due to the wash water addition at the concentrate launders, the slurry volume fed to the new Cleaner would be 60% of the current slurry volume fed to the existing Cleaner cell. Furthermore, the galena feed grade to the proposed Cleaner flotation cell would be 7.6% lower than the existing Cleaner feed. Due to significantly lower slurry volume and the additional upgrading required, the existing 30m^3 Cleaner cell would not be suitable for use in the proposed flowsheet. A series of simulations using the model could be done to determine the volume of cell needed to provide the new concentrate grade and recovery specifications.

7 CONCLUSIONS

Based on the results obtained in this study, the following conclusions could be made.

7.1 Validation testwork

7.1.1 Validated batch flotation test procedure

The results obtained from the repeatability tests showed that the batch flotation test procedure used was able to produce results that were repeatable. The cumulative recovery results of solids, lead and silver from the individual tests were found to lie within a 95% confidence level. Furthermore, the relative standard deviation for the solids, lead and silver recovery was below 5% and the error of the reconciled feed grade for lead was below 10% as per the guidelines set out for these tests. The recovery obtained after seven (7) minutes flotation time, as per the BMM SOP, was more than 10% lower than the infinite recovery time. The flotation time required for the hot batch flotation tests was set to be 20 minutes since the cumulative lead recovery achieved was 97.3% of the infinite time recovery based on the Klimpel model (1980).

7.1.2 Metal recovery negatively affected after a period of standing time

It was concluded that the metal recovery of lead and silver was significantly reduced when the sample was allowed to stand for longer than three (3) hours. Furthermore, since some reduction in metal recovery was observed even after one (1) hour standing time, although not significant, it was decided that the hot batch flotation sample would be floated immediately after sample collection.

7.2 Data reconciliation

7.2.1 Circuit data reconciled

The circuit appeared to be sufficiently stable when the circuit survey was conducted, based on the percent solids data obtained from the nine (9) individual Rougher concentrate samples. The relative standard deviation of percent solids of the streams was 2.2%, 1.4% and 1.3% for the 1st Rougher, 2nd Rougher and 3rd Rougher concentrate streams respectively. Overall, the circuit data was reconciled satisfactorily since there was good correlation between most of the experimental and balanced data, i.e. of the 36 assay data points that were fitted only six (6) assay data points had a weighted sum of squared error greater than 5.

7.2.2 Representivity of intermediate tailings samples compromised

The intermediate tailings streams were more difficult to reconcile and were found to have the weakest correlation between the experimental and balanced data compared to the other streams. Inconsistencies were observed for the experimental percent solids, assays and hot batch flotation tests of these streams. It is thought that the sample representivity and integrity were compromised due to the method of sampling used, i.e. using a dip sampler.

7.3 Characterisation of the Lead flotation circuit using the Floatability Component Model

It can be concluded that the Lead flotation circuit was characterised using the Floatability Component Model approach in conjunction with the Woodburn and Wallin (1984) matrix methodology and was done so using data that was obtained easily, inexpensively and in a manner which was not disruptive to the operation. The model was able to predict reasonably well the circuit recovery of galena, within 99% confidence level based on the average historical galena recovery observed at BMM. However, the model was not able to accurately predict the silver recovery and this was due to the lack of mineralogical information pertaining to the extent of association of silver metal with chalcopyrite.

7.3.1 Residence time and water recovery

The calculated residence time, based on the model predicted tailings flows, correlated well with the data obtained from the circuit survey. It can be concluded that the galena recovery achieved within the Lead flotation circuit residence time was sufficient since additional residence time would result in the undesired additional recovery of sulphide gangue minerals, i.e. chalcopyrite and sphalerite.

It can be concluded that the calculated water recovery was consistent with that observed from the circuit survey data, with the exemption of the 3rd Rougher flotation cell. It can also be concluded that due to the low water recovery across all the flotation cells considered in this study, the recovery of entrained non-sulphide gangue, i.e. the remainder, was significantly low ranging from 0.0% to 0.2%.

7.3.2 Bubble surface area flux (S_b) and froth recovery (R_f)

Although the experimental bubble surface area flux (S_b) of the Rougher and Scavenger flotation cells was significantly lower than that obtained for a similar size flotation cell used in the platinum industry, it was found to be comparable with data obtained from the Elura Lead Concentrator (Grano, 2006) where the pulp conditions were similar to BMM. It can,

therefore, be concluded that the bubble surface area flux observed for the BMM Lead flotation circuit was consistent with values measured at another Lead Concentrator.

It can be concluded that due to the mineralisation of the sulphides in the Lead flotation circuit as well as the sulphides having varying degrees of hydrophobicity, a global froth recovery per flotation cell could not be used. Furthermore, based on the exceptionally high model fitted froth recovery of sphalerite in the 3rd Rougher flotation cell, i.e. 90.3%, it can be concluded that froth recovery of sphalerite in the batch flotation cell was likely lower than 100%.

7.3.3 Characteristics of galena

Galena was characterised into three (3) sub-classes, i.e. fast, slow and non-floating, which was consistent with other studies conducted on lead operations. Although the fast floating fraction was considerably smaller compared to the studies conducted at the Red Dog and Cannington operations, the floatability constant of BMM galena was considerably higher (Runge et al., 1997; Welsby et al., 2010). A significant amount of slow floating galena (14.6%) was lost into the Scavenger tailings stream and was possibly made up of fine, liberated galena. However, size-by-size data was not available for this study and it was not possible to confirm this hypothesis.

7.3.4 Characteristics of silver minerals

Silver was classified as fast, slow and non-floating. As highlighted in the literature, although silver was found to be associated with galena it was concluded that the flotation response of silver could not be entirely predicted in terms of the response and recovery of galena. Additional mineralogical information is required to better understand the distribution of silver in association with other minerals that are non-floating, in particular the chalcopyrite that has been shown to be associated with in the Deeps ore BMM is treating. It can be concluded that the model obtained from this study cannot accurately predict the circuit recovery of silver.

7.3.5 Characteristics of chalcopyrite

Since the Copper flotation circuit preceded the Lead flotation circuit, the fact that the chalcopyrite was characterised as having no fast floating material was to be expected. Although the assay of chalcopyrite in the lead concentrate does not pose any problems from a concentrate quality perspective, it can be concluded from the findings of this study that there was an opportunity for BMM to improve the chalcopyrite recovery in the Copper flotation circuit as some of the slow floating chalcopyrite was still present in the Lead flotation circuit feed. However, as suggested by the almost linear correlation observed from the chalcopyrite

recovery versus water recovery profile, a portion of the chalcopyrite could have been recovered as a result of entrainment. Since no size-by-size data was available from this study, it was not possible to validate the transport mechanism of chalcopyrite from the pulp to the froth.

7.3.6 Characteristics of sphalerite

It was assumed that all sulphide minerals, including sphalerite, were recovered by true flotation and sphalerite was, therefore, classified as fast, slow and non-floating with almost 28% being floatable. This floatability distribution of sphalerite, and more specifically the fact that two floating classes were identified, suggested that the depression of sphalerite was not sufficient. This could be due to under-dosage of depressant, since the control loop used to control the sodium cyanide (NaCN) and zinc sulphate ($ZnSO_4$) solutions was typically run on a manual basis and not based on the mass of sphalerite entering the Lead flotation circuit. Alternatively, it could have been due to insufficient residence time for the depressant within the Conditioning stage.

Alternatively, as shown by the almost linear correlation between sphalerite and water recovery, a portion or all of the sphalerite could have been recovered by entrainment. Since no size-by-size data was available, it was not possible to validate whether the observed sphalerite recovery was by true flotation and/or entrainment.

7.3.7 Characteristics of non-sulphide gangue minerals

The remainder was assumed to be entirely non-floating and the degree of entrainment was predicted to be 0.07. Based on the low recovery of the remainder, i.e. cumulative recovery of 0.5% in the Lead flotation circuit, it can be concluded that the recovery of the gangue did not pose significant problems to the concentrate quality of the Lead flotation circuit.

7.3.8 Identified circuit improvement opportunities

It can be concluded that the model that was developed for the Lead flotation circuit could easily be used to simulate the response of the circuit, as shown in Section 6.3.5, when alternative process conditions are tested, e.g. when reagent screening is done and the effect in the plant-scale operation would like to be understood. Furthermore, the same methodology could be used to characterise and model the Cleaner stage of the Lead flotation circuit or it could be extended to characterise the Copper and/or Zinc flotation circuit(s).

If it was assumed that the bubble surface area flux of the flotation cells was increased to double the measured value without adversely affecting the froth performance, the galena recovery of the circuit would increase to 91.0%, i.e. a potential increase of 7.5%. As

highlighted in the literature review, the aeration rate and bubble size influence the S_b observed in the flotation cell. Without having to change the installed equipment, the effect of the aeration rate, impeller speed and/or frother dosage on S_b, froth recovery as well as mineral recovery could be investigated in order to optimise the galena recovery in relation to the recovery of the sulphide gangue minerals, i.e. chalcopyrite and sphalerite.

Similarly, improving the froth recovery of the Scavenger flotation cell without changing the bubble surface area flux had the potential to increase the galena circuit recovery to 87.7%. Therefore, the model predicted loss of slow floating galena could have been reduced by 4.1%. The froth recovery of the Scavenger flotation cell could be improved by investigating the effect the operating froth depth has on mineral recovery in the Scavenger flotation cell.

The above-mentioned scenarios are examples of how the modelling approach could be used to investigate possible opportunities, by means of simple desktop simulations, to develop strategies to increase the recovery of galena in the Rougher and Scavenger bank.

Another opportunity identified in this study would be to increase the floatability of the slow floating fraction of galena in order for it to be recovered within the residence time of the circuit. Currently S.E.X. is used as the collector in the Lead flotation circuit. A possibility of increasing the floatability of the slow floating fraction could be to use a mixture of collectors, as it has been shown that the mineral recovery could improve significantly compared to that obtained when a single collector was used (McFadzean et al., 2012).

From a perspective of the mineral floatability distribution of galena, it can be concluded that the current flowsheet design is not ideal since streams are being mixed without taking into account the floatability classes present in the streams, and the 1st Rougher concentrate is being fed to the Cleaner stage although already at final concentrate quality level. However, due to the restrictions in terms of the flotation equipment, i.e. a single Cleaner flotation cell was being used, the possibility of re-routing streams is not likely since it would require the installation of additional Cleaner flotation equipment. In the event BMM was considering upgrading the Concentrator and re-routing the concentrate streams, it can be concluded that the methodology used in this study could be extended to the existing Cleaner circuit in order to generate a representative model. Thereafter, a series of simulations could be run to predict the optimal cell volume required to produce a final concentrate that meets the Concentrator's final concentrate target requirements.

8 RECOMMENDATIONS

Based on the findings of this study, the followings recommendations are made.

8.1 Alternate sampling method to be considered for intermediate tailings streams

As a result of the poor sample integrity and representivity of samples collected using the dip sampler, an alternate sampling technique has to be considered to obtain samples from these streams if it is included in any future investigations. An alternative for sampling, for example, would be to use a peristaltic pump that would pump out material from the cell near the tailings valve. In the event a suitable alternative to sampling these streams is not available, it should be omitted from further investigations since the data and test results obtained from these samples were not representative.

8.2 Increase the residence time of the batch flotation test

It is recommended, based on the findings of Phase One, that the batch flotation test procedure used by BMM is amended such that the lead Rougher stage batch flotation test is conducted using 20 minutes flotation time. It is also recommended that the copper and zinc batch flotation test procedures be reviewed.

8.3 Opportunities to improve galena recovery

It is recommended that, based on the reasonable accuracy of the model predicted galena recovery, the model can be used by the metallurgical team to quantify the possible improvement in galena recovery for the following investigations.

8.3.1 Improve the Scavenger flotation froth performance

In order to improve the recovery of slow floating galena, the performance of the Scavenger flotation cell has to be investigated. Based on the experimental data, the bubble surface area flux did not appear to be problematic and, hence, the low froth recovery could have been as a result of incorrect froth depth. It is recommended that the Scavenger flotation cell is operated at various froth depths and samples should be taken of Scavenger concentrate and tailings streams at each operational froth depth in order to ascertain the assay, percent solids and mass flow of the streams. This information should then be used to determine the froth depth where the Scavenger concentrate grade and galena recovery is optimised.

8.3.2 Increase aeration rate to increase mineral kinetics and recovery

The kinetics and recovery of galena could be improved significantly by increasing the bubble surface area flux observed in all the flotation cells through the optimisation of the aeration rate. Since an increase in S_b would result in an increase in the kinetics of all floating species, including sulphide gangue minerals, the optimal operating S_b would have to be determined based on the trade-off of improved galena recovery and minimising the recovery of chalcopyrite and sphalerite, since this would possibly reduce the concentrate grade and result in additional loss of payable zinc in the lead concentrates.

8.3.3 Increase floatability of slow floating galena

The floatable galena fed to the Lead flotation circuit was classified as being made up fast floating and slow floating material. The fast floating fraction was recovered in the 1st and 2nd Rougher flotation cells whereas the slow floating fraction was not fully recovered within the residence time of the Lead flotation circuit. In order to increase the recovery of the slow floating fraction within the given residence time, the kinetics or floatability would have to be increased. Two studies are recommended to investigate opportunities to increase the floatability of slow floating galena. The first is based on the assumption that the S.E.X. dosed in the Conditioning stage of the Lead flotation circuit did not have sufficient time to adsorb onto the entire mineral surface. It is recommended that batch flotation tests are conducted using the procedure as outlined in Section 4.5.2 and varying the conditioning time of the collector, using the conditioning time in the procedure as the reference test, i.e. three (3) minutes conditioning time.

The second study would be to investigate, also using batch flotation tests as outlined in Section 4.5.2, whether an alternative collector would increase the floatability of the slow floating galena. The alternative collector could either be added alone or in conjunction with S.E.X. This study would, therefore, have to be conducted in two parts where the first would be to determine the effect the alternative collector has on the floatability of slow floating galena and the second would be to determine the effect on floatability when dosing the alternative collector in conjunction with S.E.X. The results from this two-part study would have to be compared to the reference test mentioned above, i.e. S.E.X. conditioned for three (3) minutes, in order to quantify the effect thereof.

The floatability constant for each scenario mentioned above would be calculated, assuming the mass distribution species of galena remains unchanged, by means of Equation 2.17 in Section 2.7.

Similar to the investigation of the aeration rate, the proposed investigations would have to consider the effect conditioning time and collector type has on the recovery of sulphide gangue minerals.

8.4 Determine the reason for sphalerite floatability in the Lead flotation circuit

8.4.1 Perform size-by-size analysis of sphalerite in Lead flotation circuit streams

In order to better understand and characterise the behaviour of sphalerite minerals within the Lead flotation circuit, size-by-size data should be obtained from the Rougher feed, Rougher concentrates and Scavenger concentrate streams. This would give insight as to whether the sphalerite was recovered due to true flotation and/or entrainment.

8.4.2 Review the methodology used for sphalerite depression

As some sphalerite recovery was undoubtedly due to true flotation, the efficiency of sphalerite depression has to be investigated. It is possible that the dosage rate of the sodium cyanide (NaCN) and zinc sulphate ($ZnSO_4$) and/or the residence time for conditioning of depressant was not sufficient for the amount of sphalerite entering the circuit. It is recommended that two studies are conducted using batch flotation tests, i.e. increase depressant dosage and increase conditioning time, with samples from the Copper Tails Thickener underflow and using the procedure outlined in Section 4.5.2. An improvement in sphalerite depression would be indicated by a reduction in the sphalerite recovery in the batch flotation tests compared to the reference test where a dosage of 240 g/t NaCN and 48 g/t $ZnSO_4$ is used and a conditioning time of two (2) minutes.

It is recommended for the first study that the depressant dosage is tested at three (3) increased dosages, i.e. increased by 10%, 20% and 50% from the reference dosage rate, with a fixed conditioning time of two (2) minutes. For the second study, it is recommended that the Concentrator target dosage of 240 g/t NaCN and 48 g/t $ZnSO_4$ is used and the conditioning time is varied, i.e. three (3) minutes, four (4) minutes and five (5) minutes conditioning time.

8.5 Include mineralogical analysis to understand silver response

If it is desired by the operation to better understand and predict the behaviour of silver in the Lead flotation circuit, mineralogical analysis would have to be included as a result of the silver association with both chalcopyrite and galena.

8.6 Incorporate knowledge of galena floatability distribution into future flotation circuit design

It is recommended that any future expansion or re-design at BMM should also consider the floatability distribution of minerals and not just the grade of the streams. It is, therefore, recommended that the 1st Rougher concentrate stream is pumped to the Lead Concentrate thickener and the 2nd Rougher, 3rd Rougher and Scavenger concentrate streams are treated in a single Cleaner flotation cell such that the capital and operating costs for the Cleaning stage are minimised and the upgrading of the Rougher and Scavenger concentrates are optimised.

8.7 Extend characterisation methodology to Copper and Zinc flotation circuits

It was highlighted in this study that there was an opportunity to improve the chalcopyrite recovery in the Copper flotation circuit as some of the chalcopyrite was still recovered by true flotation in the Lead flotation circuit. In order to determine the recovery as a result of true flotation and/or entrainment, it is recommended that size-by-size analysis is done of samples taken from the Rougher feed, Rougher concentrate and Scavenger concentrate streams in the Lead flotation circuit. It is, therefore, recommended that the methodology used in this study be extended to the Copper flotation circuit to understand improvement areas to increase the recovery of floatable chalcopyrite. It is further recommended that in order to complete the understanding of the role of the pulp and froth in the entire BMM circuit, the methodology should also be extended to the Zinc flotation circuit. Size-by-size analysis should be done of the circuits' samples to quantify entrainment of minerals in the various flotation circuits, and some mineralogical analysis should be done. The use of mineralogical data would be specifically useful for the Copper and Lead flotation circuits to quantify the association of the sulphide minerals.

REFERENCES

Albijanic, B., Odzemir, O., Nguyen, A.V. & Bradshaw, D. 2010. A review of induction and attachment times of wetting thin films between air bubbles and particles and its relevance in the separation of particles by flotation. *Advances in Colloid and Interface Science*. 159: 1–21.

Alexander, D.J., Franzidiz, J.P. & Manlapig, E.V. 2003. Froth recovery measurement in plant scale flotation cells. *Minerals Engineering*. 16: 1197–1203.

Ata, S. 2012. Phenomena in the froth phase of flotation – a review. *International Journal of Mineral Processing*. 102-103: 1–12.

Ata, S., Ahmed, N. & Jameson, G.J. 2003. The study of bubble coalescence in flotation froths. *International Journal of Minerals Processing*. 72: 255–266.

Bartlett, H.E. 2002. Design of primary samplers for slurries in concentrators and statistical methods for measuring components of variance in sampling. *The Journal of South African Institute of Mining and Metallurgy*. 102: 485–490.

Bowen, O.E. 1962. *Rocks and Minerals of the San Francisco Bay region*. United States of America : University of California Press. 32.

Bramdeo, S., Dhlamini, S., Scharneck, Y. & Magudulela, B. 2008. *Mineralogical results: Black Mountain circuit survey.* (Mineralogy Report No.: M/07/33). South Africa : Anglo Research Mineralogical Research Department.

Brand, S. & Horsh, H. 2006. *Mineralogical characterisation of a Black Mountain feed to float sample.* (Mineralogy Report No.: M06/177). South Africa : Anglo Research Mineralogical Research Department.

Brezani, I. 2010. *Flotation kinetics – equation fitting.*

Available:

http://www.mathworks.com/matlabcentral/fileexchange/28583-flotation-kinetics-equation-fitting/content/html/Flotation_fitting.html [6 May 2015].

Chamber of Mines of South Africa. 2014. *Lead.*

Available:

http://chamberofmines.org.za/mining-industry/minerals/-south-africa [5 May 2015].

Collins, D.A., Schwarz, S. & Alexander, D.J. 2009. Designing modern flotation circuits using JKFit and JKSimFloat. In *Recent Advances in Mineral Processing Plant Design*. D. Malhotra, P.R Taylor, E. Spiller & M. LeVier, Eds. United States of America : SME. 197–203.

Crowson, P. 2006. Lead. In *Base Metals Handbook*. M Thompson, Ed. United Kingdom : Woodhead Publishing Limited. 4.

Deglon, D.A., Egya-Mensah, D. & Franzidis, J.P. 2000. Review of hydrodynamics and gas dispersion in flotation cells on South African platinum concentrators. *Minerals Engineering*. 13 (3): 235–244.

Gomez, C.O. & Finch, J.A. 2007. Gas dispersion measurements in flotation cells. *International Journal of Mineral Processing*. 84: 51–58.

Gorain, B.K., Franzidis, J.P. & Manlapig, E.V. 1995a. Studies on impeller type, impeller speed and air flow rate in an industrial scale flotation cell – Part 1: Effect on bubble size distribution. *Minerals Engineering*. 8 (6): 615–635.

Gorain, B.K., Franzidis, J.P. & Manlapig, E.V. 1995. Studies on impeller type, impeller speed and air flow rate in an industrial scale flotation cell – Part 2: Effect on gas holdup. *Minerals Engineering*. 8 (12): 1557–1570.

Gorain, B.K., Franzidis, J.P. & Manlapig, E.V. 1996. Studies on impeller type, impeller speed and air flow rate in an industrial scale flotation cell – Part 3: Effect on superficial gas velocity. *Minerals Engineering*. 9 (6): 639–654.

Gorain, B.K., Franzidis, J.P. & Manlapig, E.V. 1997. Studies on impeller type, impeller speed and air flow rate in an industrial scale flotation cell – Part 4: Effect on bubble surface area flux on flotation performance. *Minerals Engineering*. 10 (4): 367–379.

Gorain, B.K., Napier-Munn, T.J., Franzidis, J.P. & Manlapig, E.V. 1998. Studies on impeller type, impeller speed and air flow rate in an industrial scale flotation cell – Part 5: Validation of k-S_b relationship and effect of froth depth. *Minerals Engineering*. 11 (7): 615–626.

Grano, S. 2006. Effect of impeller rotational speed on the size dependent flotation rate of galena in full scale plant cells. *Minerals Engineering*. 19: 1307–1318.

Hathaway, J.E., Schalltje, G.B., Gilbert, R.O., Pulsipher, B.A. & Matzke, B.D. 2008. Determining the optimum number of increments in composite sampling. *Environmental and Ecological Statistics*. 15: 313–327.

Herbst, J.A. & Flintoff, B. 2012. Recent Advances in Modelling, Simulation, and Control of Mineral Processing Operations. In *Separation Technologies for Minerals, Coal, and Earth Resources*. C.A. Young & G.H Luttrell, Eds. United States of America : SME. 671.

Jameson, G.J., Nguyen, A.V. & Ata, S. 2007. The flotation of fine and coarse particles. In *Froth Flotation: A Century of Innovation*. M.C. Fuerstenau, G. Jameson & R-H Yoon, Eds. United States of America : SME. 339-341.

Jenniker, S. 2005. *An investigation of the Ore and Metallurgical characteristics of the Deeps Orebody, Broken Hill Deposit, Aggeneys*. In-house Black Mountain Mining (Pty) Ltd. report

Kawatra, S.K. 2011. Fundamental Principles of Froth Flotation. In *SME Mining Engineering* Handbook. Rev. 3rd ed. P. Darling, Ed. United States of America : SME. 1517–1531.

Leja, J. 1982. *Surface chemistry of froth flotation*. New York : Springer. 1–20.

Mathe, Z.T., Harris, M.C. & O'Connor, C.T. 2000. A review of methods to model the froth phase in non-steady state flotation system. *Minerals Engineering*. 13 (2): 127–140.

McFadzean, B., Castelyn, D.G. & O'Connor, C.T. 2012. The effect of mixed thiol collectors on the flotation of galena. *Minerals Engineering*. 36 - 38: 211–218.

Naik, S. & van Drunick, W. 2007. Anglo Research (AR) experiences with integrated comminution and flotation plant modelling. *Proceedings of The Fourth South African Conference on Base Metals*. August 2007. 273–292.

Available:
http://www.saimm.co.za/Conferences/BM2007/273-292_van%20Drunick.pdf [19 May 2015]

Nelson, M.G., Lelinski, D. & Gronstrand, S. 2009. Design and operation of mechanical flotation machines. In *Recent Advances in Mineral Processing Plant Design*. D. Malhotra, P.R. Taylor, E. Spiller & M. LeVier, Eds. United States of America : SME. 168–196.

Nesset, J.E., Harnandez-Aguilar, J.R., Acuna, C., Gomez, C.O. & Finch, J.A. 2006. Some gas dispersion characteristics of mechanical flotation machines. *Minerals Engineering*. 19: 807–815.

Nguyen, A.V. & Schultze, H.J. Ed. 2004. *Colloidal Science of Flotation, Volume 118 of Surfactant Science Series*. United States of America : CRC Press. 173–182.

Ramlall, N.V. & Loveday, B.K. 2015. A comparison of models for recovery of mineral in a UG2 platinum ore by batch flotation. *The Journal of South African Institute of Mining and Metallurgy*. 115: 221–228.

Available:
http://www.saimm.co.za/Journal/v115n03p221.pdf

Rao, S.R. Ed. 2004. *Surface chemistry of froth flotation, Vol 1: Fundamentals.* Rev. 2nd ed. New York : Springer Science and Business Media. 18

Rozendaal, A. & Stalder, M. 2007. *AOL Deeps Project: Mineralogy and Genesis of the Deeps orebody – Final report.* In-house Black Mountain Mining (Pty) Ltd. report

Runge, K., Harris, M.C., Frew, J.A. & Manlapig, E.V. 1997. Floatability of streams around the Cominco Red Dog Lead cleaning circuit. *Proceedings of the 6th Annual Mill Operators' Conference.* 6-8 October 1997. 157-163.

Available:
http://www.metso.com/miningandconstruction/mct_service.nsf/WebWID/WTB-120118-22576-803FB/$File/164.pdf [19 May 2015]

Runge, K.C., Franzidis, J.P. & Manlapig, E.V. 2003a. A study of the flotation characteristics of different mineralogical classes in different streams of an industrial circuit. *Proceedings of XXII International Mineral Processing Congress.* L. Lorenzen & D.J. Bradshaw, Eds. 29 September – 3 October 2003. 962–972.

Available:
http://mapag.biz/miningandconstruction/mct_service.nsf/WebWID/WTB-120118-22576-1FB59/$File/151.pdf [19 May 2015]

Runge, K.C., Franzidis, J.P. & Manlapig, E.V. 2003b. Structuring a flotation model for robust prediction of flotation circuit performance. *Proceedings of the XXII International Mineral Processing Congress.* L. Lorenzen & D.J. Bradshaw, Eds. 29 September – 3 October 2003. 973-984.

Available:
http://www.metsoendress.com/miningandconstruction/mct_service.nsf/WebWID/WTB-120118-22576-E788F/$File/152.pdf [19 May 2015]

Saleh, A.M. 2010. A study on the performance of second order models and two phase models in iron ore flotation. *Physiochemical Problems of Mineral Processing.* 44: 215-230.

Savassi, O.N., Alexander, D.J., Franzidis, J.P. & Manlapig, E.V. 1998. An empirical model for entrainment in industrial flotation plants. *Minerals Engineering.* 11 (3): 243–256.

Shanthaveerappa, S.C., Sharma, N.K., Tamekar, G.G. & Ravindranath, K. 1995. A comprehensive investigation on Rajpura-Dariba 60:40 Calc Silicate : Graphite Mica schist ore.

In *Mineral Processing: Recent Advances and Future Trends*. S.P. Mehrotra & R. Shekar, Eds. New Delhi : Allied Publishers Limited. 432.

Singh, N. 2013. Factors driving entrainment in flotation systems and implications for bank management. MSc dissertation. McGill University

Snodgrass, R.A. 1986. Lead in South Africa. *Journal of South African Institute of Mining and Metallurgy*. 86 (4): 97–111.

Available:

http://www.saimm.co.za/Journal/v086n04p097.pdf [6 May 2015]

Stechemesser, H. & Nguyen, A.V. 1999. Time of gas–solid–liquid three-phase contact expansion in flotation. *International Journal of Mineral Processing*. 56: 117–132.

Subasignhe, G.K.N. & Albijanic, B. 2014. Influence of the propagation of the three phase contact line in flotation recovery. *Minerals Engineering*. 57: 43–49.

Sutherland, D.N. 1981. A study on the optimisation of the arrangement of flotation circuits. *International Journal of Mineral Processing*. 7: 319–346.

Sweet, J.A. 1999. Investigation of a methodology to decouple physical and chemical effects for flotation circuit performance evaluation. MSc dissertation. University of Cape Town

Vera, M.A., Franzidis, J.P. & Manlapig, E.V. 1998. Simultaneous determination of collection zone rate constant and froth zone recovery factor. In *Frothing in Flotation II*. J.S. Laskowski & E.T Woodburn, Eds. India : Gordon and Breach Science Publishers. 178.

Vera, M.A., Franzidiz, J.P. & Manlapig, E.V. 1999. Simultaneous determination of collection zone rate constant and froth zone recovery in a mechanical flotation environment. *Minerals Engineering*. 12 (10): 1163–1176.

Wang, L., Peng, Y., Runge, K. & Bradshaw, D. 2015. A review of entrainment: Mechanisms, contributing factors and modelling in flotation. *Minerals Engineering*. 70: 77 – 91

Welsby, S.D.D., Vianna, S.M.S.M. & Franzidis, J.P. 2010. Assigning physical significance to floatability components. *International Journal of Mineral Processing*. 97: 59–67.

Wills, B.A. 1988. *Mineral Processing Technology: An Introduction to the Practical Aspects of Ore Treatment and Mineral Recovery*. 4th edition. Great Britain : Pergamon Press. 457-482.

Zheng, X., Franzidiz, J.P. & Johnson, N.W. 2006. An evaluation of different models of water recovery in flotation. *Minerals Engineering*. 19: 871–882.

APPENDIX A – Phase One raw data

Repeatability tests

ASSAY RESULTS		
Sample ID	Pb (%)	Ag (ppm)
Test 1 Feed	6.4	32
Test 1 30s	73.5	334
Test 1 3m	70.0	397
Test 1 1m	66.9	384
Test 1 2 m	60.9	219
Test 1 7m	48.7	312
Test 1 11m	30.9	244
Test 1 15m	22.8	195
Test 1 20m	17.6	124
Test 1 Tails	1.1	9
Test 2 Feed	6.1	33
Test 2 30s	73.9	399
Test 2 3m	71.9	240
Test 2 1m	69.7	318
Test 2 2 m	60.5	386
Test 2 7m	52.0	363
Test 2 11m	28.8	180
Test 2 15m	17.8	138
Test 2 20m	167	121
Test 2 Tails	11	9
Test 3 Feed	6.2	33
Test 3 30s	72.9	252
Test 3 3m	71.6	415
Test 3 1m	67.5	403
Test 3 2 m	59.2	385
Test 3 7m	42.5	313
Test 3 11m	25.0	209
Test 3 15m	16.2	124
Test 3 20m	13.9	113
Test 3 Tails	1.0	8

SAMPLE MASSES		
Sample ID	Wet (g)	Dry (g)
Test 1 Feed	15.2	7.9
Test 1 30s	30.5	30.8
Test 1 3m	44.6	17.2
Test 1 1m	32.4	21.4
Test 1 2 m	8.6	13.7
Test 1 7m	47.9	26.4
Test 1 11m	71.4	15.5
Test 1 15m	67.1	8.9
Test 1 20m	16.8	7.7
Test 1 Tails	2 363.5	1 247.9
Test 2 Feed	14.6	7.5
Test 2 30s	26.3	30.4
Test 2 3m	18.1	16.4
Test 2 1m	24.7	21.7
Test 2 2 m	20.5	12.9
Test 2 7m	53.7	23.7
Test 2 11m	142.9	17.2
Test 2 15m	162.3	12.1
Test 2 20m	64.6	6.2
Test 2 Tails	2 198.8	1 240.2
Test 3 Feed	15.7	8.1
Test 3 30s	32.7	35.7
Test 3 3m	23.3	20.5
Test 3 1m	29.6	22.0
Test 3 2 m	20.0	12.0
Test 3 7m	83.0	25.8
Test 3 11m	126.1	16.9
Test 3 15m	114.0	11.1
Test 3 20m	87.0	7.4
Test 3 Tails	2 176.1	1 235.0

Ageing tests

ASSAY RESULTS		
Sample ID	Pb (%)	Ag (ppm)
Fresh Feed	4.1	58
Fresh 30s	77.0	699
Fresh 3m	73.2	753
Fresh 1m	68.9	724
Fresh 2 m	58.8	712
Fresh 7m	46.2	610
Fresh 11m	32.9	470
Fresh 15m	24.6	361
Fresh 20m	17.0	281
Fresh Tails	0.4	11
1 Hour Feed	4.6	56
1 Hour 30s	77.8	702
1 Hour 3m	72.8	713
1 Hour 1m	70.7	720
1 Hour 2 m	68.9	707
1 Hour 7m	59.3	703
1 Hour 11m	47.0	594
1 Hour 15m	40.0	540
1 Hour 20m	25.8	413
1 Hour Tails	0.7	16
3 Hours Feed	4.6	56
3 Hours 30s	75.5	712
3 Hours 3m	72.8	714
3 Hours 1m	72.2	707
3 Hours 2 m	64.8	707
3 Hours 7m	54.4	625
3 Hours 11m	32.4	435
3 Hours 15m	21.2	362
3 Hours 20m	10.5	198
3 Hours Tails	0.9	15
1 Day Feed	4.2	58
1 Day 30s	63.8	653
1 Day 3m	64.9	654
1 Day 1m	62.1	647
1 Day 2 m	62.4	640
1 Day 7m	60.4	628
1 Day 11m	53.8	579
1 Day 15m	44.1	538
1 Day 20m	31.1	418
1 Day Tails	1.9	29

SAMPLE MASSES	
Sample ID	Dry (g)
Fresh Feed	10.2
Fresh 30s	37.0
Fresh 3m	25.0
Fresh 1m	27.2
Fresh 2 m	14.3
Fresh 7m	24.8
Fresh 11m	13.3
Fresh 15m	14.3
Fresh 20m	9.3
Fresh Tails	2 486.9
1 Hour Feed	9.2
1 Hour 30s	39.5
1 Hour 3m	23.7
1 Hour 1m	28.1
1 Hour 2 m	17.0
1 Hour 7m	40.3
1 Hour 11m	12.9
1 Hour 15m	6.5
1 Hour 20m	15.7
1 Hour Tails	2 749.1
3 Hours Feed	16.0
3 Hours 30s	34.2
3 Hours 3m	22.5
3 Hours 1m	28.3
3 Hours 2 m	19.8
3 Hours 7m	45.3
3 Hours 11m	15.2
3 Hours 15m	11.3
3 Hours 20m	11.9
3 Hours Tails	2 488.9
1 Day Feed	9.6
1 Day 30s	8.9
1 Day 3m	6.1
1 Day 1m	12.8
1 Day 2 m	11.2
1 Day 7m	38.5
1 Day 11m	22.8
1 Day 15m	13.4
1 Day 20m	13.3
1 Day Tails	2 665.3

APPENDIX B – Phase Two raw data

Circuit assays and slurry mass measurements

ASSAY RESULTS				
Sample ID	**Cu (%)**	**Pb (%)**	**Zn (%)**	**Ag (ppm)**
Rougher feed	0.1	2.2	2.5	38
1st Ro Conc	1.1	68.1	3.1	654
1st Ro Tails	0.2	3.0	4.0	34
2nd Ro Conc	3.2	52.7	6.6	649
2nd Ro Tails	0.2	2.1	4.8	32
3rd Ro Conc	4.2	34.0	11.3	575
3rd Ro Tails	0.1	0.7	3.2	14
Scav Conc	4.7	27.1	13.6	523
Scav Tails	0.1	0.2	2.7	18

SLURRY MASS MEASUREMENTS			
Stream Name	**Sample ID**	**Slurry Mass (g)**	**Solids Mass (g)**
Rougher Feed	A1	6 402.6	3 509.1
	A2	5 864.9	3 250.1
	A3	6 138.0	3 308.5
1st Ro Conc	B1	1 438.7	543.3
	B2	1 249.0	585.6
	B3	1 492.5	575.8
1st Ro Tails	C1	5 134.4	1 145.5
	C2	6 967.6	1 561.7
	C3	7 473.3	1 794.8
2nd Ro Conc	D1	862.1	326.5
	D2	945.3	374.5
	D3	880.8	345.8
2nd Ro Tails	E1	6 676.1	1 226.0
	E2	6 919.6	1 232.2
	E3	6 841.0	1 246.0
3rd Ro Conc	F1	836.4	258.3
	F2	791.6	227.4
	F3	829.6	259.3
3rd Ro Tails	G1	7 210.2	2 556.2
	G2	8 311.5	3 048.2
	G3	8 353.1	3 016.1
Scav Conc	H1	7 025.3	127.6
	H2	7 917.4	106.4
	H3	7 652.0	87.7
Scav Tails	I1	7 667.5	3 642.1
	I2	5 101.3	2 383.6
	I3	5 085.7	2 207.7

Mass flow measurements

Stream Name	Sample number	Slurry mass (g)	Sample time (s)	Calc'd slurry mass flow (kg/h)	Solids mass (g)
1st Ro conc	1	140.0	2.2	10 309.1	46.3
	2	198.2	2.5	12 843.4	89.2
	3	251.9	2.8	14 574.2	101.7
	4	253.3	2.7	15 198.0	95.7
	5	316.2	2.9	17 663.6	120.5
	6	423.4	4.0	17 147.7	235.9
2nd Ro conc	1	152.2	2.9	8 502.2	45.9
	2	119.9	2.9	6 697.9	44.6
	3	114.5	2.8	6 624.6	43.0
	4	135.6	3.3	6 656.7	55.1
	5	102.9	2.7	6 174.0	41.3
	6	158.4	4.2	6 109.7	73.0
3rd Ro conc	1	118.2	3.7	5 175.2	39.2
	2	110.9	2.8	6 416.4	31.1
	3	106.9	3.2	5 411.8	39.8
	4	144.1	2.9	8 049.7	38.3
	5	119.5	2.1	9 218.6	30.2
	6	181.0	4.1	7 151.7	45.9
Scav conc	1	7 605.7	7.3	3.7	107.1
	2	9 731.0	8.7	4.0	483.8
	3	8 855.1	8.3	3.8	364.7
	4	8 678.2	7.3	4.3	32.5
	5	10 057.5	14.7	2.5	692.9
	6	4 556.8	7.5	2.2	109.4

where Calc'd denotes calculated

Hot batch flotation test data

ASSAY RESULTS				
Sample ID	**Cu (%)**	**Pb (%)**	**Zn (%)**	**Ag (ppm)**
Ro feed 30s	0.3	79.3	1	666
Ro feed 1min	0.7	75.6	1.3	680
Ro feed 2min	0.8	73.7	1.7	701
Ro feed 3min	1.4	66.3	2.5	661
Ro feed 10min	2.1	54.2	4.4	598
Ro feed 20min	2.7	33.7	7	491
Ro Feed Tails	0.1	0.4	2.6	8
1st Ro Tails 30s	0.8	64.2	3.3	613
1st Ro Tails 1min	1.3	47.5	5.9	493
1st Ro Tails 2min	1.7	32.5	8.2	391
1st Ro Tails 3min	1.6	17.7	10.3	264
1st Ro Tails 10min	1.2	9.8	11.8	170
1st Ro Tails 20min	0.9	6.4	12.5	118
1st Ro Tails Tails	0	0.3	3.6	5
2nd Ro Tails 30s	1.6	37.2	7.5	439
2nd Ro Tails 1min	1.5	24.9	9.8	313
2nd Ro Tails 2min	1.7	21.9	11.2	281
2nd Ro Tails 3min	1.8	16.9	12.9	246
2nd Ro Tails 10min	1.6	13	14.1	199
2nd Ro Tails 20min	1.2	9.3	14.5	160
2nd Ro Tails Tails	0.1	0.6	5	46
3rd Ro Tails 30s	1.7	28.3	8	364
3rd Ro Tails 1min	1.7	23	9.4	338
3rd Ro Tails 2min	1.8	20.3	10	309
3rd Ro Tails 3min	2.2	21.2	11	339
3rd Ro Tails 10min	2.1	17.6	11.4	291
3rd Ro Tails 20min	1.8	13.6	11.7	256
3rd Ro Tails Tails	0.1	0.2	3.2	6

ASSAY RESULTS (continued)				
Sample ID	Cu (%)	Pb (%)	Zn (%)	Ag (ppm)
Scav Conc 30s	5.7	32.6	9.4	681
Scav Conc 1min	5.3	32.3	13.6	566
Scav Conc 2min	5.1	31.6	14.6	610
Scav Conc 3min	5.1	32.1	15	600
Scav Conc 10min	4.6	30.5	15.7	558
Scav Conc 20min	4.5	31.2	16.3	555
Scav Conc Tails	2.3	17.6	17.7	344
Scav Tails 30s	1.0	13.7	13	35
Scav Tails 1min	1.2	14.5	15	66
Scav Tails 2min	1.2	14.3	16.7	57
Scav Tails 3min	0.9	8.2	18.6	46
Scav Tails 10min	0.6	1.5	20.8	45
Scav Tails 20min	0.5	1.5	21.7	77
Scav Tails Tails	0.1	0.2	2	4

SAMPLE MASSES		
Sample ID	Wet (g)	Dry (g)
Ro feed 30s	236	34
Ro feed 1min	125.8	16
Ro feed 2min	171.6	22.4
Ro feed 3min	180.7	21.5
Ro feed 10min	374.7	16.8
Ro feed 20min	383.5	14.3
Ro Feed Tails	-	2825.1
1st Ro Tails 30s	169.4	21.5
1st Ro Tails 1min	114	12.5
1st Ro Tails 2min	139.9	18.2
1st Ro Tails 3min	154.7	19.1
1st Ro Tails 10min	339.6	15.1
1st Ro Tails 20min	398.8	14.1
1st Ro Tails Tails	-	784
2nd Ro Tails 30s	109.2	13.2
2nd Ro Tails 1min	92.4	11.2
2nd Ro Tails 2min	115	11.7
2nd Ro Tails 3min	112.2	11.5
2nd Ro Tails 10min	325.5	13.3
2nd Ro Tails 20min	366.8	12.5
2nd Ro Tails Tails	-	985

SAMPLE MASSES (continued)		
Sample ID	**Wet (g)**	**Dry (g)**
3rd Ro Tails 30s	95.7	10.7
3rd Ro Tails 1min	80.7	9.2
3rd Ro Tails 2min	94.9	8.9
3rd Ro Tails 3min	89.9	8.6
3rd Ro Tails 10min	294.9	9.9
3rd Ro Tails 20min	347.8	8.6
3rd Ro Tails Tails	-	1403.8
Scav Conc 30s	85.7	8.5
Scav Conc 1min	83	8.4
Scav Conc 2min	117.6	9.9
Scav Conc 3min	132.9	12.5
Scav Conc 10min	395.4	14.8
Scav Conc 20min	477.7	15.7
Scav Conc Tails	-	25.9
Scav Tails 30s	95.8	10.4
Scav Tails 1min	98.2	10.6
Scav Tails 2min	124.7	11.8
Scav Tails 3min	140.5	14.3
Scav Tails 10min	423.9	17.2
Scav Tails 20min	428.1	14.4
Scav Tails Tails	-	2658.7

APPENDIX C – Assigned relative standard deviation for hot batch flotation tests

RELATIVE STANDARD DEVIATION (%)				
Sample ID	Cu	Pb	Zn	Ag
Ro feed 30s	15	10	15	10
Ro feed 1min	15	10	15	10
Ro feed 2min	15	10	15	10
Ro feed 3min	10	8	10	8
Ro feed 10min	10	8	10	8
Ro feed 20min	8	5	8	5
1st Ro Tails 30s	200	200	200	200
1st Ro Tails 1min	200	200	200	200
1st Ro Tails 2min	200	200	200	200
1st Ro Tails 3min	200	200	200	200
1st Ro Tails 10min	200	200	200	200
1st Ro Tails 20min	200	200	200	200
2nd Ro Tails 30s	200	200	200	200
2nd Ro Tails 1min	200	200	200	200
2nd Ro Tails 2min	200	200	200	200
2nd Ro Tails 3min	200	200	200	200
2nd Ro Tails 10min	200	200	200	200
2nd Ro Tails 20min	200	200	200	200
3rd Ro Tails 30s	200	200	200	200
3rd Ro Tails 1min	200	200	200	200
3rd Ro Tails 2min	200	200	200	200
3rd Ro Tails 3min	200	200	200	200
3rd Ro Tails 10min	200	200	200	200
3rd Ro Tails 20min	200	200	200	200
Scav Conc 30s	15	10	15	10
Scav Conc 1min	15	10	15	10
Scav Conc 2min	15	10	15	10
Scav Conc 3min	10	8	10	8
Scav Conc 10min	10	8	10	8
Scav Conc 20min	8	5	8	5
Scav Tails 30s	15	10	15	10
Scav Tails 1min	15	10	15	10
Scav Tails 2min	15	10	15	10
Scav Tails 3min	10	8	10	8
Scav Tails 10min	10	8	10	8
Scav Tails 20min	8	5	8	5

APPENDIX D – Sample calculations for Phase One and Phase Two

Validation testwork calculations

1. Reconciled feed grade (% or ppm)

This calculation is based on lead for Test 1. The same method was repeated for Test 2 and Test 3, and the average of the three (3) reconciled feed grades was determined.

$$\text{Feed}_{Pb}(\%) = \frac{\sum Conc_{Pb} + \sum Tails_{Pb}}{\text{Concentrate} + \text{Tails}} \times 100 = \frac{(78.4 + 14.2)\text{g}}{(141.6 + 1\,247.9)\text{g}} \times 100 = 6.7\%$$

where: $\sum \text{Conc}_{Pb}$ is the total mass of lead in the concentrate samples (g)

$\sum Tails_{Pb}$ is the total mass of lead in the tailings sample (g)

Concentrate is the mass of solids in the concentrate samples (g)

Tails is the mass of solids in the tailings sample (g)

2. Propagated allowed error for reconciled silver feed grade (%)

The tolerated deviation of the BMM Analytical Laboratory based on the bias associated with the ICP-MS technique used to analyse samples for their silver content is 9,2% for low grade samples and 6,3% for high grade samples (i.e. concentrates). The calculation shown is for the repeatability tests in order to determine the allowed error between the measured and reconciled feed grade of silver.

$$\text{Error}_{Silver}(\%) = \sqrt{(\sigma_{30s})^2 + (\sigma_{1m})^2 + (\sigma_{2m})^2 + (\sigma_{3m})^2 + (\sigma_{7m})^2 + (\sigma_{11m})^2 + (\sigma_{15m})^2 + (\sigma_{20m})^2 + (\sigma_{Tails})}$$

$$= \sqrt{(6.3)^2 + (6.3)^2 + (6.3)^2 + (6.3)^2 + (6.3)^2 + (6.3)^2 + (6.3)^2 + (9.2)^2}$$

$$= 20.2\%$$

3. Feed grade relative error (%)

This calculation is based on average lead feed grade. The same method was repeated for silver using the average measured and reconciled feed grade values.

$$\text{Error}_{Pb_{feed}}(\%) = \frac{|Measured_{Avg\ Pb} - Reconciled_{Avg\ Pb}|}{\text{Measured}_{Avg\ Pb}} \times 100 = \frac{|6.2 - 6.7|\ \%}{6.2\%} \times 100 = 6.9\%$$

where: $\text{Measured}_{Avg\ Pb}$ is the average measured feed grade of lead for Test 1 through 3 (%)

$\text{Reconciled}_{Avg\ Pb}$ is the average reconciled feed grade of lead for Test 1 through 3 (%)

This calculation was used in all instances in this study where the relative error between two variables was determined.

4. Experimental recovery (%)

This calculation is based on lead for the concentrate recovered after one (1) minute flotation time. The same method was used for all concentrates and was also used to calculate the solids and silver recovery per flotation time.

$$\text{Rec}_{Pb\_1min}(\%) = \frac{Conc_{Pb\_1min}}{Feed_{Pb}} \times 100 = \frac{17.2\ g \times 70.0\%}{92.6\ g} \times 100 = 24.5\%$$

where: Conc_{Pb_1min} is the mass of lead recovered into the one (1) minute concentrate (g)

Feed_{Pb} is the total mass of lead in the feed sample (g)

The cumulative recovery was determined by the summation of the individual recovery per flotation time.

5. Infinite recovery using Klimpel (1980) model (%)

This calculation is based on lead for a cumulative flotation time of one (1) minute. An estimate was assigned for the flotation rate constant (k) and the infinite time recovery (R_∞). The sum of squared error between the experimental and Klimpel recovery was minimised by adjusting the flotation rate constant and infinite time recovery. The calculation below shows the fitted flotation rate constant and infinite recovery.

$$\text{Rec}_{Pb\_1min}(\%) = R_\infty\left(1 - \frac{1}{k\tau}(1 - e^{-k\tau})\right) = 87.6\%\left(1 - \frac{1}{1.3 \times 1}(1 - e^{-1{,}3 \times 1})\right) = 38.7\%$$

Mass balance calculations

1. Percent solids for the experimental data (%)

This calculation is based on a sample collected from the 1st Rougher concentrate.

$$\%Solids_{R1C\_1} = \frac{Solids\ mass_{R1C\_1}}{Slurry\ mass_{R1C\_1}} \times 100 = \frac{46.3\ g}{140\ g} \times 100 = 33.1\%$$

The same method was used to calculate the percent solids for all the six (6) samples that were collected to determine the mass flow rate. The average percent solids was calculated using the individual percent solids per sample.

$$\%Solids_{R1C\_Avg} = \frac{\sum_{i=6}^{1} \%Solids_{R1C\_i}}{6} = \frac{(33.1 + 45.0 + 40.4 + 37.8 + 38.1 + 55.7)\%}{6} = 41.7\%$$

2. Experimental slurry mass flow (kg/h)

This calculation is based on a sample collected from the 1st Rougher concentrate.

$$\text{Slurry flow}_{R1C\_1} = \frac{Slurry mass_{R1C\_1}}{Sample\ time_{R1C\_1}} \times \frac{3\,600\ \text{sec}}{hour} \times \frac{Perimeter_{1st\ Ro}}{Length_{Sampler}} \times \frac{1\ ton}{10^3\ kg}$$

$$= \frac{140.0\ g}{2.2\ \text{sec}} \times \frac{3\,600\ \text{sec}}{hour} \times 45 \times \frac{1\ ton}{10^3\ kg} = 10\,309.1\ \text{kg/h}$$

The same method was used to calculate the slurry mass flow for all the six (6) samples that were collected to determine the mass flow rate. The average slurry mass flow was calculated using the individual mass flow per sample.

$$Slurry flow_{R1C_{Avg}} = \frac{\sum_{i=6}^{1} Slurry flow_{R1C_i}}{6}$$

$$= \frac{(10\,309.1 + 12\,843.4 + 14\,574.2 + 15\,198.0 + 17\,663.6 + 17\,147.7)\ kg/h}{6}$$

$$= 14\,622.7\ kg/h$$

3. Average experimental solids mass flow (kg/h)

This calculation is based on the average of the samples collected from the 1st Rougher concentrate.

$$Solids\ flow_{R1C\_Avg} = \text{Slurry}_{R1C\_Avg} \times \%Solids_{R1C\_Avg} = 14\,622.7\ tph \times 41.7\% = 6\,094.1\ tph$$

4. Calculating the relative standard deviation from circuit survey data (%)

This calculation is based on the solids mass flow of the 1st Rougher concentrate stream.

$$Error_{Sol,R1C} = \frac{StdDev_{Solids\_R1C}}{Solids\ flow_{R1C\_Avg}} \times 100 = \frac{1\,990.1\ kg/h}{6\,094.1\ kg/h} \times 100 = 32.7\%$$

5. Experimental water mass flow (kg/h)

This calculation is based on the 1st Rougher concentrate using the average experimental data.

$$Water_{R1C} = Slurry\ flow_{R1C} - (\%Solids_{R1C} \times Slurry\ flow_{R1C})$$

$$= 14\,622.7\ tph - (41.7\% \times 14\,622.7 tph) = 8\,527.1\ kg/h$$

6. Experimental mineral mass flow (kg/h)

This calculation is based on the 1st Rougher concentrate using the average experimental data of copper.

$$Chal_{R1C} = \frac{\%Cu_{R1C} \times Solids\ flow_{R1C}}{\frac{Copper}{Chalcopyrite}} = \frac{1.1\% \times 6\,094,.kg/h}{\frac{63.5\ g}{183.5\ g}} = 193.4\ kg/h$$

The same calculation applies for galena and sphalerite. To calculate the mass flow of silver, the following calculation was used.

$$Silver_{R1C} = \frac{ppm\_Silver_{R1C} \times \text{Solids flow}_{R1C}}{10^6} = \frac{654\ ppm \times 6\,094.1\ kg/h}{10^6} = 4.0\ kg/h$$

7. Experimental mass flow of gangue/remainder (kg/h)

This calculation is based on the 1st Rougher concentrate using the average experimental data.

$$Rem_{R1C} = Solids\ flow_{R1C} - Chal_{R1C} - Gal_{R1C} - Sphal_{R1C} - Silver_{R1C}$$

$$= (14\,622.7 - 193.4 - 4\,795.2 - 277.9 - 4.0)\ kg/h = 827.6\ kg/h$$

8. Experimental assay of gangue/remainder (%)

This calculation is based on the 1st Rougher concentrate using the average experimental data.

$$\%Rem_{R1C} = \frac{Rem_{R1C}}{Solids\ flow_{R1C}} \times 100 = \frac{827.6\ \text{kg/h}}{6\,094.1\ kg/h} \times 100 = 13.6\%$$

9. Balanced species mass flow in concentrate and tailings streams

This calculation is based on water in the 1st Rougher concentrate and 1st Rougher tailings streams using the mass balanced data.

$$Water_{R1T} = -Water_{Feed} X_{Water,R1}{}^{-1} = -204\,111.0\ kg/h \times -0.975 = 198\,995.3\ kg/h$$

$$Water_{R1C} = g_{Water,R1} \text{Water}_{R1T} = 2.6\times10^{-2} \times 198\,995.3 \frac{\text{kg}}{\text{h}} = 5115.7\ kg/h$$

The same calculation applies for solids, chalcopyrite, galena, sphalerite and silver.

10. Balanced percent solids (%)

This calculation is based on 1st Rougher concentrate using the mass balanced data.

$$\%Solids_{R1C} = \frac{Solids\ flow_{R1C}}{Solids flow_{R1C} + Water\ mass_{R1C}} \times 100 = \frac{3\,655.4\ \text{kg/h}}{(3\,655.4 + 5\,115.7)\ kg/h} \times 100$$

$$= 41.7\%$$

11. Balanced assay of flotation streams (% and ppm)

This calculation is based on 1st Rougher concentrate using the mass balanced data of copper (%) and silver (ppm).

$$\%Copper_{R1C} = \frac{\text{Chal}_{R1C} \times \frac{Copper}{Chalcopyrite}}{\text{Solids flow}_{R1C}} = \frac{109.1\ kg/h \times \frac{63.5\ g}{183.5\ g}}{3\,655.4\ \text{kg/h}} = 1{,}0\%$$

$$ppm\_Silver_{R1C} = \frac{\text{Silver}_{R1C}}{\text{Solids flow}_{R1C}} \times 10^6 = \frac{2.4\ \text{kg/h}}{3\,655.4\ \text{kg/h}} = 650\ \text{ppm}$$

12. Balanced mass flow of remainder (kg/h)

This calculation is based on the 1st Rougher concentrate for the mass balanced data.

$$Rem_{R1C} = Solids\ flow_{R1C} - Chal_{R1C} - Gal_{R1C} - Sphal_{R1C} - Silver_{R1C}$$

$$= (3\,655.4 - 109.1 - 2\,940.8 - 166.1 - 2.4)\ \text{kg/h} = 439.5\ kg/h$$

13. Balanced species recovery (%)

This calculation is based on the solids in 1st Rougher concentrate for the mass balanced data.

$$\%Rec\_Solids_{R1C} = \frac{Solids\ flow_{R1C}}{Solids\ flow_{Feed}} \times 100 = \frac{3\ 655.4\ kg/h}{246\ 564.6\ kg/h} \times 100 = 1.5\%$$

14. Weighted sum of squared error calculation

This calculation is based on the solids in the 1st Rougher concentrate for the mass balanced data.

$$Solids\ Error_{R1C} = \left[\frac{Solids\ flow_{R1C,Exp} - Solids\ flow_{R1C,Bal}}{Solids\ flow_{R1C,Exp} \times Error_{Sol,R1C}}\right]^2 = \left[\frac{(6\ 094.1 - 3\ 655.4)\ kg/h}{6\ 094.1\ kg/h \times 35\%}\right]^2$$

$$= 1.3$$

Modelling calculations

1. Enhancement factor for species based on model fitted parameters

This calculation is based on the fast floating galena in the 1st Rougher concentrate, exiting the 1st Rougher flotation cell, for the model predicted data.

$$g_{Gal,F,R1} = P_{Gal,F} S_{b,R1} R_{f,Gal,R1} \tau_{R1} = 2.8\times 10^{-2} \times 937.2\ min^{-1} \times 22.9\% \times 9.2\ min = 55.9$$

The same calculation applies to chalcopyrite, sphalerite and silver for all sub-classes. The enhancement factor of the remainder, i.e. the entrained non-floating fraction, is shown below using the 1st Rougher concentrate stream for the model predicted data.

$$g_{Rem,NF} = \frac{\mathrm{ENT}_G R_{Water,R1}}{1 - R_{Water,R1}} = \frac{0.07 \times 2.5\%}{1 - 2.5\%} = 1.8 \times 10^{-3}$$

2. Model predicted mass flow of species in tailings streams (kg/h)

This calculation is based on the fast floating galena in the 1st Rougher tailings stream for the model predicted data.

$$Gal_{F,R1T} = -Gal_{Feed} m_{Gal,F} X_{Gal,F,R1}{}^{-1} = -6\ 309.4\ kg/h \times 0.2 \times -0.018 = 23.2\ kg/h$$

3. Model predicted mass flow of species in concentrate streams (kg/h)

This calculation is based on the fast floating galena in the 1st Rougher concentrate for the model predicted data.

$$Gal_{F,R1C} = g_{Gal,F,R1} \times \mathrm{Gal}_{F,R1T} = 55.9 \times 23.2\ \mathrm{kg/h} = 1\ 298.8\ kg/h$$

4. Overall model predicted mass flow of species (kg/h)

This calculation is based on galena in the 1st Rougher concentrate for the model predicted data.

$$Gal_{\mathrm{R1C}} = \mathrm{Gal}_{F,R1C} + Gal_{S,R1C} + Gal_{NF,R1C} = (1\ 298.8 + 1\ 511.4 + 0.0) kg/h = 2\ 810.2\ kg/h$$

5. Overall model predicted mass flow of solids (kg/h)

This calculation is based on the 1st Rougher concentrate for the model predicted data.

$$Solids_{R1C} = \sum_{i=1}^{3} Chal_{R1C} + \sum_{i=1}^{3} Gal_{R1C} + \sum_{i=1}^{3} Sphal_{R1C} + \sum_{i=1}^{3} Silver_{R1C} + \sum_{i=1}^{1} Rem_{R1C}$$

$$= (72.4 + 2\,810.2 + 119.9 + 2.4 + 411.4)\ kg/h = 3\,416.3\ kg/h$$

6. Model predicted mass flow of water in flotation streams (kg/h)

This calculation is based on the 1st Rougher concentrate for the model predicted data. Since the density of the solids was not known, the mass flow of the solids was used.

$$Q_W = aQ_S{}^b = 2.4 \times \left(\frac{3\,416.3}{1000}\right)^{0.6} = 5\,064.2\ kg/h$$

The mass of water in the tailings streams was calculated by difference, i.e. the water in the feed to the flotation cell less the water recovered into the concentrate produced by that flotation cell. An example using the 1st Rougher tailings is shown below.

$$Water_{R1T} = Water_{Feed} - Water_{R1C} = (204\,111.0 - 5064.2)kg/h = 199046.8\ kg/h$$

7. Model predicted percent solids of flotation streams (%)

This calculation is based on 1st Rougher concentrate using the model predicted data.

$$\%Solids_{R1C} = \frac{Solidsflow_{R1C}}{Solidsflow_{R1C} + Watermass_{R1C}} \times 100 = \frac{3\,416.3\ kg/h}{(3\,416.3 + 5\,064.2)kg/h} \times 100$$

$$= 40.3\%$$

8. Model predicted residence time (minutes)

This calculation is based on the 1st Rougher flotation cell where the 1st Rougher tailings stream exits the flotation cell. Since the density of the slurry was not known, the solids was assumed to have a density of 4 t/m³.

$$\tau_{R1} = \frac{V_{R1}}{Q_{R1T}} = \frac{40\ m^3}{\left(\frac{243\,157.7\ tph}{\frac{4\ t}{m^3}} + 199\,046.8\ m^3\right)} \times 60\ minutes = 9.2\ minutes$$

9. Model predicted assay of flotation streams (% and ppm)

This calculation is based on chalcopyrite and silver in the 1st Rougher concentrate stream for the model predicted data.

$$\%Chal_{R1C} = \frac{Chal_{R1C}}{Solids\ flow_{R1C}} \times 100 = \frac{72.4\ kg/h}{3\,416.3\ kg/h} \times 100 = 2.1\%$$

The same calculation applies for galena, sphalerite and remainder.

$$ppm\_Silver_{R1C} = \frac{Silver_{R1C}}{Solids\ flow_{R1C}} \times 10^6 = \frac{2.4\ kg/h}{3\,416.3\ kg/h} \times 1000 = 708\ ppm$$

10. Model predicted circuit recovery for all species (%)

This calculation is based on chalcopyrite in the 1st Rougher concentrate for the model predicted data.

$$\%Rec\_Chal_{R1C} = \frac{Chal_{R1C}}{Chal_{Feed}} \times 100 = \frac{72.4\ kg/h}{911.5\ kg/h} \times 100 = 8.0\ \%$$

The same calculation applies for solids, water, galena, sphalerite and remainder.

11. Model predicted batch flotation recovery for a sub-class of species for a certain flotation time (%)

This calculation is based on fast floating galena in the Rougher feed hot batch flotation test for a cumulative flotation time of one (1) minute.

$$Rec\_Gal_{F,1min} = m_{Gal,F}(1 - e^{-k_{Gal,F}\tau_{1min}}) = m_{Gal,F}(1 - e^{-P_{Gal,F}S_{b,Batch}\tau_{1min}})$$

$$= 0.2 \times \left(1 - e^{-2.8 \times 10^{-2}} \times 1200\ min^{-1} \times 1\ minute\right) = 21.0\%$$

12. Total model predicted batch flotation recovery for a certain flotation time (%)

This calculation is based on galena in the Rougher feed hot batch flotation test for a cumulative flotation time of one (1) minute.

$$Rec_{Gal_{Total,1min}} = Rec_{Gal_{F,1min}} + Rec_{Gal_{F,1min}} + Rec_{Gal_{NF,1min}} = (21.0 + 10.0 + 0.0)\%$$

$$= 31.0\%$$

13. Weighted sum of squared error calculation for the circuit

This calculation is based on the galena in the 1st Rougher concentrate for the model predicted data.

$$Galena\ Error_{\mathrm{R1C}} = \left[\frac{Gal_{R1C,Bal} - Gal_{R1C,Mod}}{Gal_{R1C,Bal} \times Error_{Gal,\mathrm{R1C}}}\right]^2 = \left[\frac{(2\,940.8 - 2\,810.2)\ kg/h}{2\,940.8\ kg/h \times 8\%}\right]^2 = 0.3$$

14. Weighted sum of squared error calculation for the bath flotation tests

This calculation is based on the galena in the Rougher feed hot batch flotation test for a cumulative flotation time of one (1) minute.

$$Batch\_Error_{Gal,2} = \left[\frac{\mathrm{Rec}_{\mathrm{Gal}\,Exp,Feed,1min} - \mathrm{Rec}_{\mathrm{Gal}\,Mod,Feed,1min}}{\mathrm{Rec}_{\mathrm{Gal}\,Exp,Feed,1min} x \mathrm{Error}_{\mathrm{Feed}\,Gal,SD}}\right]^2 = \left[\frac{41.3\% - 40.0\%}{41.3\% \times 10\%}\right]^2 = 0.2$$